TU WIEN Informatics

IoT Sensor Swarm for Agricultural Microclimate Measurement

DIPLOMARBEIT

zur Erlangung des akademischen Grades

Diplom-Ingenieur

im Rahmen des Studiums

Technische Informatik

eingereicht von

Thomas Puchinger, BSc
Matrikelnummer 0928809

an der Fakultät für Informatik

der Technischen Universität Wien

Betreuung: Univ.Prof. Dipl.-Ing. Dr.rer.nat. Radu Grosu
Mitwirkung: Proj.Ass. Dipl.-Ing. BSc Christian Hirsch

Wien, 8. Dezember 2020

Thomas Puchinger | Radu Grosu

Technische Universität Wien
A-1040 Wien ▪ Karlsplatz 13 ▪ Tel. +43-1-58801-0 ▪ www.tuwien.at

TU WIEN Informatics

IoT Sensor Swarm for Agricultural Microclimate Measurement

DIPLOMA THESIS

submitted in partial fulfillment of the requirements for the degree of

Diplom-Ingenieur

in

Computer Engineering

by

Thomas Puchinger, BSc
Registration Number 0928809

to the Faculty of Informatics

at the TU Wien

Advisor: Univ.Prof. Dipl.-Ing. Dr.rer.nat. Radu Grosu
Assistance: Proj.Ass. Dipl.-Ing. BSc Christian Hirsch

Vienna, 8th December, 2020

Thomas Puchinger	Radu Grosu

Technische Universität Wien
A-1040 Wien ▪ Karlsplatz 13 ▪ Tel. +43-1-58801-0 ▪ www.tuwien.at

Erklärung zur Verfassung der Arbeit

Thomas Puchinger, BSc

Hiermit erkläre ich, dass ich diese Arbeit selbständig verfasst habe, dass ich die verwendeten Quellen und Hilfsmittel vollständig angegeben habe und dass ich die Stellen der Arbeit – einschließlich Tabellen, Karten und Abbildungen –, die anderen Werken oder dem Internet im Wortlaut oder dem Sinn nach entnommen sind, auf jeden Fall unter Angabe der Quelle als Entlehnung kenntlich gemacht habe.

Wien, 8. Dezember 2020

Thomas Puchinger

Danksagung

Dem Leiter des Forschungsbereiches Cyber Physical Systems Univ.Prof. Dipl.-Ing. Dr. rer nat. Radu Grosu gilt mein aufrichtiger Dank - für die Betreuung und Begutachtung dieser Arbeit. Meinen KollegInnen der TU Wien, Dipl.-Ing. Christian Hirsch BSc, Dipl.-Ing. Michael Platzer und Ing. Leo Mayerhofer für ihren fachlichen Rat und ihre kompetente Unterstützung, sowie Viktoria Vasalik, die sich mit ihrer Englischkompetenz eingebracht hat und mir bei teils schwierigen Übersetzungen zur Seite stand.

Für die mentale Unterstützung danke ich meiner Familie. Meiner Frau Tamara für das Gegenlesen der Thesis und ihren Rat sowie meinen Eltern für ihre Unterstützung, sodass es mir möglich war, meine Studien abzuschließen.

Stetige Motivation und fachliches Feedback waren mir eine große Stütze, danke hierfür für die langjährige Freundschaft, Alexander, Bernhard und Christoph.

Acknowledgements

A special “Thank you” to the Head of the Research Unit Cyber Physical Systems, Univ.Prof. Dipl.-Ing. Dr.rer.nat. Radu Grosu, for supervising this thesis. I am grateful to my colleagues at the TU Wien, Dipl.-Ing. Christian Hirsch BSc, Dipl.-Ing. Michael Platzer and Ing. Leo Mayerhofer for their professional advice and competent support. Thanks to Viktoria Vasalik as well, who stood by my side with her language skills and helped translate difficult phrases into English. I am grateful to my family for the mental support, to my wife, Tamara, for reading my thesis and her constructive criticism and to my parents, who helped me finish my studies.

Constant motivation and professional feedback were a great support for me, thanks for the long friendship, Alexander, Bernhard and Christoph.

Kurzfassung

Mit dem Internet verbundene vernetze Sensor Systeme, auch Internet of Things (IoT) genannt, haben sich in den letzten Jahren rasch weiterentwickelt. Dadurch sind viele neue Anwendungsfälle und Einsatzmöglichkeiten entstanden und sie entstehen kontinuierlich. Damit die heutige Landwirtschaft kostendeckend wirtschaften kann, wird es immer notwendiger, Agrarflächen noch genauer und verteilter zu messen. Grund hierfür sind die steigenden Kosten für Löhne, Material und Verbrauchsmittel. Aufgrund des starken Wettbewerbes stagnieren jedoch die Marktpreise. Um die notwendigen Arbeitsschritte im Pflanzenschutz genauer planen zu können, sind genaue Messwerte der Umwelt erforderlich. Zwei hierfür relevante Messwerte sind die Blattfeuchte und der Ultraviolet Radiation (UV) Wert. Ziel dieser Arbeit ist es, einen Prototyp zu entwickeln, der diese beiden Messwerte sensorisch erfasst. Diese Messwerte sollen ins Internet übertragen werden, dazu sind der Entwurf und Aufbau eines entsprechenden Sensor Netzwerkes, auch Sensor Swarm genannt, erforderlich. Während des gesamten Entwicklungsprozesses wird darauf geachtet, die Kosten für den Sensor so gering wie möglich und den Stromverbrauch niedrig zu halten, um die Autarkheit des Sensors zu gewährleisten.

Der durchgeführte Feldtest zeigt, dass der selbst gebaute Sensor autark arbeiten kann und die Zuverlässigkeit bei mindestens 87 Prozent liegt. Die Kosten für einen Sensor liegen unter 150 € pro Stück und unterschreiten damit die Erwerbskosten kommerziell erhältlicher Produkte. Auch wenn vor einer potenziellen Markteinführung des Systems noch Hürden genommen werden müssten, konnte durch diese Arbeit nachgewiesen werden, dass das geschaffene Sensor Netzwerk sich auch in der Praxis bewährt hat.

Abstract

Networked sensor systems connected to the Internet, also called Internet of Things (IoT), have rapidly developed in the past few years. This has created and is continuing to create many new applications and possible use cases. To enable today's agricultural organizations to cover their costs, more accurate and distributed measurements of the agricultural land are necessary. The reason for this are the rising salaries and the rising costs of materials and consumables. However, the market prices of agricultural products are stagnating due to strong competition. To be able to plan the necessary steps in plant protection more precisely, accurate measurements of the environment are required. Two relevant measured values are leaf wetness and UV value. The aim of this thesis is to develop a prototype that measures these two values. These measured values are to be transmitted to the Internet; to do this, a corresponding sensor network, also called sensor swarm, has to be designed and constructed. Throughout the development process, the costs of the sensor and the power consumption are kept as low as possible to ensure the self-sufficiency of the sensor. The field test carried out shows that the self-built sensor can operate autonomously and the reliability is at least 87 percent. The cost of a sensor is less than €150 per unit, which is less than the purchase cost of commercially available products. Even if a potential market launch would prove difficult in the beginning, this thesis establishes that the created sensor network has proven itself in practice.

Contents

CHAPTER 1

Introduction

This chapter describes the problem and explains the motivation behind the aim to build an agricultural sensor swarm for microclimate measurements.

1.1 Problem Description and Motivation

Today, the number of devices that are able to transfer data over networks keeps increasing [LL15]. This system of different devices that are connected together to share data is called Internet of Things (IoT) and it is present, for example, in households, in the entertainment and mobility sectors. The aim is to exchange data, e.g. weather measurements, in order to make decisions, create statistical evaluations or to take remote actions. Such systems can also be used in agriculture to provide farmers with measured data so that they can make their spraying and irrigation systems more intelligent and can detect diseases easier [MPB+16]. The following parameters are relevant to disease detection in agricultural microclimate systems [HRG18]:

- Temperature
- Humidity
- Solar radiation
- Color of the leaves and the berries
- Water content of the berries
- Raindrops on the berries
- Ripeness of the berries

Table 1.1: Wavelengths of the different UV types.

Type	low Value	high Value
Ultraviolet C (UVC)	200nm	280nm
Ultraviolet B (UVB)	280nm	320nm
Ultraviolet A (UVA)	320nm	400nm
visible light	400nm	750nm

The leaf wetness describes how wet or dry the surface of a leaf is. Based on this value, a disease warning system can alert the farmer to possible infections [MFP+16]. Ultraviolet Radiation (UV) is an electromagnetic radiation, which has too short a wavelength to be seen by humans. Artificial UV light can be created by mercury vapour lamps, back light or UV Light Emitting Diodes (LEDs). Table 1.1 lists the different types of UV light and their respective wavelengths. The UV light affects the photosynthesis and is therefore of interest to the farmer [KBD+99]. First of all, these measured values are collected over a period of years and then models are created. Farmers are then provided with information that was obtained on the basis of these models and current measured values. Vitimeteo [Vit] is a model well known and much used by winemakers. It calculates the life cycle of the Plasmopara viticola, which is a disease of the grapevine [BKK+08] and can cause significant economic damages.

1.2 Aim of This Work

To create disease models, as much data as possible is needed. The aim of this work is to collect the data with the help of a sensor swarm. This swarm consists of a network in which the sensors can exchange messages and are able to store the measurements on a server in the cloud. The sensors should be distributed on a field, vineyard or orchard where no infrastructure is given, i.e. there is no electricity, no buildings and no Internet connection via cable available. Therefore, outdoor installation must be possible. The swarm network should contain sensors that measure the leaf wetness and the UV radiation.

1.3 Methodological Approach

The first step is to read the relevant literature and compare the prevailing transmission methods and protocols. Then we will compare the existing agricultural microclimate measurement systems with respect to the technical function of weather stations, Leaf Wetness Sensor (LWS) and UV sensors. Based on this comparison and our defined requirements, we will choose an existing system or a combination of different systems, or we will develop our own system from zero. Different data flows will be evaluated and compared, this includes the testing of different transmission methods, e.g. Bluetooth and Thread. The sensitivity of different LWSs will be evaluated, the best one then selected for the prototypes. After finishing the hardware and software development of the prototypes, we will test them and solve problems that arise. After a problem-free indoor test, the sensors will be mounted in the field for testing. If problems occur, the tests will be stopped until the equipment is fixed. At the end of the tests, the collected data will be evaluated.

1.4 Structure of This Work

After the Introduction, Chapter Two gives an overview of state-of-the-art techniques for wired and wireless data transmission. In addition, existing systems and methods for measuring the values related to microclimate in agriculture are reviewed. Chapter Three specifies our requirements for an agricultural microclimate measurement system and describes our resulting decision for an existing system, a combination of systems, or whether we will develop our own system from zero. Chapter Four describes the design of the system. Chapter Five explains the hardware and Chapter Six the software implementation. In Chapter Seven we evaluate the measured data. Chapter Eight summarizes the implementation, evaluation and the encountered problems. It also presents the results we have reached and future tasks.

CHAPTER 2

State of the Art

This chapter presents existing methods to measure microclimate. Innovations of the past few years have improved the techniques and with the help of IoT sensor swarms, which consist of many individual sensors, measuring is more reliable [TGL+07]. The protocols and standards to build such networks are constantly evolving [KK19]. Existing concepts and standards for transmitting data over networks are studied and compared at the beginning of this chapter.
To simplify the usage of System on Chips (SoCs) in IoT applications, the manufacturers provide chips with built-in wireless (e.g. Bluetooth Low Energy (BLE), Zigbee, Thread, 802.15.4, Near Field Communication (NFC)) and wired technologies. They also provide software stacks for these mesh networks. This decreases the time necessary for the development of new devices for mesh networks. Unfortunately, most of the software stacks are closed-source, which means that the developer does not know what the code looks like and cannot modify it either. To go around this problem, the developer could use one of different open-source Real Time Operating Systems (RTOSs).

2.1 Transmission Methods

In principle, there are three ways to transmit data: wired, wireless and optical. Himanshu Jha studies and compares wired, wireless and optical networks in his Journal [Jha17]. From this study we extracted the properties that are important for our agricultural sensor network and compared these in Table 2.1. For our purpose, throughput and latency are not relevant - because the arrival of the data is not time-dependent. On the other hand, mobility is very important.

Table 2.1: Comparison of wired and wireless networks [Jha17].

Properties	Wired	Wireless	Optical
Latency	medium	high	low
Throughput	medium	low	high
Mobility	limited	not limited	limited

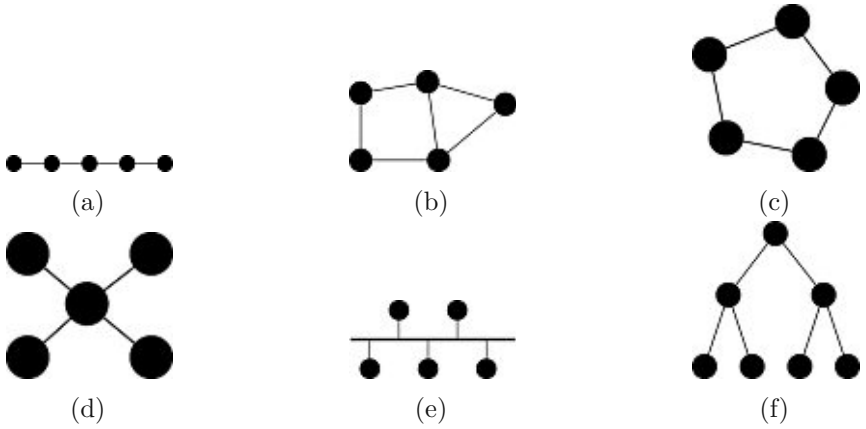

Figure 2.1: Different Network Topologies, where the lines illustrate the possible communication paths. The connected nodes can build a Line (a), Mesh (b), Ring (c), Star (d), Bus (e) or a Tree (f).

2.1.1 Network Topologies

For the construction of sensor networks, there are different topologies available and they are illustrated in Figure 2.1. K. Pandya [Pan13] describes the different topologies and their advantages and disadvantages, which are listed below.

Line: In this topology each node can have two neighbors at the most. It supports long distances, but the disadvantage is that if one node fails, the whole chain is interrupted.

Mesh: In a Mesh it is possible that each node communicates with every other node. Therefore, the network can adapt its routing if a node fails. It also supports long distances, by building a chain. The disadvantages are that the routing through the network can get complex and that the setup and maintenance is more time-consuming than that of the other topologies.

Ring: In a Ring network each node has exactly two neighbors and therefore each node can be accessed from two sides. This is important if, for example, one path is damaged. The disadvantages are the expensive and difficult installation and the detection of a faulty node.

Table 2.2: Comparison of protocols that define the physical layer for wired networks.

Protocol	Cable	Speed	Topology
Ethernet	Twisted Pair, Fiber	10 Mbps	Bus, Star
Fast Ethernet	Twisted Pair, Fiber	100 Mbps	Star, Mesh
1-Wire	Twisted Pair	16.3 kbps	Bus
RS-485	Twisted Pair	10 Mbps	Bus

Star: In a Star topology all nodes in the network are connected to the central hub. This hub is responsible for routing the data packets to the destination. The disadvantages are that the central hub is a Single Point of Failure (SPOF) and that the reachable distance is limited.

Bus: In a Bus topology a single cable is needed to connect all nodes. Therefore, it is reliable in small networks and requires the least amount of cable. To enlarge the network, only the bus cable has to be extended. The disadvantages are that the sending nodes can interrupt each other and so they use a lot of bandwidth and each additional connected node weakens the electric signal.

Tree: The Tree topology is a nested star topology. The hubs can have other hubs connected to them. The installation of the network is well-ordered and thanks to this, a faulty node can be found by following the traces. The disadvantages are that a failure in the central hub brings the whole network to a halt and more cabling is required compared to the Bus topology.

2.1.2 Wired Network

In wired networks, information is transmitted through a solid medium, e.g. copper or glass fiber. To set up a wired network, the topology has to be known in advance. Wired networks are not prone to interferences, they support high speeds (up to 1 Gbit/s) and the possible distances are long [KM14]. In Table 2.2 different protocols for wired networks are compared. The Ethernet standard (IEEE 802.3) has many extensions, e.g. Fast Ethernet (IEEE 802.3u) [IEEb]. With the help of Shortest Path Bridging (SPF) [AAB+10], which is specified in IEEE 802.1aq, all routes in an Ethernet network can be used. This way, a mesh network can be created. 1-Wire [Awt97] describes a serial protocol from the company Dallas Semiconductor. It only needs data and a ground line. It is used, for example, in home automation [Ste16] and agriculture [Awt98] to measure temperature or humidity. RS-485 (EIA-485) [cco99] is defined by the Electronic Industries Alliance (EIA), the differential signaling over twisted pair cables improves the robustness towards interferences. Therefore, it can be used over long distances [cco99].

2.1.3 Wireless Network

In wireless communication, information is transmitted through electromagnetic waves. Wireless sensors can be added to, moved within and removed from the network with less effort than in the case of wired networks because there is no cabling necessary. Therefore, wireless sensor networks have recently been used in more and more applications [PDHM14]. Standardization organizations are trying to avoid problems with interoperability between applications, by defining unique standards.

These standards try to meet requirements of low power consumption, low latency, high reliability, scalability and security. Mostly, they define a unique Physical, Data Link, Network and Application Layer. Some important organizations and standards are presented below.
The Institute of Electrical and Electronics Engineers Standards Association (IEEE-SA) [IEEc] defines the Physical and Data Link Layer for the Institute of Electrical and Electronics Engineers (IEEE) 802.15.4, IEEE 802.15.1 (Bluetooth) and IEEE 802.11ah (WiFi). The Zigbee Alliance [Zig] is a group of companies that maintain and define the Zigbee standard. Zigbee is based on IEEE 802.15.4, for low-power wireless networks. The Internet Engineering Task Force (IETF) [IETa] is a non-profit organization that defined IPv6 over Low power Wireless Personal Area Network (6LoWPAN).
The Bluetooth Special Interest Group (SIG) [BLSb] developed and distributed Bluetooth. In comparison to IEEE, which is an organization, the SIG is a consortium of companies that are interested in the development and distribution of Bluetooth.

2.2 OSI Model

The Open System Interconnection (OSI) model [fSI94] represents an abstraction of network protocols, it is defined by the International Organization for Standardization (ISO). It defines 7 layers starting at the physical medium and ending with the applications. Each layer has its own area of responsibility and in between there are standardized interfaces. The aim is to simplify the communication and to support further development. Table 2.3 shows an overview of three stack examples and the corresponding protocols. Based on this, these technologies are analyzed and compared.

2.3 Physical and Data Link Layer

The physical layer is the lowest one and provides functionality for activating and deactivating physical connections. The data link layer controls access to the transmission medium and is responsible for reliable and error-free transmission.

Table 2.3: Stack examples according to the OSI model. Column (a) shows protocols that are used with Thread. The orange cells are fixed because they are defined in the Thread standard. Column (b) shows protocols that are used with Ethernet. The blue cells are fixed because they are defined in the Ethernet standard. In the book [BS01] the Bluetooth stack, which does not comply with the OSI model, is correlated with the OSI Layers; this is shown in Column (c).

OSI Layer	(a) **Thread**	(b) **Ethernet**
Application	HTTP	HTTP, FTP, DNS
Presentation	SSL, TLS	SSL, TLS
Session	MQTT, CoAP	PPTP
Transport	UDP (DTLS)	TCP (TLS), UDP (DTLS)
Network	6LoWPAN	IP, ARP, ICMP
Data Link	IEEE 802.15.4	IEEE 802.3
Physical Layer		

(c) **Bluetooth**
Applications
RFCOMM
L2CAP
HCI
Link Manager
Link Controller
Baseband
Radio

2.3.1 IEEE 802.3

IEEE 802.3 is a standard for cable-based networks and has established itself as the most important specification for Local Area Network (LAN) [IEEa]. Carrier Sense Multiple Access (CSMA)/Collison Detection (CD) is used for communication. First, this algorithm listens on the shared transmission medium whether it is free or not. A transmission is only started, if it is available. Nonetheless, if a collision occurs, a retransmission is performed after a random period of time. This process is carried out until the maximum specified trials are exceeded, then an error is returned to the higher layers. For this, a bus or a star topology can be used.

2.3.2 IEEE 802.15.4

The IEEE 802.15.4 [IEE12] standard defines a protocol for Wireless Personal Area Networks (WPAN).

It describes the Physical and Data Link Layer of the OSI model. The main features are low power consumption, low costs, reliability and low latency, which are the main requirements for home automation (e.g. Zigbee) [GYYL09], industrial automation [CTGD09] and smart cities [San14].
As presented in Figure 2.2, the supported topologies are star and peer-to-peer networks. In a star topology the nodes can only communicate with the Personal Area Network (PAN) Coordinator, this limits the overall distance. In a peer-to-peer-network each node can communicate with every other node. There are special nodes that are able to route traffic through the network. Therefore, the overall distance can be increased. The different nodes and their features are listed below:

Full Function Device (FFD): Has full functionality and can perform routing with the help of routing tables, network coordination for one PAN at the most and can send and receive data.

Reduced Function Device (RFD): Is an end device, typically a switch or a sensor. An RFD can only communicate with an FFD. Since it does not perform routing, it can turn off the radio transmission to save power.

PAN Coordinator: Is an FFD that manages the network.

The tasks that are performed by an FFD do not allow that the radio transmission be turned off. Therefore, the power consumption of an FFD node is higher than that of an RFD.

The physical layer defines the operation of IEEE 802.15.4 on the 2.4GHz Industrial, Scientific and Medical (ISM) band. In addition, in some countries there are further frequencies allowed, see Table 2.4 for details. The maximum range between two devices could be 10 to 100 meters [KC14]. The Physical Layer is responsible for the following functions:

- Sending and receiving packages;
- Enabling and disabling the radio transmission;
- Energy Detection (ED), it estimates the power of the received signal so that the Data Link layer can avoid interference;
- Link Quality Indication (LQI);
- Clear Channel Assessment (CCA), it checks whether a channel is available.

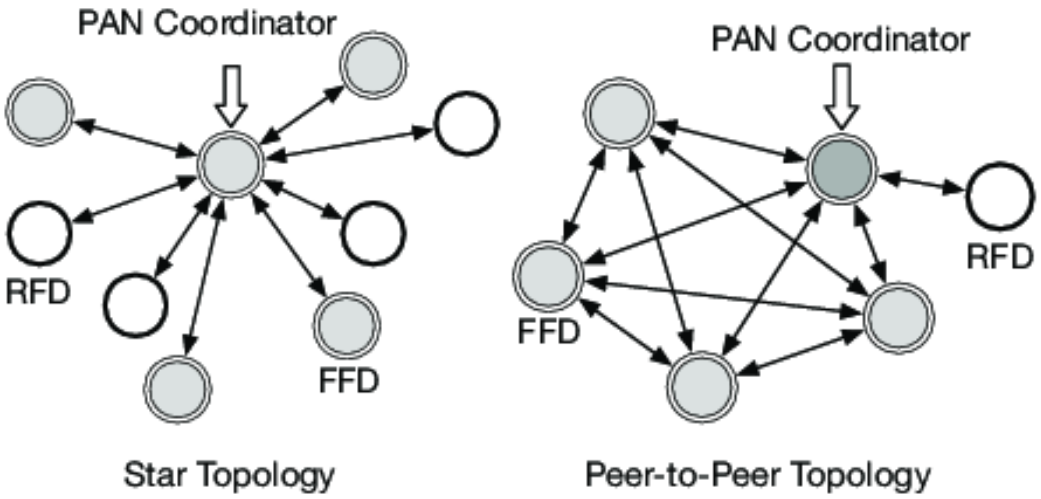

Figure 2.2: Schematic of a star and peer-to-peer network topology supported by the IEEE 802.15.4 standard [ASA+18].

Table 2.4: IEEE 802.15.4 Frequency bands and channel details.

Frequency band [MHz]	868-868.6	902-928	2400
Region	Europe	America	Worldwide
Channels available	1	10	16
Throughput [kbps]	20	40	250

IEEE 802.15.4 uses Direct Sequence Spread Spectrum (DSSS), a spread spectrum modulation technique, which multiplies the data signal with a pseudo-random spreading sequence. Its advantage is the reduction of overall signal interference.

The Data Link Layer controls the access to the channel. To avoid collisions, the CSMA with Collison Avoidance (CA) algorithm is used. This measures the signal strength from the antenna before transmitting and starts sending if the channel is unused. If the channel is used, it waits for a random period of time and retries.
There are two different modes: Beacon Enabled (BE) and Non-Beacon Enabled (NBE).

Beacon Enabled mode: In the BE mode the PAN Coordinator splits the channel into so-called superframes, as illustrated in Figure 2.3. A superframe starts with a beacon that is sent by the PAN Coordinator; the remaining time until the next superframe is sent and is split into an active an inactive period. The active period is divided into 16 time slots, the first time slot is reserved for the beacon. The others contain the Contention Access Period, which is followed by the Contention Free Period. In the Contention Access Period, nodes can send messages with CSMA with CA. In the Contention Free Period, Time Division Multiple Access (TDMA) is used to assign each node to a fixed time slot, which can be used for sending.

Time slots are assigned by the PAN Coordinator; if a node needs a time slot, it has to inform the PAN Coordinator in the Contention Access Period.
The time between two beacons is specified with the Beacon Interval (BI), which is calculated with the Formula 2.3. With the Beacon Order (BO), which can take values between 0 and 14, the duration between two beacons can be configured. The Superframe Duration (SD) specifies the duration of the active superframe period and is calculated with Formula 2.5. Superframe Order (SO) configures the duration of the active period and can take values between 0 and 14, but must be less than or equal to BO. This splits the superframe into an active and inactive period. If SO is 15, then there is no active period after the beacon. The maximum Number of Superframe Slots (NSFS) is 16. The default value for the Base Super Frame Duration (BSFD) is 60μs. The Symbol Period (SP) is defined for 2,4GHz with 16μs. This results in 2,4GHz in a length of a superframe between 15ms and 246s [ASA+18].

$$0 \leq \text{BO} \leq 14 \tag{2.1}$$

$$\alpha = NSFS * BSFD * SP \tag{2.2}$$

$$BI = 2^{BO} * \alpha \tag{2.3}$$

$$0 \leq \text{SO} \leq \text{BO} \leq 14 \tag{2.4}$$

$$SD = 2^{SO} * \alpha \tag{2.5}$$

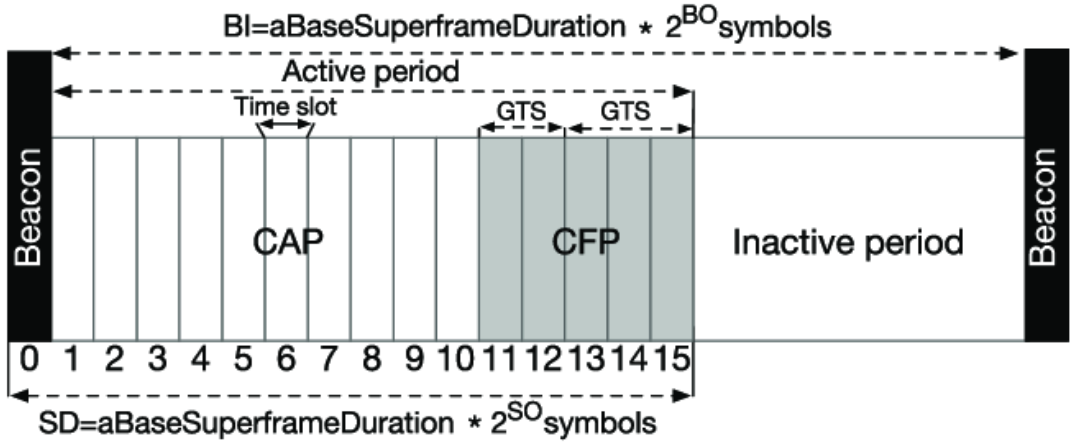

Figure 2.3: The superframe structure of the BE Data Link mode of IEEE 802.15.4 standard [ASA+18].

Non-Beacon Enabled mode: In the NBE mode the node checks before each send with CSMA/CA whether the channel is free. This mode needs no administration by the PAN Coordinator.

2.4 Network Layer

This layer is responsible for switching connections in the case of line-oriented transmission and for forwarding packets in the case of packet-oriented transmission. The network layer contains the routing of packets.

2.4.1 6LoWPAN

6LoWPAN stands for IPv6 over Low power Wireless Personal Area Network and is standardized by IETF. It is designed for networks where Internet Protocol Version 6 (IPv6) support is necessary, but the networks could not fulfill this requirement themselves. The first problem is that the IPv6 header is very large, it has a size of 40 Bytes. As an example, IEEE 802.15.4 has a Maximum Transmission Unit (MTU) of 127 Bytes. If we now subtract 25 Bytes for the Data Link Layer, another 21 Bytes for an optional Advanced Encryption Standard (AES)-Counter with CBC-MAC (CCM) encryption, another 40 Bytes for the IPv6 header and 8 Bytes for User Datagram Protocol (UDP), there are only 33 Bytes left for payload data.
With the header compression of 6LoWPAN, the size needed for the IPv6 and UDP header can be reduced to 7 bytes in the best case [IETc].

The second problem is that IPv6 claims a minimum MTU of 1280 Bytes, but IEEE 802.15.4 supports only a maximum of 127 Bytes. To meet the requirements of IPv6 regarding MTU, the 6LoWPAN Adaption Layer pretends a higher MTU to the upscale OSI layers by fragmentation. It splits the packets and gives them to the Data Link Layer for sending. Received packets are joined and then passed to the upper layer.
Furthermore, 6LoWPAN manages IPv6 routing in mesh networks, normal IP routing is not optimal because nodes can leave and rejoin somewhere else, for example.

2.5 Transport Layer

This layer enables the end-to-end communication. Transmission Control Protocol (TCP) [Staa] and UDP [Stab] are transport protocols, which define the exchange of information between network components. TCP is connection-oriented and UDP is connectionless.

2.6 Session, Presentation and Application Layer

These layers include protocols, which exchange application specific data over the network infrastructure. A communication protocol is an agreement of two or more devices, on how the data is transmitted. Models for this are Client/Server (Request/Response) and Client/Broker (Publish/Subscribe). They are located in the session, presentation or application layers of the OSI model. Hypertext Transfer Protocol (HTTP) is an application layer protocol and is commonly used with TCP. It functions as a Request/Response protocol and is used in the world wide web. Constrained Application Protocol (CoAP) and Message Queuing Telemetry Transport (MQTT) are communication protocols for IoT devices, which are examined in the next sections. Table 2.5 shows a comparison of CoAP, HTTP and MQTT.

2.6.1 HTTP

HTTP is an application layer protocol and is defined by the IETF [IETa]. It uses TCP as default transport protocol and Transport Layer Security (TLS)/Secure Sockets Layer (SSL) for security [Ily13], thus it is a connection-oriented protocol. HTTP uses request and response to handle the exchange of data between client and server. HTTP supports Representational State Transfer (REST), which defines constraints for the style of software architecture. Services that conform to the REST architecture provide interoperability between computer systems. HTTP is predominantly used in the web. CoAP, which inter-operates with HTTP, was developed for IoT networks.

Table 2.5: Comparison of CoAP and MQTT [Nai17].

Criteria	**MQTT**	**CoAP**	**HTTP**
Architecture	Client/Broker	Client/Server or Broker	Client/Server
Abstraction	Publish/Subscribe	Request/Response or Publish/Subscribe	Request/Response
Semantics	Connect, Disconnect, Publish, Subscribe, Unsubscribe, Close	Get, Post, Put, Delete	Get, Post, Head, Put, Patch, Options, Connect, Delete
Standards	OASIS	IETF	IETF and W3C [W3C]
Transport Protocol	TCP	UDP	TCP
Security	TLS/SSL	DTLS, IPSec	TLS/SSL

2.6.2 CoAP

CoAP is defined by the IETF [IETa] in RFC7252 [IETd]. CoAP is a Client/Server protocol and supports Machine-to-Machine (M2M) communication and Multicast. It is located in the session layer of the OSI model. Since CoAP is similar to HTTP, it is possible that a CoAP server communicates with a HTTP client and conversely, to accomplish this, a CoAP to HTTP Proxy is needed. CoAP is based on the REST model. It is designed for low-power and lossy networks as they occur in IoT applications. To accomplish this, the aim of the design was to keep the message overhead as small as possible. CoAP uses UDP, which is less reliable than TCP and therefore easier to manage and with a smaller packet size. A. Paventhan et al. [SPS+12] utilized CoAP for a real-time monitoring agriculture sensor network.

2.6.3 MQTT

MQTT is a publish/subscribe communication protocol developed by Andy Stanford-Clark from International Business Machines (IBM) and Arlen Nipper from Cirrus Link Solutions. Nowadays it is standardized by the Organization for the Advancement of Structured Information Standards (OASIS) [Cop]. MQTT clients can publish their messages to a broker (MQTT server) with a specified topic, which can be subscribed to by other clients. If no client is subscribed to, the message is buffered for future subscriptions [Nai17]. Clients can subscribe to multiple topics. The subscription uses TCP as transport protocol, so the communication between the clients and the broker is connection-oriented. To secure the transmission, TLS or SSL is used. MQTT is suitable for large networks where the nodes need to be monitored by a cloud server. Device-to-device communication and multicast messages are not well-supported [Jaf14].

Table 2.6: Comparison of different Wireless Technologies.

Technology	Range [m]	Data rate [kbps]	Frequency [MHz]	Cellular	Unlicensed band	Reference
Thread	30	250	2400	x	✓	[SKB18], [AGM+15]
WiFi	30-50	300k	2400	x	✓	[SKB18], [AGM+15]
Sigfox	3-50k	0.1	868 (Europe)	x	✓	[PAM17]
LTE-M	up to 15k	375	700-900	✓	x	[PAM17]
NFC	0.01	21-400	13.56	x	✓	[SKB18], [AGM+15]
LoRa	3-15k	0.3-37.5	868, 915	x	✓	[PAM17]
Bluetooth	10-100	800-2100	2400	x	✓	[SKB18], [AGM+15]
Zigbee	10-100	20-200	2400	x	✓	[SKB18], [AGM+15]

2.7 Wireless Technologies for IoT

The wireless technologies for IoT networks should be able to save energy and deal with interferences and loss of transmission. Thread, WiFi, Sigfox, LTE-M, NFC, LoRa, Bluetooth and Zigbee are used for IoT Sensor networks [AGM+15],[SKB18]. Table 2.6 compares these technologies. Thread and Bluetooth will be explained in more detail in the following subsections as these technologies are used in this work.

2.7.1 Thread

Thread is a mesh networking protocol based on IEEE 802.15.4. It is supported by well-known organizations, such as Google, Nest, Samsung, Nordic Semiconductors and Silicon Labs (for the full list of members see [Gro]). The protocol is reliable, has a low latency, is secure and cost-effective. It supports up to 250 devices [ASA+18]. The protocol defines the network and transport layer from the OSI model and consists of the 6LoWPAN protocol and the UDP protocol. Therefore, IPv6 capability is well supported and the devices can directly communicate over the Internet. Thread uses the Distance Vector Algorithm (DVA) to find the shortest path through the network. The complete traffic is secured with the TLS or DTLS. Each device that wants to join a Thread network has to do a discovery scan first, in order to find a Router for commissioning. After that, one of two commissioning methods is used. The first choice is to put the required commissioning information directly onto the device. The second one is to use a smart phone, tablet or the web to acknowledge the joining device.

Figure 2.4 illustrates a typical thread mesh network with all different devices shown. Thread defines Full Thread Devices (FTD) and Minimal Thread Devices (MTD), which correspond to FFD and RFD of IEEE 802.15.4. FTD and MTD can be further split into the following devices:

- **FTD:** Never shuts down radio transmission and therefore has higher power consumption. It subscribes to all the routers' multicast addresses and maintains IPv6 address mapping.
  - **Router:** Routes traffic through the network, on the basis of Internet Protocol (IP) routing tables, which are exchanged between routers. This way, each router knows at any time the amount of hops it takes to get to a specific address. Up to 32 routers can be located in a network.
  - **Router Eligible End Device (REED):** Can be upgraded to a router in order to replace a faulty router, or if the REED is the only node in the vicinity of a new End Device that would want to join the network. Conversely, it can be downgraded to an End Device if it has no children.
  - **Full End Device (FED):** Cannot be upgraded to a router.
  - **Thread Leader:** Is dynamically elected and has to administrate the network, especially the routers.
  - **Border Router:** Is the gateway between the thread network and other Networks, for example the Internet.
- **MTD:** Does not listen on multicast traffic. It only forwards all messages to its parent.
  - **Minimal End Device (MED):** Radio transmission is always on, it does not need to synchronize with its parent to communicate.
  - **Sleepy End Device (SED):** Can shut down the radio transmission to save energy and can therefore only communicate with its parent. If the SED is sleeping, messages that belong to the SED are buffered by the parent.

The device starting the network chooses a 64-bit prefix, which is used for the whole thread network; the IPv6 addressing is defined in RFC4291 [IETb]. Each device that joins the network receives a unique 16-bit address. The high byte in the address specifies the router address and the low byte is a unique random number. The low bytes from the router are set to zero. The scopes in a thread network are illustrated in Figure 2.5.

- Link Local - all devices reachable with one hop
- Mesh Local - all devices in the mesh network
- Global - all devices outside the network

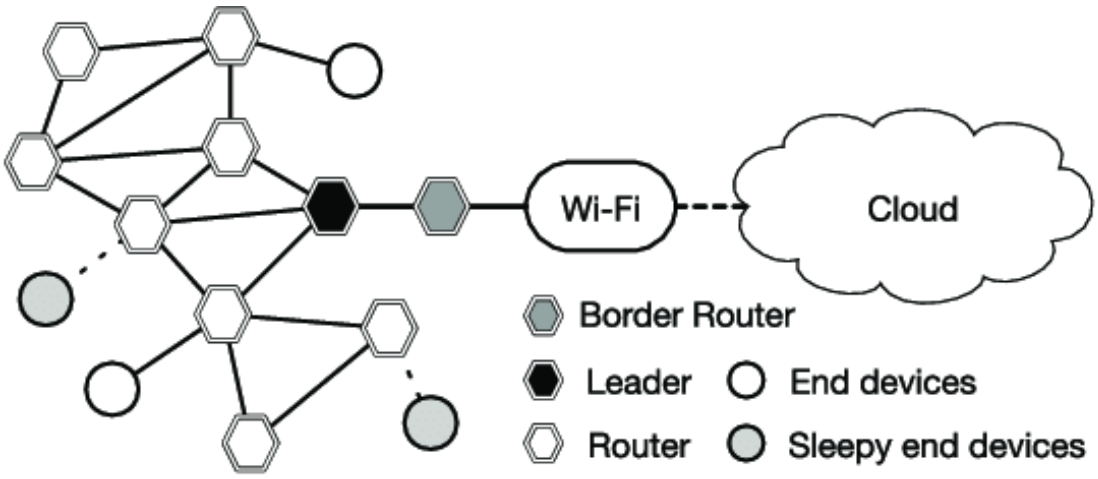

Figure 2.4: The mesh networking architecture of Thread [ASA+18].

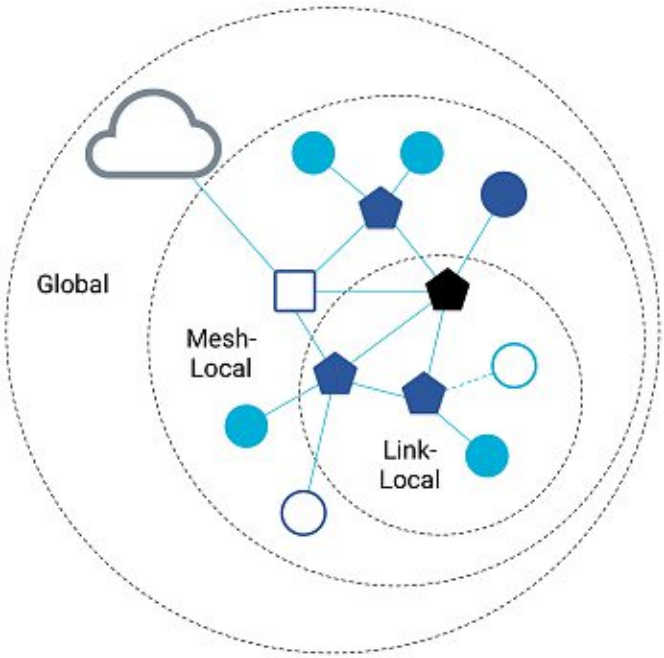

Figure 2.5: Scopes of a Thread network [IETe]

Two open-source implementations of the Thread specification are OpenThread by Google and MbedOS by ARM.

OpenThread

OpenThread [Goo] is an open-source implementation of Thread by Google. It provides a CoAP client and server as well as a Network Coprocessor (NCP).

Most of the SoC producers, for example Nordic Semicondutor or Silicon Labs, integrate OpenThread in their software stacks.

MbedOS

MbedOS [Lim] is an open-source RTOS for IoT devices and is developed by ARM and its technology partners. With the MbedOS, certified by the Thread Group, Thread is fully supported.

2.7.2 Bluetooth

Bluetooth was designed to be a wireless alternative to serial communication (RS232). The lower layers are specified in IEEE 802.15.1. Since the versions 1.1 (IEEE 802.15.1-2002) and 1.2 (IEEE 802.15.2-2005), the Bluetooth standard has evolved independently. The Bluetooth SIG [BLSb] is a consortium of companies that are interested in the development and distribution of Bluetooth. Before a new product with Bluetooth enters the market, the SIG checks it against the standard qualifications. The purpose of these checks and qualifications is to guarantee interoperability and to enforce compliance with the specifications [Gup13]. Physically, Bluetooth operates between 2.4GHz and 2.485GHz, which is in the unlicensed ISM Band and it divides the bandwidth into 79 channels, where each channel has a width of 1 MHz. Bluetooth uses Frequency Hopping Spread Spectrum (FHSS), which switches about 1600 times per second to a random channel, which is only known by the transmitter and the receiver.

In a channel, messages are transmitted by using Gaussian Frequency Shift Keying (GFSK). The Bluetooth stack does not follow the OSI model. Figure 2.6 depicts different standards with their channels and compares them in the 2.4GHz band.

BLE

BLE was introduced in the Bluetooth 4.0 specification. The Bluetooth 4.0 specification allows devices to implement BLE, classic Bluetooth or both. The aim was to reduce power consumption, so the throughput was decreased and the bandwidth was split into 40 channels, where each channel has a width of 2MHz. Due to this, BLE is not downward compatible with the so-called classic Bluetooth. As with classic Bluetooth, GFSK and FHSS are used to transmit data. BLE devices are detected through broadcasting advertising packets. The advertisement channels are presented in Figure 2.6b. A device periodically sends advertising packets on one of these advertisement channels.

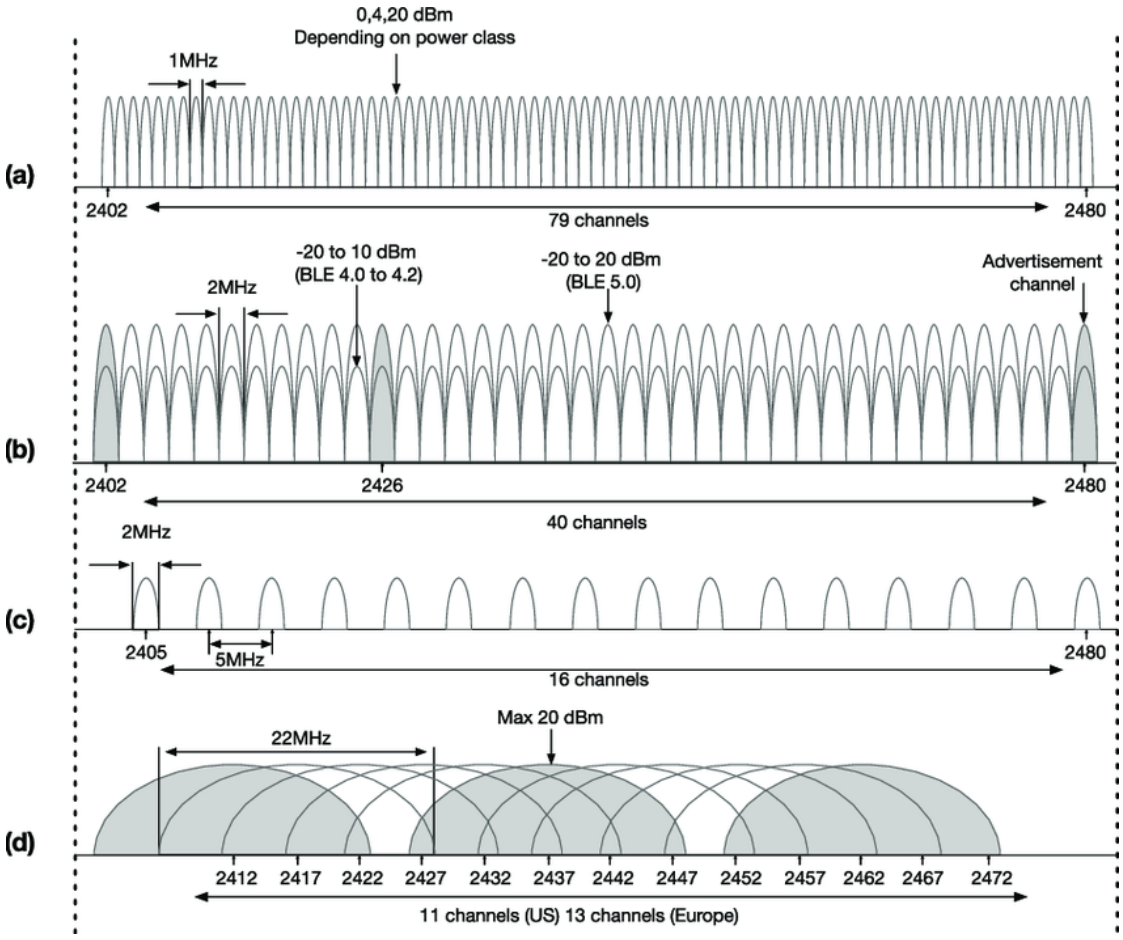

Figure 2.6: BR/EDR (a), BLE (b), IEEE 802.15.4 (c) and IEEE 802.11 (d, WLAN) sharing 2.4GHz frequency band [ASA+18]

2.7.3 Bluetooth Mesh

Bluetooth Mesh is a mesh networking technology based on BLE. It was defined by the Bluetooth SIG in 2014 and revised in 2017. The mesh network capabilities were introduced to increase the range and redundancy. BLE Mesh can be used on all devices with version 4.1 or higher [BLSa]. The components of a BLE mesh network are:

Relay Node: Forwards received messages, a maximum number of 127 hops is allowed.

Proxy Node: Provides an interface between a BLE mesh and BLE devices that have no mesh stack.

Friend Node: Buffers messages for low-power nodes and sends the messages to the nodes when they request it. It consumes more power than the low-power node.

Low-power Node: Since the friend nodes buffer messages for low-power nodes, it can go into a deep sleep mode and reduce the power consumption.

To reduce complexity, flooding is used instead of routing. This means that messages are re-transmitted by the relay nodes, except when the message is already in the cache of the relay node, which means that this message has been recently forwarded.

2.8 Sensors for Microclimate Measurement

In the following part, existing methods and products for measuring microclimate in agricultural applications are presented and reviewed. Different environmental factors are of interest in a microclimate [HRG18]. This thesis focusses on two of them: UV radiation and leaf wetness. State-of-the-art techniques to measure UV radiation and leaf wetness from the year 2019 are studied below. Soil moisture sensors are examined first because there are similarities to the way leaf wetness is measured.

2.8.1 Soil Moisture

A soil moisture sensor measures the proportion of water in the soil. This is an important measurement for research and prediction of climate [MLS12]. A specific application is the control of irrigation based on soil moisture [SBV+19]. Technologies that measure soil moisture are:

TDT and Time Domain Reflectometry (TDR) Time Domain Transmission (TDT) measures the propagation time, which is the time it takes the electromagnetic signal to travel from one end of the line to the other [Wil11]. This can be done in a closed or looped circuit. TDR analyses the reflection of an electromagnetic signal in a line. The value of dielectric permittivity depends on the wetness of the soil and thus changes the propagation behavior of the signal in the line. This allows to draw a conclusion about the soil moisture. It is independent of temperature, texture and salinity. The high price is its disadvantage [JVR+19].

Frequency Domain Reflectometry (FDR) The setup is like the TDR, but this method measures the change in frequency of the transmitted signal. The frequency changes according to the permittivity, which is related to the soil moisture [JVR+19]. The disadvantage is that due to the complex electrical field, a calibration of the sensor is necessary [OBL+15]. The CS616 [Sci], which is illustrated in Figure 2.7, is based on the FDR technique.

Figure 2.7: The CS616 [Sci] is a product from Campbell Scientific and is based on the FDR technique.

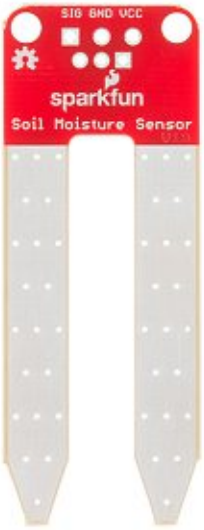

Figure 2.8: Resistor-based soil moisture sensor board from Sparkfun [Elea].

Soil Resistivity This method measures the resistance between two electrodes that are put in the soil. The moister the soil is, the lower the resistance is [CCC51]. The response time and the relatively high level of precision are advantages. Disadvantages are the necessary calibration and the unstableness of it [FJ94]. Sparkfun sells a resistor-based board [Elea], shown in Figure 2.8.

Heidi Mittelbach et al. [MLS12] compare in her journal different soil moisture sensor types and come to the conclusion that low-cost sensors, if they are calibrated, are a good alternative to the expensive TDR sensors.

(a) (b)

Figure 2.9: Schematic of resistor and capacitive measurement method. a) shows the schematic cut through the PCB for the resistor-based measurement and b) for the capacitive-based measurement.

2.8.2 Leaf Wetness

An LWS emulates a leaf, by assuming that the wetness on the sensor is the same as on the leaf. The correct emulation of a leaf depends on various factors, e.g. the color of the sensor [SMG04]. Ghobakhlou et al. compare [GAS15] different sensors and describe two methods to measure the wetness on the emulated leaf. One method is to measure the electrical resistance on a surface on which the Printed Circuit Board (PCB) tracks are not protected by a solder mask as they have to be in direct contact with the water. In case of the second method the PCB tracks are coated with a solder mask and the change in capacitance is measured. The solder mask is an additional protection for the sensor and it does not influence the measurement of the capacitance.

Leaf Resistivity The measuring surface consists of adjacent conductor tracks. These tracks are not protected by a solder mask because the water has to be in direct contact with the copper from the tracks. If moisture hits this surface, the resistance changes because a wet area conducts better than a dry one. A schematic cut through a resistor-based leaf wetness measurement PCB is presented in Figure 2.9a. Products from Campbell [Camb], Davis Instruments [Cor] and Pessl Instruments [Gmbb] are shown in Figure 2.10.

(a) (b) (c)

Figure 2.10: Different resistor-based leaf wetness sensors. a) shows the product from Campbell [Camb], b) shows the product from Davis Instruments [Cor] and c) shows the product from Pessl, which measures the conductance of a filter paper between two stainless electrodes [Gmbb].

Table 2.7: Different values for ϵ_r [VTC17].

Material	ϵ_r
Air	1
Soil mineral	3-7
Water (20°C)	80

Capacitance These sensors measure the change in humidity with the help of the change in capacitance. On the measuring surface there are conductor tracks, which do not have to come into direct contact with water, as it is the case with the resistor-based method. A schematic cut through a capacitive-based leaf wetness measurement PCB is shown in Figure 2.9b. The surface behaves like a capacitor, which is illustrated with C3 in Figure 2.9b. C3 changes according to the wetness of the surface because the relative permittivity (ϵ_r) changes according to the wetness. The respective capacitance is calculated with the Formula 2.6, where A is the area of the plate, d is the distance between the plates and ϵ_0 is the electric constant. Different values of ϵ_r are displayed in Table 2.7. Figure 2.11 shows products from Campbell [Cama], Davis Instruments [Insa] and Adcon [Adca].

$$C = \epsilon_0 * \epsilon_r * \frac{A}{d} \tag{2.6}$$

The changing capacitance is now measured by the time it takes to load the capacitor with a known current.

(a) (b) (c)

Figure 2.11: Different capacitive-based leaf wetness sensors. a) shows the product from Campbell [Cama], b) shows the product from Davis Instruments [Insa] and c) shows the product from Adcon [Adca].

2.8.3 UV Radiation

UV radiation is an electromagnetic radiation. It has too short a wavelength to be seen by humans and is emitted by the sun. Artificial sources are Mercury-vapor lamps, Black light lamps and UV- light emitting diodes [Dif02]. The electromagnetic spectrum of UV is divided into three ranges, UVA, UVB and UVC; the corresponding wavelengths are shown in Table 1.1. UV is measured in watt per square meter. UV can be harmful to humans at certain intensity [LGL+]. Therefore, the World Health Organization (WHO) introduced the UV Index (UVI) for a better handling of the intensity. Plants use photosynthesis to convert light energy into chemical energy [Ann92]. Therefore, UV radiation is important for plant growth, so the measurement is helpful for analyzing plant diseases [Hol02].

The following techniques are available to measure the UV value [Her13]:

Change in Temperature (Bolometer)

A Bolometer consists of a temperature-dependent electrical resistance, an absorptive element and a thermal reservoir. Radiation on the absorptive element causes a change in temperature, which can be measured with the help of the associated change in resistance. Bolometers have a response time of milliseconds [Dif13].

External Photoelectric Effect

The emission of electrons from the metal surface, when it is irradiated with radiation, is called external photoelectric effect. The Photomultiplier uses this effect and tubes to measure radiation [HP07].

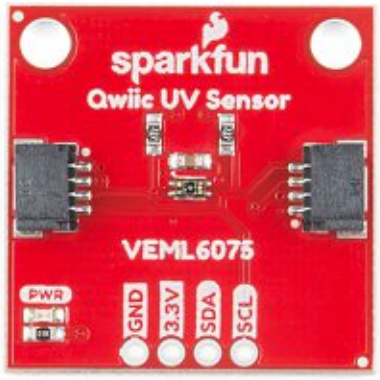

Figure 2.12: Break out board for the VEML6075 by Sparkfun [Eleb].

Internal Photoelectric Effect

The internal photoelectric effect does not emit electrons like the external one. If the metal surface is irradiated with radiation, it excites electrons to higher bands, namely from the valence band to the conduction band. This results in a photo current on the p-n junction or p-i-n junction. This effect is used in Photoresistors, Photodiodes, Phototransistors and Charge-coupled Device (CCD)/Complementary metal-oxide-semiconductor (CMOS) detectors [Her13].

In IoT development, UV sensors can be bought on break out boards for evaluation purposes. Two examples are the VEML6075 break out board from Sparkfun and the Sensor-Puck from Silicon Labs. Sparkfun offers a break out board [Eleb] that contains all the necessary components for the VEML6075 to function correctly and also header pins for connection. The board is displayed in Figure 2.12. The VEML6075 measures UVA and UVB with photo diodes. The communication is managed by Inter-Integrated Circuit (I^2C), which is a two-wire serial data bus. Silicon Labs Sensor-Puck [Labc] is an environmental and biometric sensor board, which measures UV light with the Si1114x optical sensor with the help of photo diodes. The Sensor-Puck is shown in Figure 2.13. It also includes a humidity and temperature sensor. The board can be supplied by a coin cell battery. The EFM32 microcontroller is responsible for the collection and transmission of measurement data via Bluetooth.

Figure 2.13: Sensor Puck from Silicon Labs [Labc].

2.9 Concepts for Microclimate In-Field Measurement

In the case of in-field measurement, data is collected by sensors that are scattered across the field. Each node consists of one or more sensors and one or more communication units. The following sections shortly describe the available products.

2.9.1 VitiMeteo Plasmopara

VitiMeteo Plasmopara is a computer-aided model that calculates the life cycle of the Plasmopara viticola, which is a disease of the grapevine that can cause significant economic damage [BKK+08]. The model *VitiMeteo Wachstum* is used to calculate leaf growth. It uses temperature, rain retention, relative humidity and leaf wetting data from weather stations placed in the vineyards. It supports stations from Adcon, Davis Instruments and Meteos, which are presented in the next sections.

Figure 2.14: Adcon Weather Station [Adcb]. a) is the main part called ADCON RTU.

2.9.2 Adcon

Adcon is a company with headquarters in Klosterneuburg, Austria. It offers sensors for temperature, relative humidity, rain gauge, soil moisture, leaf wetness, wind direction and wind speed [Adcb]. The main part of the weather station is the ADCON RTU shown in Figure 2.14a). It is responsible for storing the data, the battery management and for the transmission of data via radio. Supported radio technologies are Global System for Mobile Communications (GSM), General Packet Radio Service (GPRS), Universal Mobile Telecommunications System (UMTS). Data can also be transmitted via Ultra-High-Frequency (UHF) signals. With the latest version, which is the series 6, Bluetooth can also be used to transmit data or to update the firmware.

2.9.3 Metos

Metos is a company from Weiz, Austria. It offers sensors to measure leaf wetness, rain gauge, soil moisture and leaf temperature. Data is transmitted wirelessly via Long Range Wide Area Network (LoRaWAN), GPRS, Enhanced Data Rates for GSM Evolution (Edge), UMTS or WiFi in a range of about 300 to 400 meters in a star topology. Data can also be transmitted over wire with Recommended Standard 232 (RS232). The measurements are stored on a cloud server. Figure 2.15 depicts the iMetos *imt300*, which contains sensors to measure temperature, humidity, rain gauge, soil moisture, leaf wetness, wind direction and wind speed.

Figure 2.15: Metos Weather Station *imt300* [Gmba].

2.9.4 Davis

Davis is a California-based company that sells products for reliable weather monitoring. They offer weather stations for private, agriculture and safety-related measurements such as windstorms and tsunamis. Their product portfolio contains all kinds of sensors for environment measurement. The EnviroMonitor [Insb] is a self-healing, reliable mesh network of environmental sensor nodes. Figure 2.16 shows an overview of the proposed solution. The EnviroMonitor Gateway can collect data from up to 25 nodes. Depending on the environmental conditions, the distance between nodes can be up to 1200 meters. Each node can connect up to 4 different sensors. The data is transmitted in the mesh network on a license-free band, e.g. in Europe 868.0 - 868.6MHz. The nodes are peered with the gateway and configured via Bluetooth. The gateway sends the data through the cellular network, e.g. Second generation mobile network (2G) or Third generation mobile network (3G), to the Davis cloud server that is connected to the Internet. A standalone weather station, which is additionally sold by Davis, e.g. the GroWeather (illustrated in Figure 2.16), can also be connected by a wire to the gateway. Nodes and gateways are powered by a battery that is recharged with a solar panel. The gateway's battery is a 6V gel cell battery with 12Ah of capacity. It consumes about 25mA up to 1A. This way, the gateway can run for a minimum of 12h and a maximum of 20 days without charging. The node is powered by four D-cells or one lithium-ion battery (3,6V - 3,7V and about 3000mAh) and typically consumes 12mA. This way, the node can run for 5 days without charging. The company suggests using a 3W solar panel for charging. If the battery voltage is getting too low, the customer will be notified by email or a push message in the mobile app.

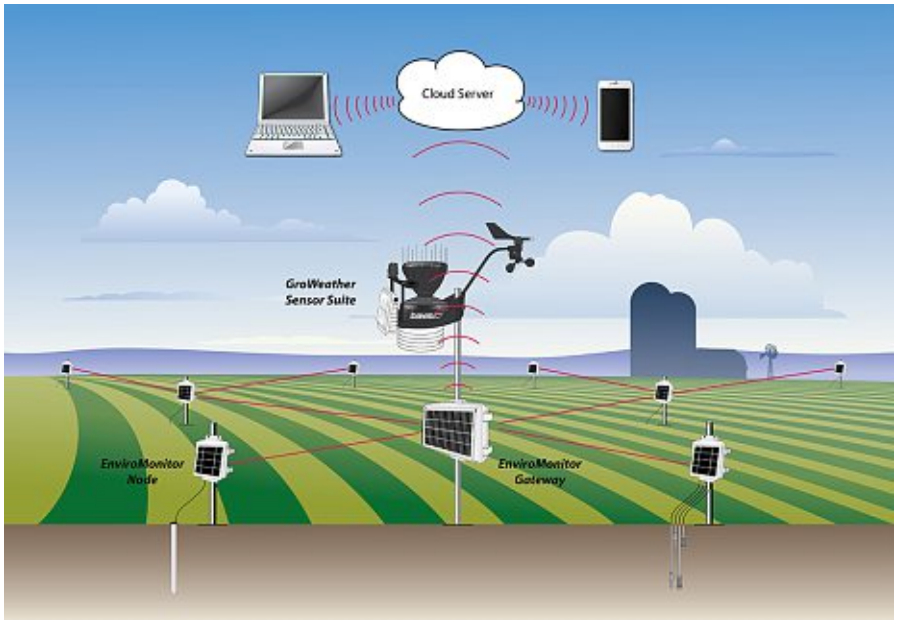

Figure 2.16: Schematic structure of the EnviroMonitor mesh network [Insb].

Table 2.8: Costs of the Davis Instruments EnviroMonitor [Insb].

Type	**one-off costs[$]**	**annual costs for 15-minute interval[$]**
Gateway	795	220
Node	395	30
Sum	**1180**	**250**

In the manual the producer claims a runtime of multiple years under optimal conditions. Problems could arise if the solar panel is shaded (by vegetation, snow or dirt) or if it is turned away from the sun. The price of an EnviroMonitor Node is $395 and that of the gateway is $795. For an update interval of 15 minutes, the yearly cost for the gateway is $220 and for one node it is $30. This means that the customer gets new data every 15 minutes; the storage is supplied by Davis Instruments. In Table 2.8 the overall costs for one year with prices as per October 2019 are listed.

2.9.5 Libelium

Libelium is a Spanish company that offers different solutions for IoT. It has two main product lines. One is based on a development board called Waspmote, which is a hardware board with various built-in features for IoT devices. The second line is the Waspmote Plug & Sense, which is a commercial product containing the Waspmote board with different sensors connected to it.

(a) (b) (c)

Figure 2.17: Waspmote and Waspmote Addons [Lib]. a) shows the hardware board Waspmote, b) shows the Waspmote 802.15.4 radio board, and c) shows the Waspmote Agriculture Sensor board, with different sensors.

Waspmote The hardware board shown in Figure 2.17a contains an ATmega1281 microcontroller and interfaces to connect different sensors and radio boards. The supported radio technologies are 802.15.4 (radio board shown in Figure 2.17b), LoRaWAN, WiFi, Fourth generation mobile network (4G) and Bluetooth. The company offers open-source Software Development Kits (SDKs) and Application-Programming-Interfaces (APIs). They support peer-to-peer, star and mesh topologies. For the mesh topology, DigiMesh [Inca] with its own radio board is used. Sensor boards are available for different use cases, e.g. for agriculture measurements, gas measurement, flood protection and smart parking [Lib]. The Waspmote consumes 17mA while active, whereas the power consumption decreases to 7μA in hibernate mode. Supported battery voltages range from 3.3V to 4.2V. The battery is charged with a solar panel or Universal Serial Bus (USB). The Waspmote hardware board with the 802.15.4 radio board costs about €240 and a sensor about €75.

(a) (b)

Figure 2.18: Ready-to-use products from Libelium [Lib]. a) shows the Waspmote Plug & Sense and b) shows the Meshlium 4.0.

Waspmote Plug & Sense The Waspmote Plug & Sense is a ready-to-use product and comes with an IP65 waterproof enclosure, which is depicted in Figure 2.18a. External devices, such as sensor probes, batteries, solar panels or USBs can be plugged in easily. Inside, the Waspmote and the radio board are installed, depending on the technology used.

Meshlium The Meshlium, presented in Figure 2.18b, is a gateway from the sensor network to the Internet. It receives data from the sensor nodes over different radio technologies and sends it over a cellular connection to a cloud server connected to the Internet. Specification:

- CPU: 1GHz
- RAM: 2GB
- SSD: 16GB
- OS: Linux, based on kernel 3.16
- Consumption: 15W, but it heavily depends on the number of activated radios

2.10 Microclimate Measurement With Satellites

Earth Observation Satellites (EOS) are obtaining information about the earth's surface. They operate in an altitude of about 36000km. The satellite data can be used to assess the canopy surface (e.g. detect the presence of weeds) or the canopy structure (e.g. measure crop height), and it can also help in decision making (by e.g. predicting yields) [ahd19]. Mark Jarman describes in his reviews [ahd19] available satellite technologies for agricultural applications. He also gives an overview of the usability of some products.

Two companies offering analysis of satellite or drone images to farmers are Descartes-Labs and FarmShots. DescartesLabs [Labb] offers the recognition of valuable data from satellite images. Their methodology is to construct models of real-world processes that are fed with relevant input (e.g. satellite imagery). FarmShots [Sho] offers the analysis of satellite and drone images.

CHAPTER 3

Requirements and Design Decision

This chapter focuses on the hardware and software requirements that are necessary to build a sensor network for agricultural microclimate measurement. Based on these specifications and the state of the art, which was looked at in the previous chapter, we will decide on the design later on.

3.1 Hardware Requirements

In this section the hardware requirements for the sensor nodes are defined. These devices are installed outdoors to measure the microclimate and should be as flexible as possible. In order to achieve this, the following features must be considered:

- **Outdoor Usage** Since the aim is to measure the agricultural microclimate, the sensor nodes have to be placed in the fields, vineyards or orchard. Therefore, they have to be constructed to be able to tackle different environmental conditions (e.g. heat, cold, humidity) without suffering damages.
- **Size** The nodes should fit into trees and walls of grapevine leaves. The leaf wetness sensor area should imitate the size of a half-grown leaf. We took the leaf of the *Grüner Veltliner* as a reference, which is about 7x7cm in size [Bau08]. The remaining part of the sensor must not exceed 10x10cm, otherwise it could influence the foliage growth.
- **Easy Installation** Since a swarm consist of many sensors, the mounting and setup should be easy and fast. Due to necessary mechanical work steps, such as vine cutting, it may be necessary to demount some sensors annually. The process should not take more than 10 minutes for a sensor.

- **Extension** After the initial configuration of the network, it should also be possible to add new sensor nodes.
- **Self-Sufficiency** The sensor nodes should be energetically self-sufficient. This means that the sensors generate the energy they require by themselves as best as possible.
- **Price** The currently available products, which were already presented in Chapter 2, are in no case available for less than €1100 per node. In order to enable smaller farms to buy a sensor network, we tried to keep the price below that of the already existing products. This means that the price of ten sensors and one relay node should not exceed €1100.
- **Different Power Sources** It should be possible to supply the device with different power sources, e.g. USB, Solar, Battery, power supply.
- **Battery Power** For the periods of time where no sunlight is available, the battery may provide the energy for the sensor. We assume that no sunlight is available for at least 12 hours on any given day. This means that the battery must be able to supply power for at least 12 hours. The aim is to provide more capacity than needed. The gateway itself can be connected to the power grid and therefore does not need a battery.
- **Solar** It is one of the available power sources to load the battery and power the system. The solar panel should minimize the need to change batteries. The size of the solar panel should be dimensioned so that it can fully charge the battery during one day. Attention should also be paid to the solar radiation of the test region that is located in Austria, in the state of Lower Austria, in the region called "Kremstal".
- **Wireless Connectivity** It should be used to transmit the data to the gateway and further to the Internet, without the need of installing wires. This way, the adaption and setup of a wireless sensor network takes less time than in the case of a wired one. The sensors should therefore use a wireless connection, on the other hand the gateway can be connected with a cable to the Internet. The disadvantages are the higher power consumption of wireless sending and the susceptibility to interferences [YKX+17].

3.2 Software Requirements

In this section the software requirements for the sensor nodes are defined.

- **Mesh Network** In order to transmit the measurement data to a cloud server connected to the Internet via a gateway, a reliable and self-healing network is necessary. As discussed in 2.1 a mesh network is the best choice for this purpose.
- **State Of Charge (SOC)** The battery voltage should be monitored for optimizing the energy consumption and for sending an alert if the battery is low.
- **Extension** It has to be possible to add new sensor nodes to the network.

3.3 Measurement Requirements

In this section we specify the requirements for the values to be measured. The following main criteria must be taken into account:

- **UV** It is essential for photosynthesis and UV measurement also helps in the analysis of plant diseases [Hol02]. UVC is blocked by the ozone layer and is not important for our measurement [SSS+06]. The sensor should thus measure UVA and UVB.
- **Leaf Wetness** The Leaf Wetness Duration (LWD) is an important variable for disease-development and disease-warning systems [Mon13]. Therefore, the leaf wetness should be measured.
- **Vicinity** The sensor should be installed near the target objects, otherwise the measurement results could be falsified. For example, if a leaf casts a shadow over a sensor, the leaf is in a different "environmental state" than the sensor that should imitate it.
- **Synchronization** It is important that the sensors record measured values at about the same time, to enable a comparison of the data. The reference to the global time is then established via the node, which has an Internet connection.
- **Frequency** The interval for taking a measurement should be adjustable according to the type of value that should be processed, the location (e.g. vineyard or orchard) and the available storage space in the sensor.

3.4 Comparison

In the following section we compare the existing solutions, which were presented in Chapter 2. All the products are suitable for outdoor usage, have wireless connectivity and optimized power consumption, are battery-powered and extensible with new sensors. All the nodes can be programmed Over The Air (OTA).

Table 3.1: Comparison of existing solutions.

Properties	Waspmote	Waspmote Plug&Sense	Adcon	Metos	Davis
Leaf Wetness Sensor	✓	✓	✓	✓	✓
UV Sensor	UVA and UVB	UVA and UVB	UVA	UVA and UVB	UVA
Mesh capabilities	✓	✓	×	×	✓
Size without sensors	73.5 x 51 mm	85 x 122 mm	160 x 60 mm	410 x 130 mm	210 x 280 mm
Price gateway [€]	1500	1500	not needed	not needed	about 795
Price node [€]	240	1025	1700	about 3000	about 395
Var. price node [€]	75 per sensor	34 per sensor	4G, 10GB about 10 monthly	4G, 10GB about 10 monthly	250 monthly for one node
Supported protocols	802.15.4, LoRaWAN, WiFi, 4G, BLE	802.15.4, LoRaWAN, WiFi, 4G, BLE	2G/3G or 4G/LTE	GSM, GPRS, EDGE, HSDPA, CDMA, UMTS, Satellit, WiFi, LoRa	GSM, UMTS
Open Source	not all	not all	×	×	×

3.5 Design Decision

Adcon and Metos are not able to build a mesh network, they only support mobile cellular networks. Therefore, each node comes with monthly costs for a Subscriber Identity Module (SIM) card to get a cellular connection. Since the aim is to place more than 10 sensors in one field, this is not an economical solution. Furthermore, the costs of the Adcon and Metos sensors exceed the previously defined budget.
Davis Instruments supports mesh networks with their own closed software on a license-free band. The price for the gateway is high (about €795), but we would need only one, so it is affordable. But the high costs of buying one node and the additional monthly costs for every node to store the data on their servers exceed the previously defined budget.
The Waspmote Plug&Sense would be the best solution for our needs, but the costs also exceed the previously defined budget. The Waspmote would be a good starting point to develop further sensors. Unfortunately, it has a lot of extensions that we don't need but cannot be deselected at purchase either. So this option also exceeds our previously defined budget.
Based on the literature survey and the analysis of existing solutions, we decide to develop our own board. It will only contain the mesh functionality and we will be able to use it as a model for further sensors in IoT applications. In the next chapter we compare and select the components for the sensors and also choose a transmission technique.

CHAPTER 4

System Design

In this chapter we list and compare possible solutions and products - that we build from self-developed hardware and software - that can fulfill the specific requirements. After this, we select the appropriate components based on the requirements, product research and the literature survey.

4.1 LWS

An LWS measures the moisture on a leaf by imitating it. The requirements for the LWS are robustness, reliability and longevity. Therefore, we choose the capacitive measurement method, which was discussed earlier in Section 2.8.2. The goal is to develop a board with high sensitivity to measure leaf wetness. To do this, three boards with different PCB layouts should be designed; Figure 4.1 provides an illustration. We will compare the boards in Chapter 7. Each of these boards changes its capacity relative to the moisture on the surface to be measured. We are not interested in measuring the exact capacity in Farad, but in getting a value related to the wetness, e.g. 0 indicates not wet and 100 means wet. Three ways to measure the change in capacity are:

Difference Method A capacitor is unloaded and the voltage is measured at two different known time points [Dja19]. With Equation 4.1 we can calculate the value of the capacitance. In Figure 4.2a the circuit and in Figure 4.2b the discharge curve is illustrated. This method is mainly used in multimeters.

$$C = \frac{t_2 - t_1}{R * ln(\frac{U_1}{U_2})} \tag{4.1}$$

(a) (b) (c)

Figure 4.1: Different conductor thicknesses to test the moisture sensitivity. a) shows the wetness area with large tracks, b) shows the wetness area with medium tracks and c) shows the wetness area with small tracks.

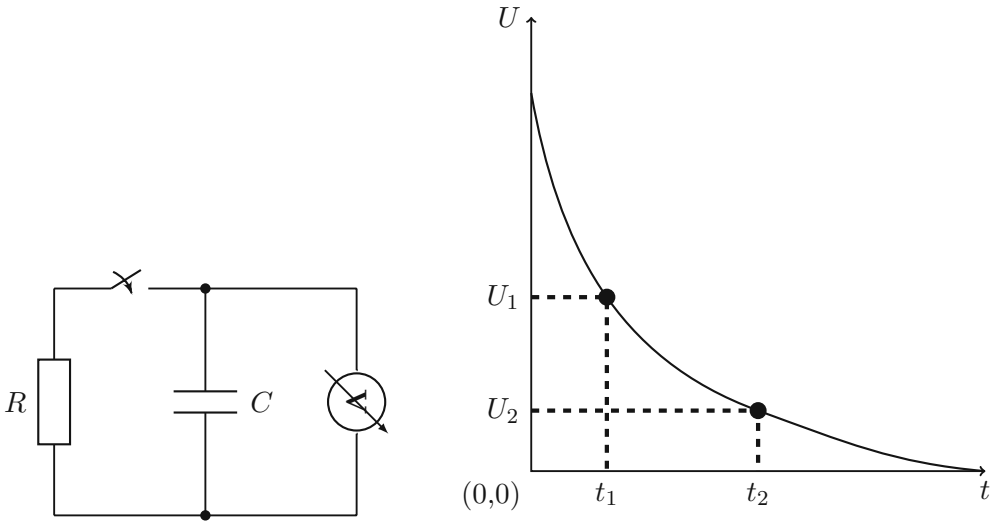

(a) Discharge circuit. (b) Discharge curve.

Figure 4.2: Capacitance measurement with the difference method.

Capacitive to Digital Converter A Capacitive to Digital Converter (CDC) is an Integrated Circuit (IC) that measures the capacitance and is mainly used in touch-screens, humidity sensing or liquid level sensing devices and pressure measurement [Nin12]. For example, the AD7746 [Dev], schematically shown in Figure 4.3, measures the capacitance with switching capacitor technology. It contains a known and fixed excitation voltage, reference voltage and an internal reference capacitance. The converted value from the Sigma-Delta modulator represents the ratio between the sensed capacitance and the reference capacitance. Different CDCs are compared in Table 4.1.

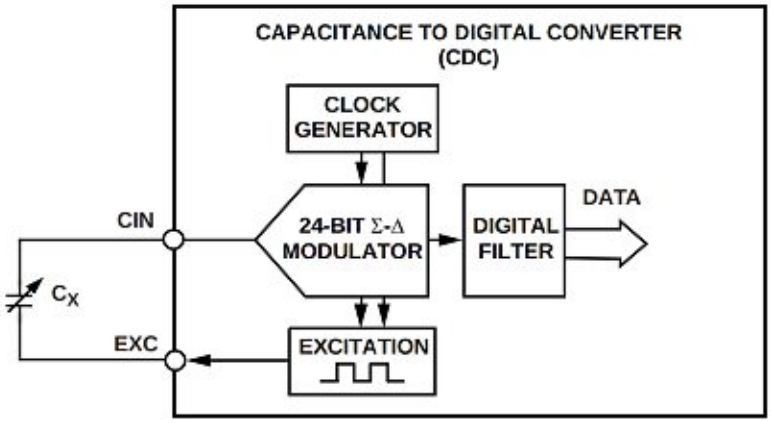

Figure 4.3: CDC Simplified Block Diagram of the Analog Devices AD7746 [Dev].

Table 4.1: Comparison of CDC.

	Price [€] (09/2019)	Size [mm]	Accuracy [fF]	Range [pF]	Supply Voltage [V]
AD7746	12	5 x 6	4	±4	2.7 - 5.25
FDC1004	5	3 x 3	0.5	±15	3.3
LC717A00AJ	1.96	8 x 6.4	0.04	±8	2.6 - 5.5

Capacitance Measurement Using Low Pass Filter With the help of a low pass filter, the change in capacitance can be measured [RSPAM19]. A low pass filter passes signals with frequencies lower than the cutoff frequency (e.g. $f1_{3db}$ in Figure 4.4) and weakens signals with higher frequencies. This is illustrated in the Bode diagram 4.4. The cutoff frequency can be calculated with Equation 4.3. A circuit for a first order low pass filter consists of a resistor and a capacitor. This is illustrated in Figure 4.5.

$$G = 20 \log \frac{U_{out}}{U_{in}} \tag{4.2}$$

$$f_{3dB} = \frac{1}{2\pi RC} \tag{4.3}$$

From Equation 4.3 we can see that if the capacitance C changes, the cutoff frequency changes. If we feed our input U_{in} with a rectangular signal with a fixed frequency f_{in} (e.g. 1MHz), the output voltage is weakened according to the capacitance. This behavior is illustrated in Figure 4.6, in the time domain for a 1nF (C_1) and a 3nF (C_2) capacity. These values were taken based on a measurement from a capacitance sensor in wet (C_2) and dry (C_1) states. The resistor was set to 330Ω. The input voltage was set to 3.2V because this will be the supply voltage. The voltage curve over the time when the capacitor is charging can be calculated with Equation 4.4, the discharging can be calculated with Equation 4.5.

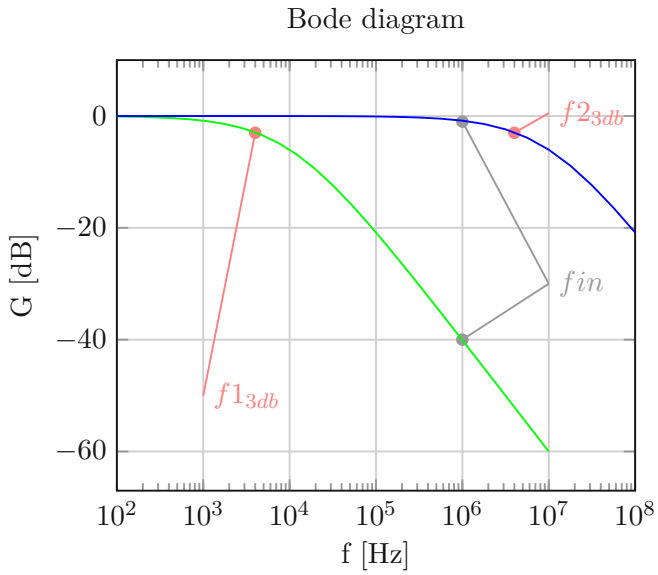

Figure 4.4: Bode diagram of a first order low pass filter. The green line with cutoff frequency ($f1_{3db}$) shows the damping of the input signal with a big capacitance and the blue line ($f2_{3db}$) for a smaller one. The frequency of the input signal is 1MHz (f_{in}).

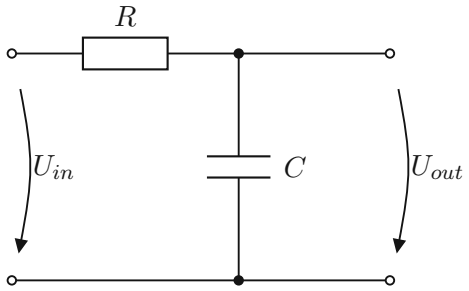

Figure 4.5: Low pass filter circuit.

Figure 4.4 shows the Bode diagram of this behavior, where f_{in} is fixed at 1MHz. The green line illustrates the damping of the input signal with a big capacitance and the blue line for a smaller one. For the high capacitance (wet area) and for the small capacitance (dry area), the input signal is damped by -20dB per decade.

$$u_c(t) = U_0 * (1 - e^{\frac{-t}{R*C}}) \tag{4.4}$$

$$u_c(t) = U_0 * e^{\frac{-t}{R*C}} \tag{4.5}$$

We are choosing the capacitance measurement using a low pass filter because the component, consisting of a resistor and a capacitor, cost €0.2 at Mouser in 2019 and this price is lower than that of a CDC.

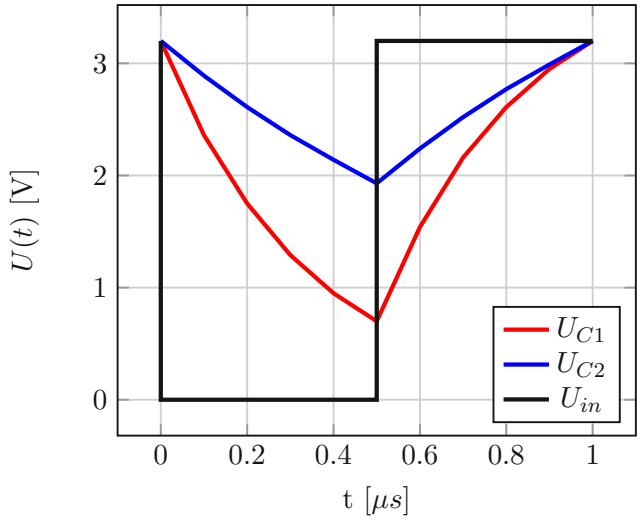

Figure 4.6: Capacitor charging and discharging curves in steady state. C_1=1nF (dry leaf) and C_2=3nF (wet leaf)

Table 4.2: Comparison of UV sensor ICs

Product	Price [€] (09/2019)	Size [mm]	Range [nm]	I^2C	Supply Voltage [V]
Si1133	1.48	2 x 2	280-400 (only UV-Index)	✓	1.62 - 3.6
VEML6070	2.36	2.35 x 1.8	320-400	✓	1.7 - 5.5
VEML6075	2.7 (End of life)	8 x 6.4	280-400	✓	1.7 - 3.6
AS7341	8.24	3.1 x 2	350 - 1000	✓	1.8

4.2 UV Sensor

The UV sensor should measure UVA (320-400nm) and UVB (280-320nm). In Table 4.2 different UV Sensors are compared. Unfortunately, the Si1133 does not directly measure UV, it only performs UV Index approximation based on the light level. The VEML6070 and VEML6075 have a light sensor to measure the UV spectrum. The VEML6075 would be the best choice because it measures UVA and UVB, but it is an end-of-life product. The VEML6070 measures only UVA. The AS7341 does not measure the full UVA spectrum. So we are choosing the VEML6070.

Table 4.3: Comparison of Bluetooth Mesh and Thread Mesh network [MLPP16].

Properties	Bluetooth Mesh	Thread
Routing techniques	Flooding	Routing and flooding
Amount of connected nodes	Low	High
Range	Low	Low
6LoWPAN support	✓	✓

4.3 Data Transmission

In the following section we examine different possibilities to transmit data from the sensor nodes to the cloud. These data transmission opportunities can be implemented without changing the hardware, only the software needs to be adapted accordingly. Figure 4.7 depicts the schematic design of the transmission network and its layers. In the first region, the sensor nodes are connected with a mesh network, this is called the sensor swarm. Based on Table 4.3, we choose Thread as protocol for the mesh network because of the lower power consumption of the routing technique [MRC+17], which is one of our discussed requirements in Section 3.1. Each node forwards received messages that do not belong to themselves to all other reachable nodes with the flooding technique. The routing technology determines the routes of the messages in advance. This is done with the help of routing tables. In the fog layer, data is collected from the mesh network over some gateway and is then forwarded to the cloud. The fog layer contains devices that can communicate with the mesh network and have an Internet connection, e.g. a smartphone, a quadrocopter or a Raspberry Pi. Since smartphones [SWA13] and the Raspberry Pi [Upt19] have Bluetooth built in, this is used to communicate with devices in the mesh network. The sensors that operate as a gateway and that are called relay nodes need to implement Thread and Bluetooth. The Internet connection can be established via cable or the cellular network. Nodes in the fog layer have higher computation power and more storage. Therefore, they can set actions based on the data. In the cloud region the data is stored on a cloud server connected to the Internet.

Figure 4.8 illustrates different transmission possibilities. They will be implemented in Chapter 6 and compared in Chapter 7.

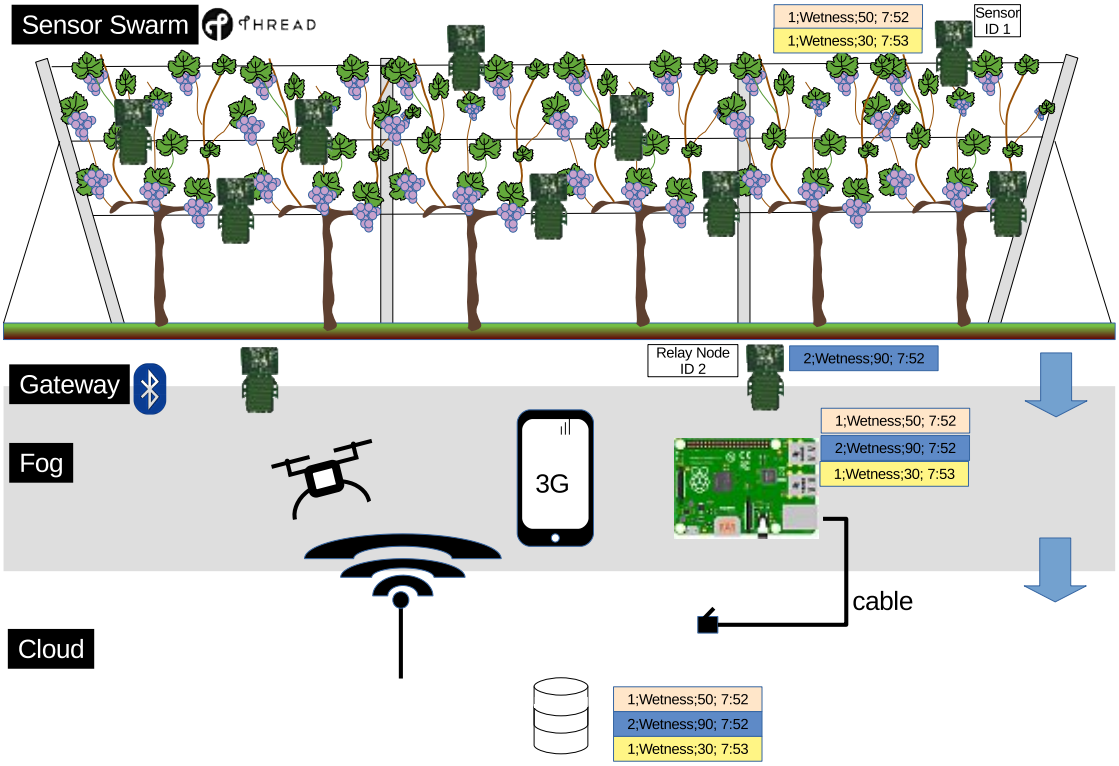

Figure 4.7: Schematic design of the sensor network.

- In variant 4.8a, called *Forward Only Method*, messages are sent periodically by each sensor. The relay node forwards these messages immediately to a connected fog node. If no fog node is available, the message is lost. On the one hand this is the disadvantage of this variant, on the other hand an advantage is that no buffer is needed.

- In variant 4.8b, called *Relay Buffered Method*, messages are sent periodically by each sensor. The relay node buffers the data until a data request from the fog node arrives. After that, it forwards all buffered data to the fog node and clears the buffer. Response technique is used as communication protocol. The disadvantage is that the buffer of the relay node is related to the number of sensors in the network. Therefore, the number of sensors in the network cannot be increased without considering the remaining free buffer space of the relay node. The advantage is that the fog node does not have to be connected to the network all the time.

- In variant 4.8c, called *Fog Request Method*, each sensor buffers the measured data until a data request from the relay node arrives. After that, each notified sensor sends its data to the relay, which then forwards it to the fog node. Response technique is used as communication protocol. The disadvantage is that each sensor needs a buffer to store the sensor values and a time synchronization. The advantage is that if a sensor loses the connection to the network, the measurement values do not get lost because they are stored locally.

The *Relay Buffered Method* and the *Fog Request Method* are based on the request and response technique, which is not supported by MQTT (see Table 2.5). Therefore, CoAP is used as communication protocol.

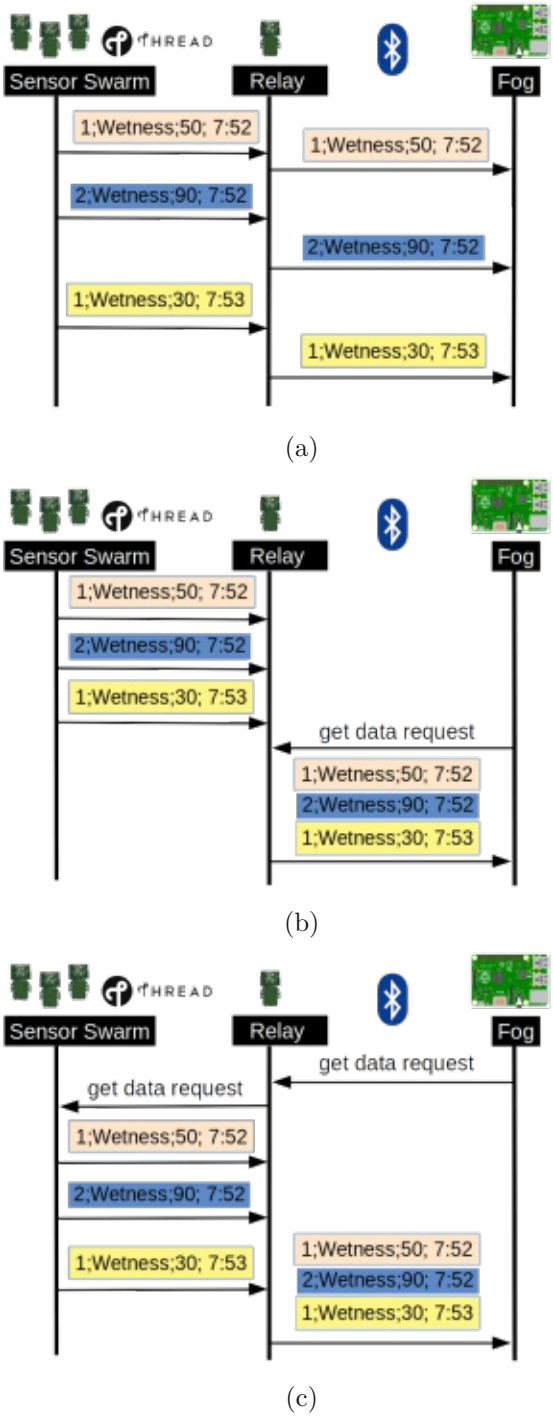

Figure 4.8: Different transmission possibilities. a) shows the *Forward Only Method*, b) shows the *Relay Buffered Method* and c) shows the *Fog Request Method*. The semicolon-separated list illustrates the following data: "ID of the sensor; Type of Measurement; Value; Time"

Table 4.4: Comparison of data storage consumption. The abbreviation for the pick-up interval is PUI, MI stands for measurement interval, NS means number of sensors and SD stands for size of data. PUI and MI are measured in seconds and SD in bytes.

Variants	Sensor Swarm [Byte]	Relay node [Byte]
Forward Only Method	0	0
Relay Buffered Method	0	$\frac{PUI}{MI} * SD * NS$
Fog Request Method	$\frac{PUI}{MI} * SD$	0

4.3.1 Data Storage

Since the available storage on the sensor nodes is limited, we have to calculate the needs and optimize the data collection in that way. We assume that the fog node (e.g. a Raspberry Pi) has unlimited storage. In the *Forward Only Method*, 4.8a, the sensor and relay node only need a buffer to store the measurement temporarily until it is transmitted to the fog node. In the *Relay Buffered Method*, 4.8b, the sensor needs a buffer to temporarily store the measurements until they are transmitted to the relay node. The relay needs a buffer to store the measurement values from all sensors until the fog node collects it. In the *Fog Request Method*, 4.8c, each sensor stores the data until it is collected from the relay node. The relay only needs a buffer to temporarily store the measurement values until they are transmitted to the fog node. Table 4.4 presents a comparison of these methods. The abbreviation for the pick-up interval is PUI, MI stands for measurement interval, NS means number of sensors and SD stands for size of data. PUI and MI are measured in seconds and SD in bytes. The leaf wetness can take values between 0 and 100 units. Therefore, it is stored in a variable with a size of one byte, which can have a maximum value of 255. The UV value, according to the data sheet of the VEML6070 [Sem19], has the size of two bytes. Two bytes are required to store the time of the measurement. This way, it is possible to store 45 days with a minute resolution and 18 hours with a second resolution. These two bytes are needed for the leaf wetness and the UV measurement values if they have different recording times. In total, 5 bytes of memory are required for the data, which corresponds to the variable SD. Table 4.5 displays the results when we collect the data every week, set the number of sensors to ten and the measurement interval to one minute.

Table 4.5: Comparison of data storage. Data storage (SD) is set to 5 bytes. The pick-up interval (PUI) is set to one week. The measurement interval (MI) is set to one minute and the number of sensors (NS) is set to ten.

Variants	Sensor Swarm [Byte]	Relay node [Byte]
Forward Only Method	0	0
Relay Buffered Method	0	$\frac{7*24*60*60}{60} * 5 * 10 = 504k$
Fog Request Method	$\frac{7*24*60*60}{60} * 5 = 50.4k$	0

4.4 System on Chip

A SoC is a chip that contains different ICs for different functionalities. A SoC can contain a processor, a voltage regulator and different interfaces and components for storage (Flash or Random Access Memory (RAM)). The SoC is the main part of the sensor board and has to fulfill the following requirements:

- **Support BLE and 802.15.4** The hardware needs to support BLE and 802.15.4, this is necessary for the wireless transmission of the data.
- **Serial Peripheral Interface (SPI) and I^2C** Necessary for the on-board communication with other ICs.
- **Analog to Digital Converter (ADC)** Necessary for converting the analog capacitive leaf wetness value to a digital value.
- **Minimum Flash** As calculated in Table 4.5, the minimum free flash storage on a relay node has to be 504kB and on a sensor node 50.4kB.
- **Bluetooth Stack** A Bluetooth stack is software that implements the Bluetooth protocol. If a Bluetooth stack is already provided by the SoC producer, the development of the transmission software takes less time because the Bluetooth stack does not have to be implemented.
- **Thread Stack** A Thread stack is software that implements the Thread protocol. If a Thread stack is already provided by the SoC producer, the development of the transmission software takes less time because the Thread stack does not have to be implemented.

Table 4.6: Comparison of SoCs.

Producer	Silicon Labs	Nordic Semiconductor	Texas Instruments	ON Semiconductor
Part number	**EFR32MG12**	**nRF52840**	**CC1352P**	**NCS36510**
MCU Core	ARM Cortex M4	ARM Cortex M4F	ARM Cortex M4F	ARM Cortex M3
Frequency [MHz]	40	64	48	32
Flash [kB]	1024	1024	256	640
RAM [kB]	256	256	80	48
Thread	✓	✓	✓	✓
BLE	✓	✓	✓	×
GPIO Pins	65	48	18	26
Package Type	BGA125	AQFN-72	VQFN48	QFN-40
Energy consumption TX [mA] at 0dBm	8.5	4.8	7	7
Price (Mouser 10/2019) [€]	10.36	5.45	9.32	5.63

Table 4.6 compares SoCs from Silicon Labs, Nordic Semiconductors, ON Semiconductors and Texas Instruments. They all have I^2C, SPI, Pulse Width Modulation (PWM) and an ADC. Based on Table 4.6 and the requirements, the nRF52840 is the best choice for our project. The NCS36510 does not support Bluetooth and BLE and therefore it does not fulfill the transmission requirements for a relay node. The EFR32MG12 and the CC1352P would also work well. However, the nRF52840 has a greater flash and a lower price. So we decide to use the nRF52840.

4.5 Power Management

The power management is responsible that the system has always enough energy. To ensure this, a solar panel and a battery are installed on the device. Furthermore, USB can be used as an optional third source. If USB is connected, this is the preferred choice for the power source as it provides reliable power. Unlike the solar panel, which depends on sunlight. If a power source is connected, disconnected or exceeds the configured maximum or minimum voltage, a seamless switch to another power source should take place. Before comparing possible components for the power management, facts for later decision making are presented.

Thermistor Thermistor is used to measures the temperature based on the resistance change. It is needed to monitor the temperature of the battery during charging because cold and hot batteries should not be charged fast [Ins18].

Voltage Proportional Current Control (VPCC)/Voltage Input Dynamic Power Management (VINDPM) It is a feature that regulates the consumed current by the voltage. If, for example, a battery charger consumes too much current from a source, the voltage drops and the consumed current is reduced. The voltage threshold is component-dependent and is either set to a fixed value or can be configured with I^2C or a voltage divider.

Dynamic Power Path Management (DPPM) Manages and controls the flow of the current based on the voltage. If the input voltage drops under a defined threshold, the charging of the battery is throttled; if the voltage drops further, the charging is stopped and the battery is used to power the system. This is all done seamlessly so that the output is powered continuously.

Dynamic Power Management (DPM) Regulates the input voltage or the input current against a threshold by modifying the current consumption. It is more efficient than using DPPM and the system voltage is always constant. But a voltage drop called brownout could crash the system.

Maximum Power Point Tracking (MPPT) Describes the way to get the maximum power out of a solar cell. It is illustrated by a black line in Figure 4.11. The maximum power from a source is obtained when the product of current and voltage is at its maximum. This is the case when the internal resistance of the source is equal to the load resistance. This operating point is commonly called Maximum Power Point (MPP) [PRSBR17].

Power Multiplexer Switches between input sources. The switch should be seamless so that the system is continuously powered all the time. Our aim is to make sure that the power Multiplexer (mux) switches to the most reliable input source and prevents damage through timely switching in the event of voltage peaks.

4.5.1 Circuits for Power Management

In the following sections, three possible power management designs are examined. The circuit that suits our needs best is then selected.

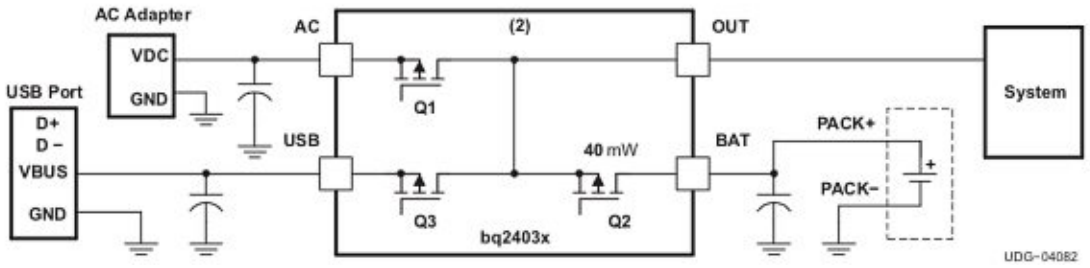

Figure 4.9: Schematic of the BQ2403x dual input charger IC from Texas Instruments [Ins14].

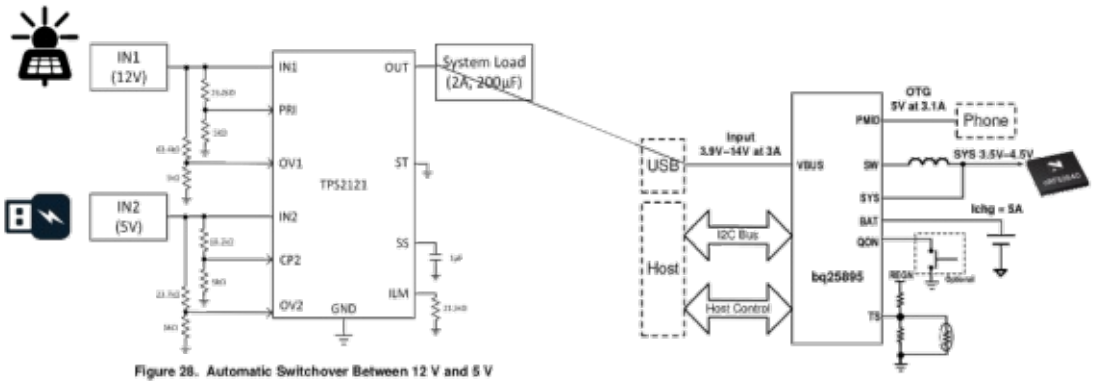

Figure 4.10: Schematic of the power mux TPS2121 connected to the battery charger BQ25895. Both components are from Texas Instruments.

Variant 1: Dual Input Charger IC

A dual input charger IC manages two inputs to load the battery and to power the system at the output pin. It uses Power Path Management (PPM) and predefined thresholds to choose one of two inputs. The schematic of the BQ2403x, which is a dual input charger IC from Texas Instruments, is shown in Figure 4.9. Table 4.7 compares the components available on the market. None of these ICs have dual input or MPPT. But they all have DPPM.

Variant 2: Power Mux With a Single Input Charger IC

In this design a power mux switches one of two inputs to the battery charger IC. Figure 4.10 shows the schematic. The battery charger IC needs only one input. Table 4.7 lists available products on the market. They all have DPPM and a Negative Temperature Coefficient (NTC). Table 4.8 lists different power muxes.

Table 4.7: Comparison of single and dual input charger ICs.

Products	Components	Price [€]	Size [mm]	VPCC [V]	MPPT	Inputs
BQ25895	8	2.85	4.8 x 4.8	3.9 - 15.3	×	1
FAN54063	8	2.5	2 x 2	3.5 - 4.5	×	1
LTC4162	15	8,57	4 x 5	4.2 - 4.6	✓	1
MAX77818	11	5.08	3.6 x 3.6	4.3 - 4.5	×	1
BQ24032	8	3.66	3.5 x 4.5	2.6 - 5	×	2
BQ24161	10	3.7	2.8 x 2.8	4.2 - 4.7	×	2
LTC4155	9	6	4 x 5	4.3	×	2
FAN54511	9	4	4 x 5	-	×	2

Table 4.8: Comparison of power muxes available on the market.

Products	Components	Price [€]	Size [mm]	Operation Range [V]
TPS2121	6	1.81	1.5 x 1.9	2.8 - 22
FPF3042	5	1	1.96 x 1.76	4 - 12.4
LTC4412	5	1.4	1.5 x 2.9	2.5 - 28

Variant 3: Single Input Charger IC

Here we only need the battery charger, the switching between battery and the input value is performed by a Metal Oxide Semiconductor Field Effect Transistor (MOSFET). The cable from the solar panel is connected with a Direct Current (DC) jack to the board. If a solar panel is plugged into the DC jack, the second input source is mechanically disconnected by it. As soon as an input voltage is applied, the system is supplied with its power and the battery is charged. We can use the MCP73871 or one of the previously described single input charger ICs as battery charger.

4.5.2 Design Decision

The problem with the dual input variant is that no product supports a solar cell very well. Figure 4.11 illustrates the origin of this problem. If we follow the orange line (marked with 1) from the right, we see that at 0.5V the current rises. At roughly 0.45V we have the MPP with 36mA and at about 0.4V the maximum current, which is 38mA, is reached. As soon as more than 38mA of current is drawn, the orange line for the voltage goes towards 0V. If a battery charger does not consider this voltage drop, it will abort the loading and continue it at a later time. This results in a non-stop charge and is therefore less efficient than charging continuously at constant current. Therefore, we need a VPCC to regulate the current consumption. The blue line in Figure 4.11 shows the MPPT.

The curves in Figure 4.11 are for one diode, where the consumption is 0.5V, due to the p-n junction. To get a higher voltage, the diodes can be put in series. The different lines indicate how strong the illumination of the sun is. For example, the orange line (marked with 1) at 38mA has the most illumination.

The BQ24032 has VPCC, but the voltage is limited to 5V, which is too low because a solar cell could have its MPPT at higher voltages, depending on the solar cells connected in series.

The power mux and the single input charger IC variant do not have to deal with this problem because both use the single input charger ICs for loading, which supports VPCC with higher voltages. The advantages of the variant with the power mux over the single input charger IC are low component costs, the over-voltage protection and the automatic switch to another input. Therefore, we will choose this variant. We use the BQ25895 as a charger IC because of its high VPCC voltage. The LTC4162, which has MPPT, would also meet our requirements, but is three times more expensive than the BQ25895.

To compensate for the lost efficiency due to not using MPPT, we use a larger solar panel. Since solar panels are available only in standard sizes, we can not order one which fits exactly our calculation. Therefore, we take the next bigger standardized panel.

4.5.3 Approximate Power Consumption

In this section, the power consumption is calculated as an approximate value. This value is needed to roughly calculate the size of the battery and the solar panel. First, we take the current consumption of the nRF52840. The values in Table 4.9 were obtained from the data sheet. The ADC is used to convert the measured analog leaf wetness value to a digital value. The watchdog monitors the digital system to detect malfunctions. If a failure is detected, the watchdog can reset the system. The radio has to be in receiving mode the whole time, otherwise the mesh network loses its function and messages can get lost. Sleepy end devices could turn off the radio and therefore need less current, but we are dimensioning the devices for the worst case, which is when the radio is powered all the time.

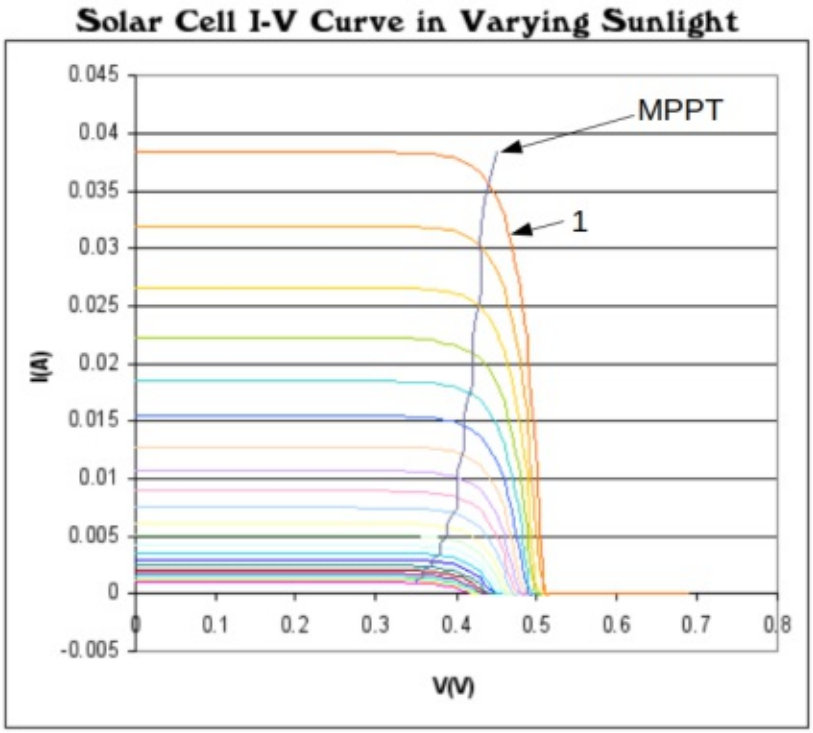

Figure 4.11: Solar Cell IV curve with MPP [Com06].

Table 4.9: Current consumption of nRF52840 [Sem16].

Radio receiving	6.53mA
ADC active	1.24mA
Watchdog active	3.1μA
Sum	7.77 mA

The current consumption of the BQ25895, if the battery is discharging, i.e. there is no voltage on VBUS, is 12μA. If the battery is charging, the BQ25895 consumes 3mA. The TPS2121 consumes 300μA if one of the two inputs power the output. If none of the inputs are connected, the TPS2121 is on standby and consumes 15μA. For the overall consumption in battery mode, we add the values as shown in Table 4.10. We get an overall current consumption of 7.9mA, which tells us that we can operate our sensor for about 5 days, with a 1,1Ah battery. This fits our requirement, which we defined in Section 3.

Table 4.10: Overall current consumption, in battery mode.

NRF52840	7.77mA
BQ25895	$12\mu A$
TPS2121	$15\mu A$
VEML6070	$100\mu A$
Sum	7.9mA

Table 4.11: Comparison of rechargeable batteries [Mor12].

Type	Specific Energy [Wh/kg]	Recharge Cycles	Life [years]	Self-Discharge Rate per month	Price per Wh [€] (09/2019)
Lead-Acid	35-50	250-1000	5	up to 20%	0.19
Nickel-Iron	50-60	2000	20	up to 40%	0.9
Nickel-Cadmium	30-60	1000 to 50k	10-15	up to 15 %	2
Nickel-Metal-Hydride	60-80	300-600	2-5	up to 25%	1.25
Lithium-Ion	80-180	3000	5+	up to 10%	0.9

4.5.4 Batteries

Batteries convert chemical energy to electrical energy. The battery for the sensor board should store the produced surplus of the solar panel for times when solar energy cannot be used. Therefore, it should be rechargeable, have a high lifetime, low self-discharge, low price per Watt hour (Wh) and low weight. The rounded-up power consumption from Table 4.10 is 8mA. For 24 hours a minimum battery capacity of 192mAh is needed. Morris [Mor12] compares the different batteries. All batteries relevant for the sensor device are summarized in Table 4.11. We defined in Chapter 3 a portable and small sensor, so we need a light-weight battery. The Lithium-Ion is the best choice. It is cheap and has the lowest self-discharge rate. The battery has to be charged only once a day, so the maximum number of recharge cycles will be reached in about 8 years. A recharge cycle indicates how many times the battery can be fully charged and discharged [Dav10].

4.5.5 Solar Panel Dimensioning

The solar panel is dimensioned in a way so it can produce the energy that is needed to power the system for 24 hours (192mAh) in about one hour, under full sunglight. We made this assumption because not each day is fully cloudless. To calculate the necessary size of the solar panel, we first have to look at the Photovoltaic (PV) power potential map, shown in Figure 4.12, at the location where the sensors will be placed. This location is marked by a cross. In this region we have an average annual sum of $1000kWh/m^2$ and this means we have an average of $114Wh/m^2$ per hour. The efficiency rate of affordable solar panels is approximately 18% [Laba]. If we multiply the power per square meter with the efficiency rate of a solar panel ($114Wh/m^2 * 0.18$), we get a consumable energy of $20.52Wh/m^2$. We need about 710mWh to power the system with a 3.7V battery voltage ($192mAh * 3,7V$). The size of the panel is $0.035m^2$, this value we get by dividing the power by the existing solar radiation per square meter ($\frac{710mWh}{20.52Wh/m^2}$). And this corresponds to a size of about 20 x 20 cm, which has a price of about 70€ (09/2019).

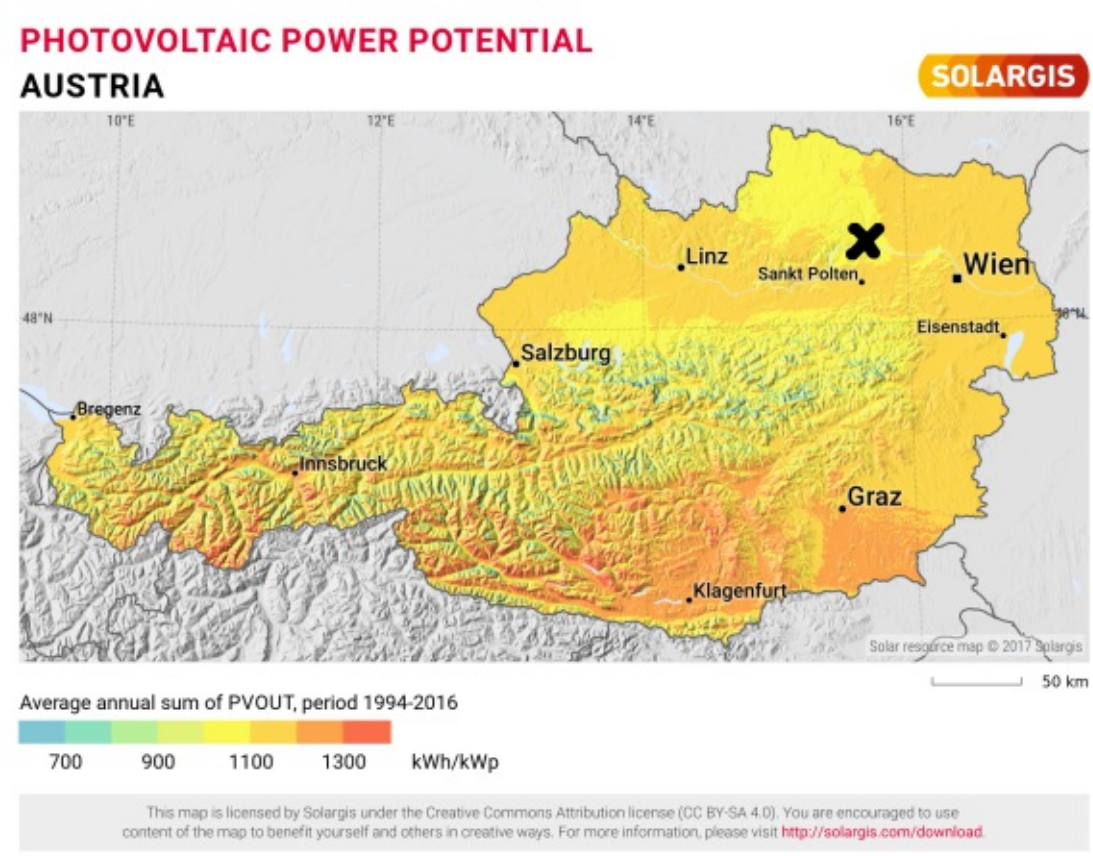

Figure 4.12: Photovoltaic power potential in Austria [Sol].

Table 4.12: Comparison of different antenna types [Aud08a].

Antenna Types	Pros	Cons
PCB antenna	• Low cost • Good performance is possible • Small size	• Difficult to design • Potentially larger size at low frequencies
Chip antenna	• Small size	• Medium performance • Medium cost
Whip antenna	• Good performance	• High cost • Large size

4.6 2.4 GHz Antenna

The antenna is responsible for transmitting messages wirelessly. We can use a Surface Mounted Device (SMD) antenna, a whip antenna or a PCB antenna. The SMD antenna is a chip that includes the antenna. The whip antenna is an external antenna and is connected with a SubMiniature version A (SMA) connector [Sol18]. In the PCB variant the antenna is printed onto the PCB [Aud08b]. Andersen compares these antenna types in his paper [Aud08a], his results are presented in Table 4.12. Based on this, we are choosing the PCB antenna because of its low cost, good performance and small size.

Our further design decisions are:

- Capacitance measurement with a low pass filter to measure leaf wetness
- VEML6070 for UV measurement
- BQ25895 as charger IC for power management
- TPS2121 as power mux
- PCB antenna to provide wireless connection to the sensor network

CHAPTER 5

Hardware Implementation

This chapter describes the hardware design. First, a schematic for each circuit part of the board is designed. In this schematic the components are wired according to the datasheets. After that, the PCB layout is created. In this layout the components are placed on the board and wires are routed. We used the open-source program KiCad [KiC] for making the schematic and designing the PCB.

5.1 nRF52840 SoC Circuit

The nRF52840 is produced by Nordic Semiconductor and is used as a computation unit. The programming is done with the help of the Serial Wire Debug (SWD) interface. The wiring is done as described in the datasheet [Sem16]. The nRF52840 uses an external 32MHz crystal and provides several clock signals. The internal RC oscillator or an external crystal oscillator can be used as low-frequency clock source (32.768kHz). The low frequency could also be synthesized from the higher clock source. We are using an external crystal oscillator, due to its higher accuracy [Sem16].

5.2 2.4 GHz Antenna

In section 4.6 we have decided to choose the PCB antenna. Now we are able to design our own antenna, which is only possible with good simulation tools and a spectrum analyzer. Or we could choose a freely provided design that has already been tested and optimized. Texas Instruments is providing such a design and we decided to use it [Aud08b]. In the reference design a copper thickness of 35μm and FR4 substrate are used. Figure 5.1 illustrates the antenna dimensions and Table 5.1 lists the antenna dimensions.

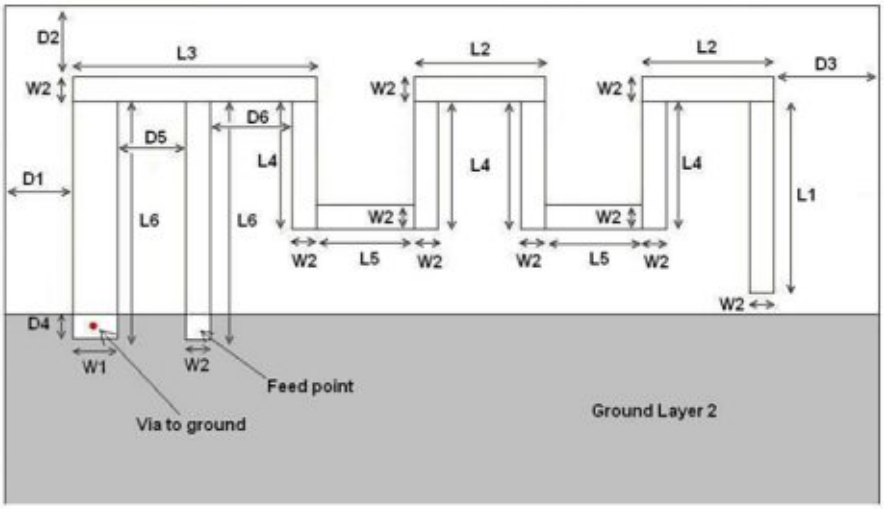

Figure 5.1: Antenna dimensions [Aud08b].

Table 5.1: Antenna dimensions [Aud08b].

Type	Length [mm]
L1	3.94
L2	2.7
L3	5.0
L4	2.64
L5	2.0
L6	4.9
W1	0.9
W2	0.5
D1	0.5
D2	0.3
D3	0.3
D4	0.5
D5	1.4
D6	1.7

The nRF52840 has a single-ended antenna output, which means that the Balanced Unbalanced Network (BALUN) is already on the chip. As shown in Figure 5.2, a matching network between the antenna and the RF pin is needed. It is necessary to match the antenna impedance to 50Ω [Sem16].

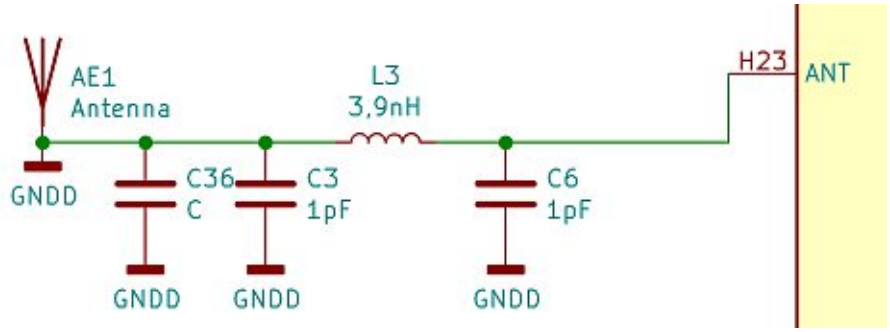

Figure 5.2: Matching network of the antenna.

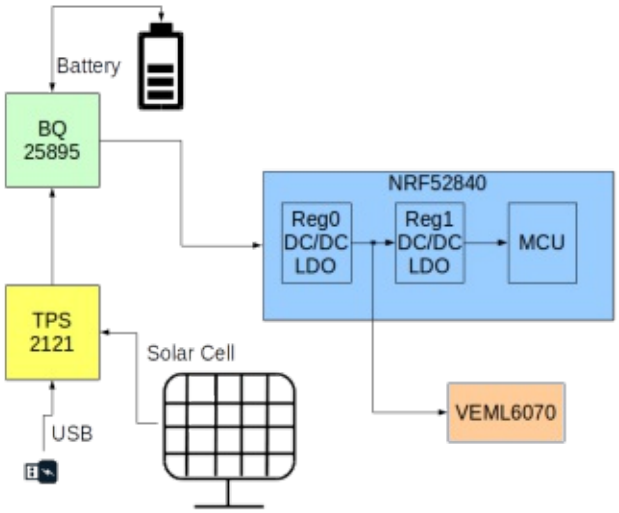

Figure 5.3: Schematic power flow.

5.3 Power Management

In the following section the implementation of the power management is studied. Figure 5.3 illustrates the schematic power flow. The nRF52840 has two stages. In the first stage we can choose between a Buck regulator (DC/DC) or a Low Dropout Regulator (LDO) by setting the register Reg0. After the first stage, up to 25mA can be drawn for external devices, in our case, e.g. for the VEML6070. In the second stage we have to choose between a DC/DC or a LDO by setting the register Reg1. The DC/DC consumes less power than the LDO, but it needs an external LC filter, which consist of two components (inductor and capacitor). We are choosing the DC/DC for both stages, therefore we need 4 external components.

5.3.1 Power Mux

Figure 5.4 shows the schematic of TPS2121 power mux [Ins19]. It is configured in the way that IN1 is preferred over IN2. IN1 can be connected to a USB port. IN2 is connected to a solar panel. To accomplish this, we have to short the CP2 pin and connect a voltage divider to the PR1 pin. The values for the resistors illustrated in Figure 5.5a are calculated with Equation 5.1. The internal reference voltage V_{PR1} is 1.06V. The voltage of IN1 (V_{IN1}) is set to 3.22V, so this input is preferred when the voltage is higher. The optimal value for R_2 is 5kΩ and for R_1 it is 10.2kΩ.

$$V_{PR1} = V_{IN1} * \frac{R_2}{R_1 + R_2} \tag{5.1}$$

The TPS2121 has an over-voltage protection, which can be configured by external resistors. If the voltage exceeds 14V, the input source is switched from IN1 to IN2. To make sure that this happens, we have chosen resistors that could handle that. Figure 5.5b illustrates the chosen voltage divider. To find the correct values for the resistors, we use Equation 5.2 and set V_{IN1} to 14V and V_{OV1} to 1.06V, which is the internal reference voltage. The resistors that fit best and are deliverable are 63.4kΩ for R_3 and 5kΩ for R_4. We go through these same steps with the over-voltage protection on the second input source.

$$V_{OV1} = V_{IN1} * \frac{R_4}{R_4 + R_3} \tag{5.2}$$

According to the datasheet [Ins19] with the resistor R5, the input current limit can be configured. With Equation 5.3 we get a resistor value of 21.5kΩ for an input limit of 4.5A.

$$I_{LM} = \frac{71.5}{R_{ILM}^{0.9}} \tag{5.3}$$

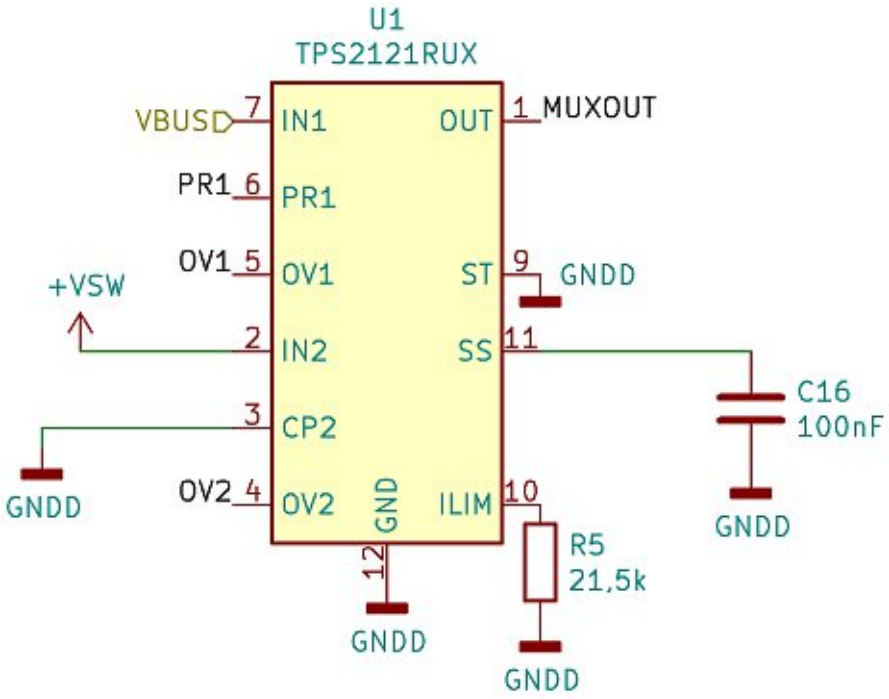

Figure 5.4: Schematic of the TPS2121 power mux.

5.3.2 Battery Charger

The BQ25895 by Texas Instruments is an I^{2}C-controlled single-cell battery charger [Ins18], its schematic is shown in Figure 5.6. The wiring was performed by the components specified in the datasheet. On the open drain *STAT* pin, a LED is connected to display the state of charging; it is switched off if no charging process takes place. SCL and SDA are for the I^{2}C communication, the SCL pin is needed for the timing signal and the SDA pin is for the data. With this the configuration and information exchange between the nRF52840 and the battery charger is done. The *OTG* pin is set to ground because the boost mode is not necessary. The *ILIM* pin is disabled because the configuration is done by I^{2}C.

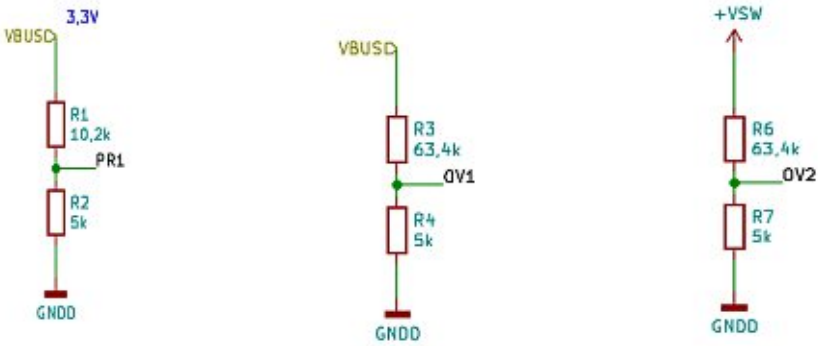

(a) (b) (c)

Figure 5.5: Configuration of TPS2121. a) shows the voltage divider for the input source priority, b) shows the voltage divider for the over voltage protection on VIN1 and c) shows the voltage divider for the over voltage protection on VIN2.

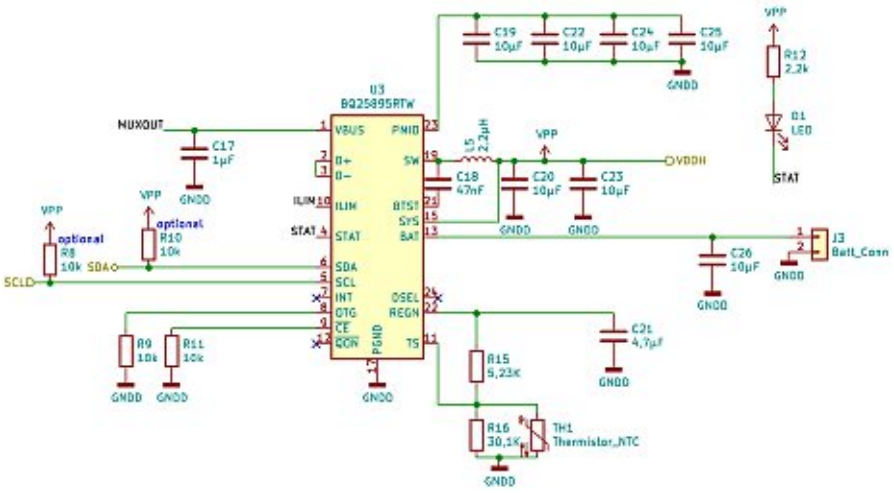

Figure 5.6: Schematic of the BQ25895 battery charger.

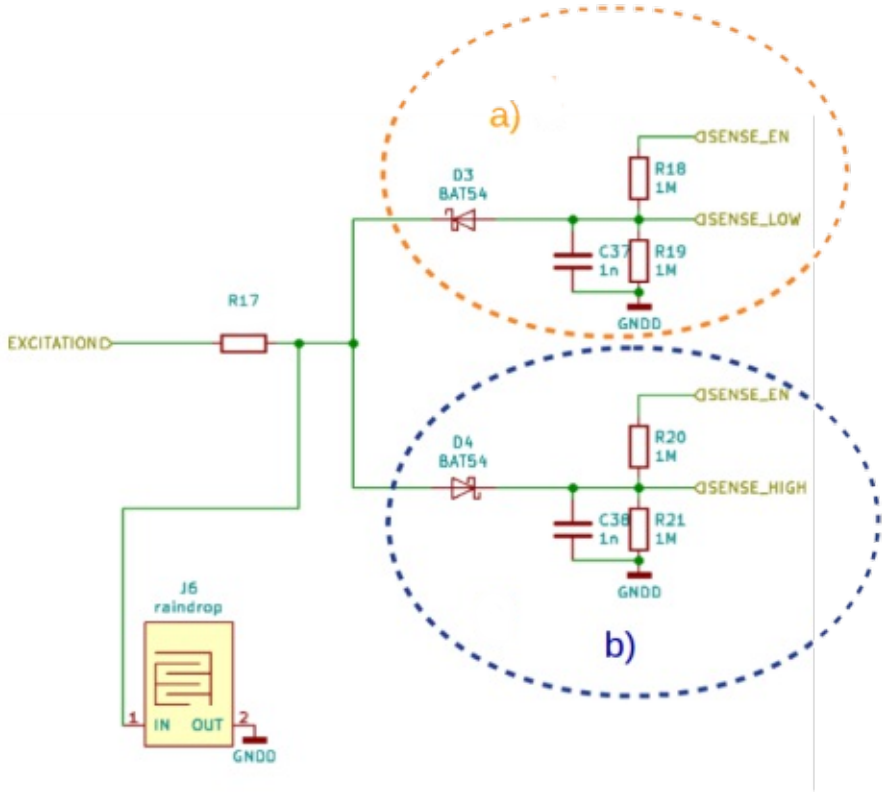

Figure 5.7: Capacitance leaf wetness measurement circuit.

5.4 Leaf Wetness Measurement

In the following section the values for the components of the leaf wetness measurement circuit are determined. Figure 5.7 depicts the whole circuit. *J6* is the capacitive sensor area. The *EXCITATION* pin is fed with a PWM signal. Figures 5.7a and 5.7b show how the output signal is rectified. Figure 5.7a shows how the discharging voltage is measured and Figure 5.7b shows this for charging voltage. For the measurement values we take the difference of both values to achieve a higher range of sensitivity.

The *SENSE_HIGH* and *SENSE_LOW* Pin are converted to a digital value by the ADC from the nRF52840. The ADC has a resolution of 12 bit and is able to divide the input voltage range, which is in our case 0V to 3.2V, into 4096 values [Sem16]. Because the number of values is limited, we have to calculate *R17* in a way that the voltage range between the dry and wet state is the largest. To get the optimal value of the resistor *R17*, we first have to calculate the capacitance of the measurement area in dry and wet state. The capacitance C of the measurement area can be calculated with Equations 5.4 to 5.8 for the inter-digital capacitor [AM12]. $K(x)$ is the complete elliptic integral of the first kind.

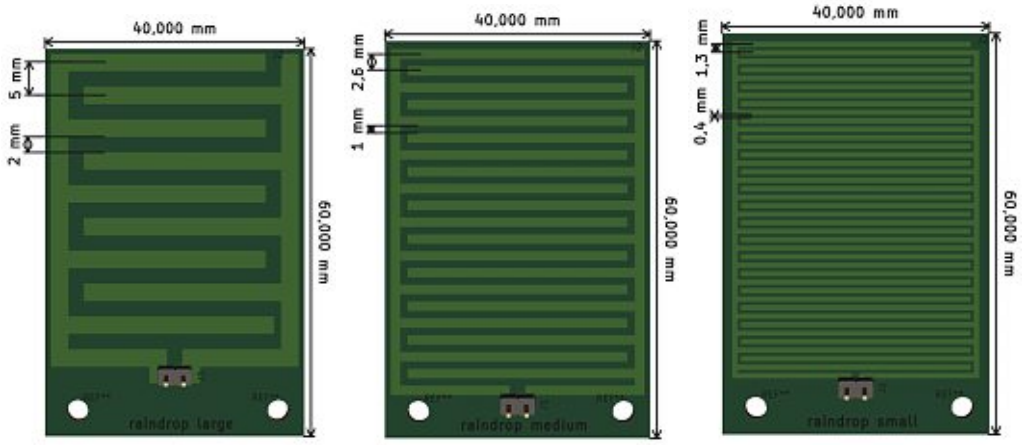

(a) (b) (c)

Figure 5.8: LWS boards with dimensions for the calculations. a) shows the wetness area with large tracks, b) shows the wetness area with medium tracks and c) shows the wetness area with small tracks.

As described in Section 4.1, three different leaf wetness boards are designed and compared. The boards with the dimensions for the calculation are presented in Figure 5.8 and also listed in Table 5.3, where they are abbreviated *small*, *medium* and *large*. Figure 5.9 schematically displays the parameters necessary for the calculations and Table 5.2 lists the values, which are the same for all three boards.

$$C = C_{UC}(N-1)L \tag{5.4}$$

$$C_{UC} = C_1 + C_2 + C_3 \tag{5.5}$$

$$C_1 + C_3 = \epsilon_0(\frac{\epsilon_1 + \epsilon_3}{2})(\frac{K(\sqrt{1-k^2})}{K(k)}) \tag{5.6}$$

$$C_2 = \epsilon_0\epsilon_2\frac{h}{a} \tag{5.7}$$

$$k = \frac{a}{b} \tag{5.8}$$

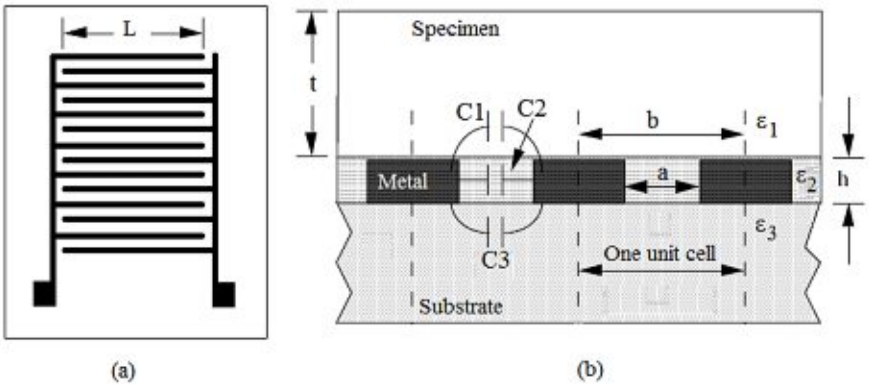

Figure 5.9: (a) Top view (b) Cut through view [AM12].

Table 5.2: Common parameters for the capacitor calculation.

Parameters	Value	Description
L	40mm	length of a probe
ϵ_0	$8.854 * 10^{-12}$	electric constant, permittivity of vacuum
ϵ_1	1	relative permittivity of air
ϵ_1	80	relative permittivity of water at 20° Celsius
ϵ_2, ϵ_3	5.4	relative permittivity of FR4
h	$35\mu m$	thickness of PCB track

Table 5.3: Distinctive parameters for the capacitor calculation for each board.

Parameters	large	medium	small	Description
a [mm]	2	1	0.4	clearance between PCB tracks
b [mm]	5	2.6	1.3	distance between the PCB tracks from the middle point
N	9	20	40	Number of unit cells

In order to find the best value for R17, we calculate the charging curve with Equation 4.4. In this calculation we combine different resistor values from Table E6 with different capacity values for C_{air} and C_{water} from Table 5.4. The E series specify standard resistor values to simplify manufacturing, handling and purchasing. It is defined in the DIN EN 60063 [DIN15]. The voltage U_0 is set to 3.2V and the time t is fixed for the calculation at 0.5μs. This is the switching point of the input rectangle, which has a frequency of 1MHz, which is illustrated in Figure 4.6. 1MHz was chosen because it is the highest frequency that can be generated by the nRF52840.

Table 5.4: Results of the capacitance calculation for the three different boards.

Capacitance	large	medium	small
C_{air} [nF]	0.015	0.035	0.08
C_{water} [nF]	0.2	0.45	1.01

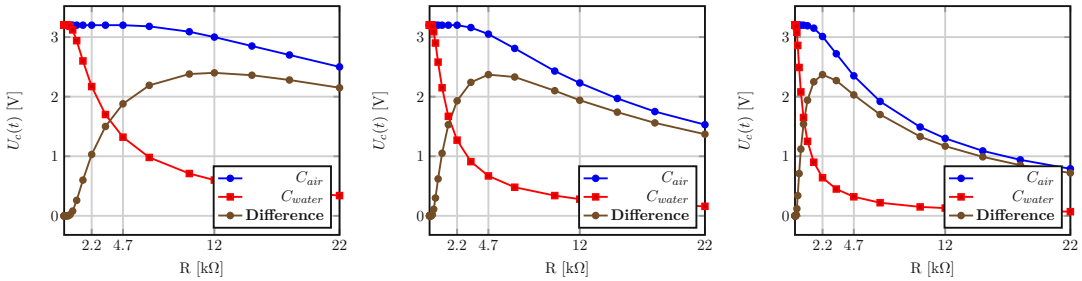

(a) (b) (c)

Figure 5.10: Capacitor charging voltage differences for resistor values from the E6 table. a) shows it for the large tracks, b) shows it for the medium tracks and c) shows it for the small tracks.

We take the resistance where the voltage difference is the greatest. This is demonstrated in Figure 5.10. Our tests reveal that the optimal value is 12kΩ for the large tracks, 4.7kΩ for the medium tracks and 2.2kΩ for the small tracks. These values are chosen because the difference in voltage and in capacity after a charge cycle between the dry and wet state is the greatest. As there are now more values between the dry and wet state, the measuring range becomes finer.

5.5 UV Measurement Circuit

The VEML6070[Sem19] is used to measure the UV value. Figure 5.11 shows the schematic of the VEML6070. The ACK, SDA and SCL pins are connected to the nRF52840, the other values of the components are taken from the datasheet [Sem19]. The IC cannot be protected from environmental impacts like rain or sun, so the wiring contacts are protected by epoxy resin.

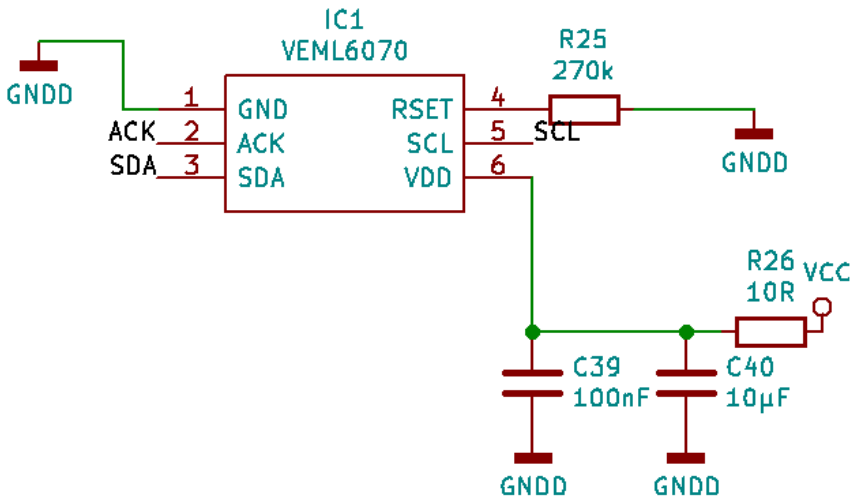

Figure 5.11: Schematic of the VEML6070 circuit.

5.6 Finished Board

Figure 5.12 illustrates the finished PCB layout of the board. A plastic case, shown in Figure 5.13b, is used to protect the electronics from environmental influences. The wetness area and the VEML6070 are not protected by this case. The mounting is done through the mounting holes with rope clamps [dp] shown in Figure 5.13a.

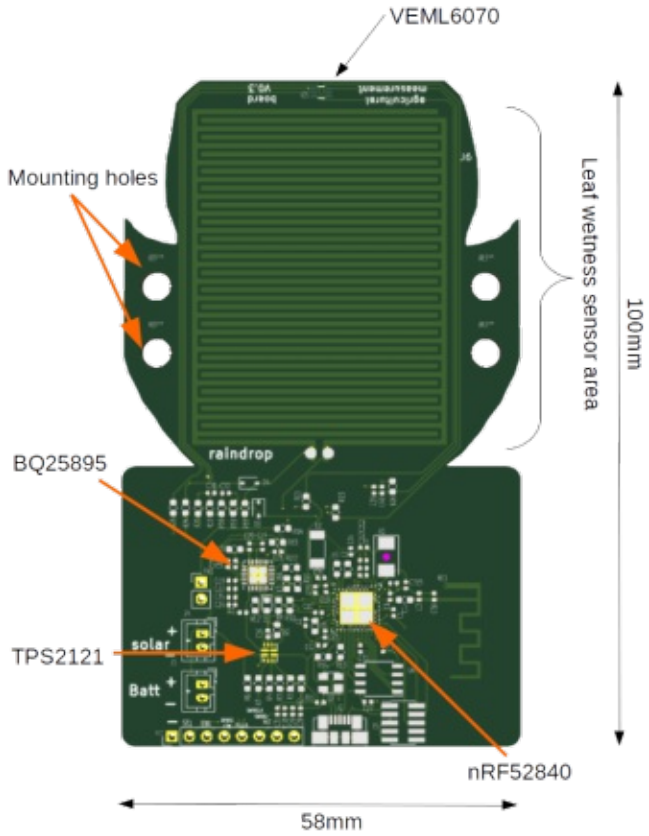

Figure 5.12: PCB layout of the finished board.

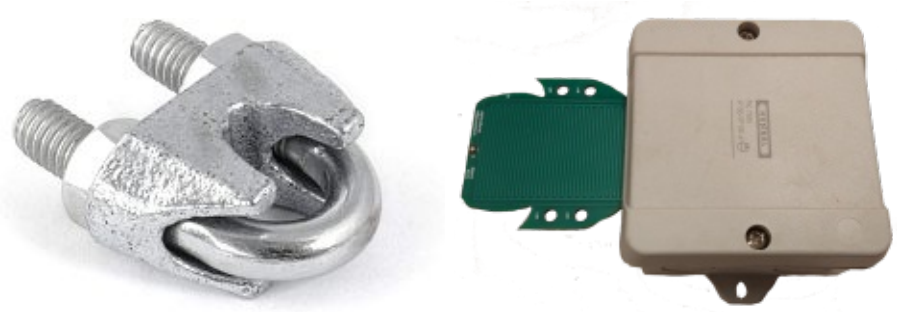

(a) (b)

Figure 5.13: a) shows the rope clamp to mount the sensor board [dp] and b) shows the case.

CHAPTER 6

Software Implementation

This chapter describes the programming of the sensors, the relay node and the Raspberry Pi, which operates as the fog node. The program for the nRF52840 is written in the programming language C. There are two ways to put the program into the memory of the nRF52840 [Sem20]. The first option is to do it with the help of the nRF52840 Development Kit (DK) [Sem20], which is connected to the PC via USB. The self-designed board is connected with the DK over the SWD pins. Nordic provides a Graphical User Interface (GUI) and a console program called nrfjprog [Sem], which uses the SEGGER J-LINK program [LLC]. The second possibility is to use the program OpenOCD [Deb18] and an SWD Programmer with USB interface. The Raspberry Pi is running the *Raspberry Pi Operating System* and is executing a python script.

6.1 Sensor Node

The sensor node is responsible for collecting, storing and transmitting the measurement data. In this section, we first examine the data storage and the configurations, which are managed by the software. Then we describe the state machine for the software components.

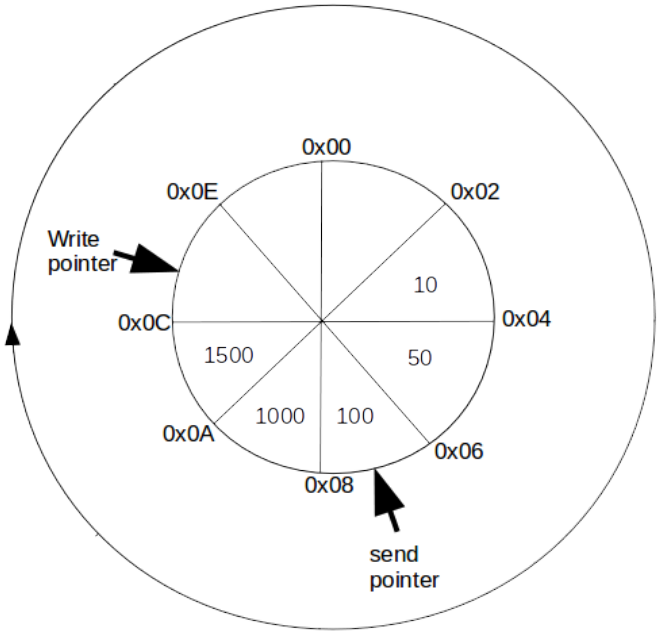

Figure 6.1: Ring buffer, where the write pointer indicates the next position to be written into the memory and the send pointer indicates the value that is transmitted next.

6.1.1 Data Storage

The data storage uses a ring buffer to handle the measurement values. Figure 6.1 shows the ring buffer for the 2-byte UV values. This example can store 8 values. The write pointer indicates the next position that is going to be written in the memory and the send pointer indicates the value that is transmitted next. The ring buffer is necessary because the size of the data packets is limited and should be kept low to avoid fragmentation. Thread has a minimum payload of 63 bytes, while 6LoWPAN [Incb] and CoAP together need a minimum of 4 bytes of overhead [IETd]. This leaves a maximum size of 59 bytes for a packet. The transmission of values is then independent of the collection of measurements.

Figure 6.2 displays the memory layout of the nRF52840. The flash has a size of 1024kB. The size of the bootloader settings, the Master Boot Record (MBR) parameter storage, the bootloader, the softdevice and the MBR are taken from the Nordic libraries [Sem18a]. After the compilation of the source code, the size of the application can be determined and it is 354kB. The Application Data has a size of about 90kB. Therefore, the free space is 492kB and the sensor node with *Fog Request Method* (6.4b) can store up to 98400 values if one value has a size of 5 bytes, according to Section 4.3.1.

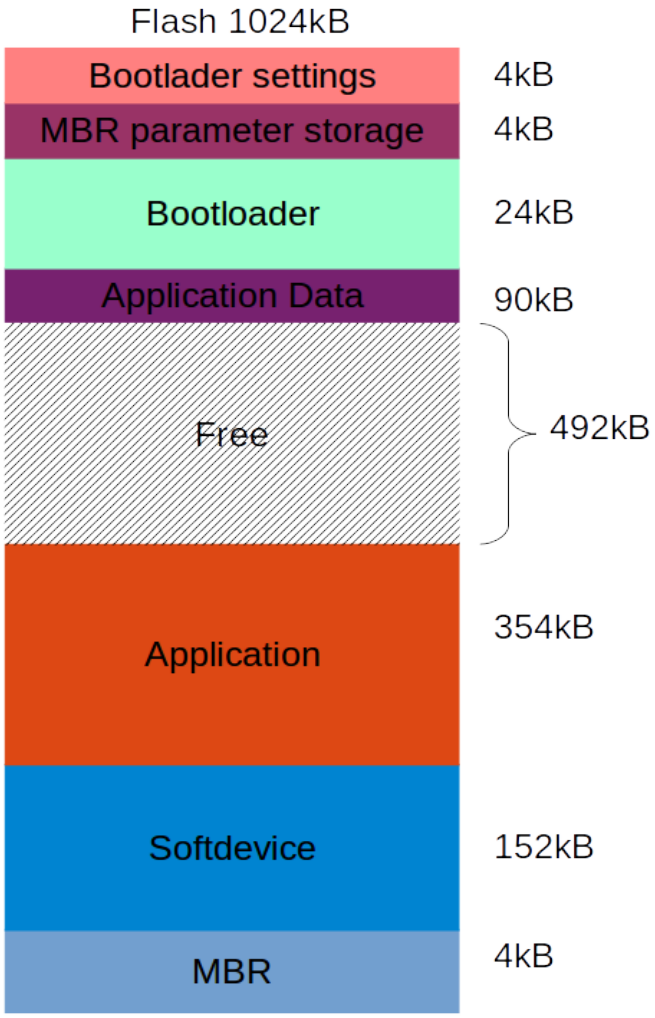

Figure 6.2: Memory layout for the nRF52840, with a flash size of 1024kB.

6.1.2 ADC

The ADC converts the analog measured wetness value to a digital one. The internal reference voltage of 0.6V is used and the single ended mode is activated. The gain factor of the input is set to 1/16 and the acquisition time to $10\mu s$. The burst mode is disabled.

6.1.3 I^2C

The I^2C bus technology is used to communicate with the BQ25895 and the VEML6070. The speed is set to 400kbps.

6.1.4 PWM

The PWM is needed for the excitation of the leaf wetness area. The nRF52840 has a built-in module to generate up to 4 independent PWM signals with programmable frequency. We are using channel 0, a base clock of 16MHz (prescaler of 1), an up counter with a top value of 8. If the value 8 is reached, then the counter is reset to zero. This results in a PWM signal with 50 percent duty cycle and a time period of $1\mu s$, which results in a frequency of 1MHz. In order to get the optimal duty cycle and frequency for the wetness measurement, some duty cycles are tested and compared in Chapter 7.

6.1.5 WDT

The Watchdog Timer (WDT) offers a protection against application lockup. It is a counter that decrements a specified register. If the value in the register reaches zero, the watchdog resets the system. So the CPU has to periodically set the watchdog register to the starting value. The nRF52840 has a WDT module built in, which we use in default configuration.

6.1.6 VEML6070

The VEML6070 is configured over I^2C, it has one slave address for writing (0x70) and two slave addresses for reading (0x73 and 0x71). First, the initial value of 0x06 has to be sent to the write address. Second, the configuration can be sent to the write address, which includes the disabling of the acknowledge signal, an integration time of 500ms and the disabling of the shutdown mode. The 2-byte UV value is split into two 1-byte parts, which can be retrieved with the two slave read addresses.

6.1.7 BQ25895

The BQ25895 can be configured and the status information can be read over I^2C. We can choose between a continuous battery voltage ADC or a discrete one. For reading the battery voltage in an interval of minutes, it is more efficient to use the discrete option because the continuous one converts a new value each second. For loading the battery with the solar panel, we have to set *FORCE_VINDPM* to 1 and the *VINDPM* threshold to 4.2V. Otherwise, the BQ25895 uses a relative *VINDPM* threshold, which can lead to the problem described in Section 4.5.2.

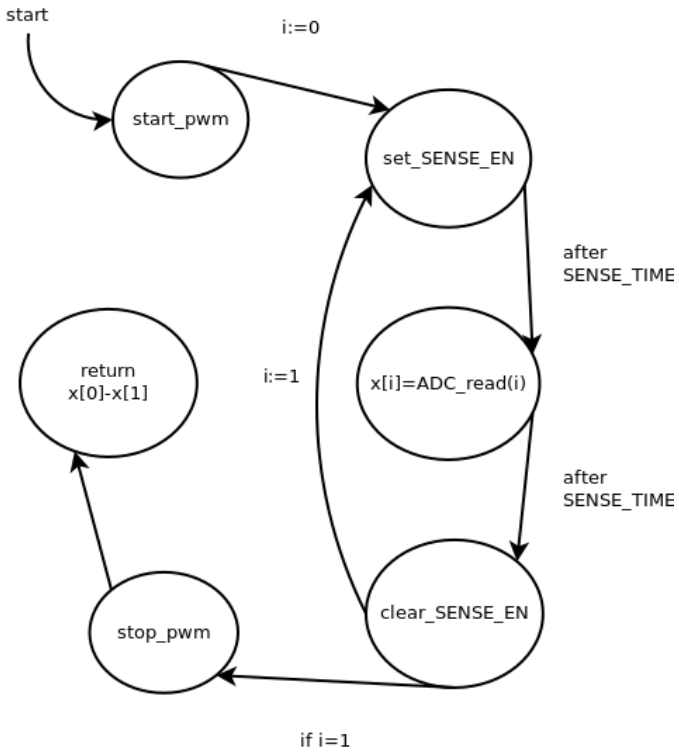

Figure 6.3: State machine to get a wetness value.

6.1.8 Leaf Wetness State Machine

A state machine is used to abstract a program flow, it can only be in one of a finite number of states. To illustrate it, a graph can be used in which the nodes describe the state of the program. The arrows indicate the possible transitions from one state to another and their conditions or assignments. Figure 6.3 depicts the state machine, with which we get a wetness value from the sensor area. The PWM is started in the *start_pwm* state and it is stopped in the *stop_pwm* state. This works because the PWM signal is only needed during the capture of a leaf wetness measurement. The PWM is configured as described in Section 6.1.4. This configuration is done in the initial part of the main program, which is shown in Figure 6.4a and 6.4b. The states *set_SENSE_EN* and *clear_SENSE_EN* are setting and clearing the *SENSE_EN* pin to high (3.2V) and low (0V). The state *ADC_read* converts the analog value of the measurement to a digital value. If i is zero, the *SENSE_HIGH* pin value is used and if i is one, the *SENSE_LOW* pin value. The value is written into the variable x on position i. Before and after converting the value, *SENSE_TIME*, which is set to a value between $1\mu s$ and $20\mu s$, has to wait before going to the next state. After reading the high and low value of the measurement, the state return subtracts the low value from the high value and stores it for later transmission.

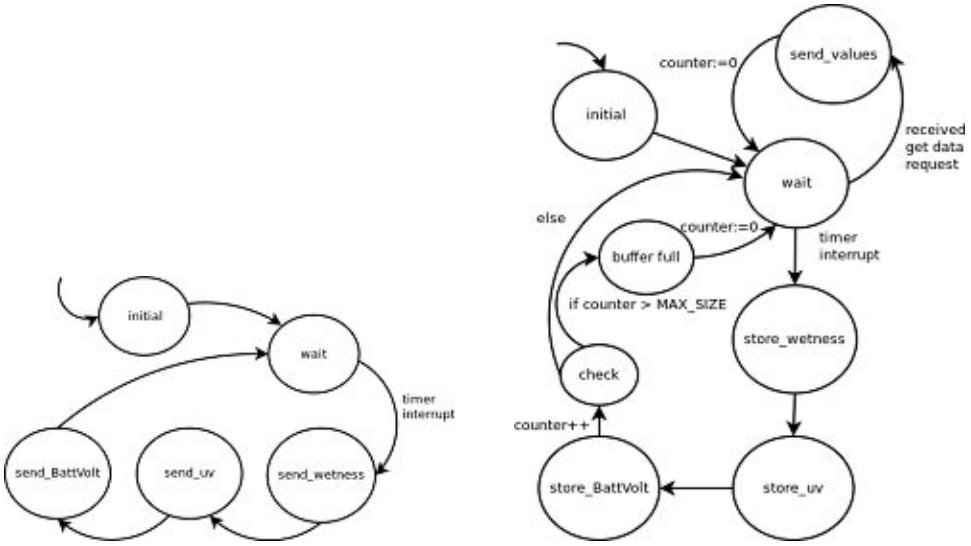

(a) (b)

Figure 6.4: State machines of the main program for the sensor nodes. a) shows the *Forward Only Method* and the *Relay Buffered Method* and b) shows the *Fog Request Method*.

6.1.9 Main Program State Machines

Figure 6.4a shows the state machine of the main program for the *Forward Only Method* (Figure 4.8a) and *Relay Buffered Method* (Figure 4.8b). In the initial state the ADC, the I^2C, the VEML6070, the BQ25895 and the PWM are configured. The *send_wetness* state receives a new wetness value, which is done with the state machine in Figure 6.3. The *send_uv* state collects the UV value from the VEML6070 over I^2C. The *send_BattVolt* state collects the battery voltage from the BQ25895. Then the values are sent over Thread to the relay node. After one minute, the outgoing transition from the wait state is taken. This interval for taking a measurement is configurable. The other transitions are used as soon as the execution of the state is finished.

Figure 6.4b shows the state machine of the main program for the *Fog Request Method* (Figure 4.8c). In the initial state the ADC, the I^2C, the VEML6070, the BQ25895 and the PWM are configured. The states *store_wetness*, *store_uv* and *store_BattVolt* collect the measured values but the data is not sent immediately. It is stored in a ring buffer. If the ring buffer is full, the counter is set to zero again and the values at the beginning of the ring buffer are overwritten, even if they have not been sent yet. The other option would be to keep the values and avoid adding new ones. In this case measured values are lost. The number of values that can be stored is described in section 6.1.1. If the node receives a *get data request*, it sends all values to the relay node and sets the counter to zero.

6.2 Relay Node

The relay node can be a sensor node with additional functions or an independent device. Its main task is to receive the messages from the sensor nodes in the Thread network and then forward them over Bluetooth to the fog node devices. For that task the relay node needs to implement Thread and Bluetooth, which are provided by Nordic. We can choose between a switched multiprotocol and a dynamic multiprotocol [Sem18b]. In the case of the switched version only one protocol is active and because of that we could miss a request, so we choose the dynamic one, where multiple protocols are active at the same time. The disadvantage of the switched protocol is that the switching has to be done at the right time, because if, for example, the relay node is currently connected to the BLE network and a sensor in the Thread network sends something, this message is lost. In the dynamic multiprotocol the disadvantage is that the throughput of one protocol can be lower because of the sharing of the radio.

6.2.1 Data Storage

In the case of *Forward Only Method* (Figure 6.4a) and the *Fog Request Method* (Figure 6.4b), the relay node forwards the received measurement data from the Thread network immediately to the fog node device. Therefore, the data does not need to be stored. But a transmit ring buffer for temporarily storing the data is necessary because the maximum packet size of Bluetooth and Thread differs. The Nordic BLE stack supports 20 bytes by default for a notification characteristic [Sem18c]. And as described in Section 6.1.1, Thread with CoAP packages can have a size of 59 bytes.

However, in the *Relay Buffered Method* (Figure 6.4a) the measurement data are stored on the relay node until a fog node collects it. A ring buffer, as described in Section 6.1.1, is used to store the data. The relay node uses 357kB for the application and the resulting free space is 489kB. Therefore, the relay node can store 97800 measurements, provided one value has a size of 5 bytes, according to Section 4.3.1. These values are valid only for the relay node and without the capability to measure values since the size of the application of the sensor node has to be added.

Table 6.1: Data packet that is sent with BLE to the subscribed fog device.

Data Byte	0 - 7	8	9	10	11	12	13	14	15	16	17	18	19
Values	ID	Value1		Time1		Value2		Time2		Value3		Time3	

6.2.2 Bluetooth

To get the measurement data, the fog device has to subscribe to one of the three BLE characteristics. The base Universally Unique Identifier (UUID) is set to a custom value of 128 bit, the service UUID is set to 0xF00D. The characteristic UUID for the wetness is 0xBEEF, for the UV value it is 0xDEEF and for the battery voltage value it is 0xFEEF. The data packet that is sent from one of the characteristics to the fog device is shown in Table 6.1. The NID is a unique number assigned to the sensor node in the whole thread network. The ID is composed of the NID and the last 6 bytes of the IPv6 address of the sensor node. The measurement values and the according measurement time are 4 bytes large.

6.2.3 State Machine

The state machine for the relay node for the *Forward Only Method* (Figure 6.4a) is shown in Figure 6.5a. In the initial state the BLE stack, the watchdog and the BLE characteristics are initialized. If a message is now received over the Thread network and a BLE device is subscribed to the characteristics, the message is forwarded, otherwise the message is discarded.

Figure 6.5b shows the state machine for the *Relay Buffered Method* (Figure 6.4a). In the initial state the BLE stack, the watchdog and the BLE characteristics are initialized. If now a message is received over the Thread network, the state is changed to store_value and the value is stored in the ring buffer. After that, it is checked whether the buffer is full. If it is, the counter is set to zero and the oldest values are overwritten. Another option would be to keep the old values and discard the new value. As soon as a BLE device subscribes to the characteristics, the data from the ring buffer is sent to it.

The state machine of the *Fog Request Method* (Figure 6.4b) is shown in Figure 6.5c. In the initial state the BLE stack, the watchdog and the BLE characteristics are initialized. If now a data request is sent from a subscribed BLE device, a received data request is sent to all members of the Thread network. After that, each sensor node sends its data to the relay, which then forwards it to the BLE device.

6.3 Raspberry Pi as Fog Device

The Raspberry Pi is used as fog device to collect the data from the Thread network over BLE to store it or to send it to a cloud server. We used Python [Fou] as programming language to write a program that subscribes to the BLE characteristics from the relay node. GattLib [LA16] is a library that offers functions to communicate with BLE devices.

Table 6.2: Example of a time stamp calculation for five measurement values. The calculation is done by the Raspberry Pi and is based on the RTC and the time stamp from the NTP. The outcome are time stamps for each measurement value.

Value	RTC	Data collection Timestamp [s]	Calculated Timestamp [s]	Description
2	0	1597568384	1597568380	= 1597568384 – 4
3	1	1597568384	1597568381	= 1597568384 – 3
5	2	1597568384	1597568382	= 1597568384 – 2
7	3	1597568384	1597568383	= 1597568384 – 1
5	4	1597568384	1597568384	= 1597568384 – 0

For testing the Thread network, the data is stored on the Raspberry Pi in a Comma Separated Values (CSV) file.

6.4 Time Synchronization

A time stamp must be assigned to each measured value in order to enable comparisons and correlations for later processing of the data. The sensor nodes and the relay nodes have a Real Time Counter (RTC), which, e.g. increments a counter every minute. For each taken measurement the current RTC value is stored. The Raspberry Pi has an Internet connection and can get the current time over a Network Time Protocol (NTP) server. Therefore, the Raspberry Pi is responsible for assigning each received measurement value a current time stamp. With this and the RTC value, we can calculate the current time stamp of each measurement value. Depending on the variant used, the assignment procedure is different; the differences are discussed below.

6.4.1 *Forward Only Method*

In this variant the measurement values are immediately forwarded by the relay node to the Raspberry Pi, which marks each received value with a time stamp taken from an NTP server.

6.4.2 *Relay Buffered Method*

In this variant the relay node has an RTC, which increments a register at configured time steps. For each received measurement data, the current value from the RTC is stored. If the data is collected by the Raspberry Pi, it stores the current time stamp from the NTP. After the transmission, the RTC register is reset to zero. So each data set at the Raspberry Pi has a tuple of 3 values: the measured value, the RTC when the measurement was taken and the time stamp. With the time stamp and the RTC values, we can calculate the time point of each measurement, by subtracting the highest RTC value from the time stamp of the lowest RTC value. An example is shown in Table 6.2.

Table 6.3: Pre-commissioning Parameters.

Parameter	Value
Radio Channel	11
PAN ID	0xABCD
Network Master Key	0x00112233445566778899AABBCCDDEEFF
Mesh-Local Prefix	FDDE:AD00:BEEF::/64

6.4.3 *Fog Request Method*

In this variant all sensor nodes have an RTC. For each measurement they store the current value of the RTC register. The further procedure, which includes the collection of the data from the Raspberry Pi, is the same as for the *Relay Buffered Method*.

6.5 OpenThread Mesh Network

The Thread SDK from Nordic is built on top of the OpenThread stack. In this section we first describe commissioning, which is the joining procedure of a node to the thread network. Then we take a look at the used CoAP configurations for the different variants.

6.5.1 Commissioning

To make the development and validation of the mesh network less time-consumable, we used hard-coded parameters presented in Table 6.3. Therefore, no commissioning is necessary and each device connects to the network with the given parameters. In a final product, this method should not be used but a commissioner [TG15]. The commissioner can be in the thread network (on-mesh commissioner) or outside the thread network (external commissioner, e.g. smart phone) and it is elected by the *Thread Leader*. The external commissioner needs a *Border Router* for forwarding the messages. The communication between the joiner and the commissioner is secured with DTLS. The Joining Device Credential (PSKd) is a passphrase used for authenticating a new joiner device and it should be unique for each device. The passphrase can be restricted to a specific 64-Bit Extended Unique Identifier (EUI-64). The network-wide master key is only known by already joined devices and is transmitted to new ones after commissioning.

Table 6.4: Data packet that is sent with CoAP over the Thread network.

Data Byte	0	1	2	3	4	5	6	7	8	9	10	11	12
Values	NID	Value1		Time1		Value2		Time2		Value3		Time3	

6.5.2 CoAP

The CoAP protocol is used to manage the transmission of the measurement data. The CoAP server waits for messages on specific resources and the CoAP client can send messages to these resources. We defined three resources: *raindrop* for the leaf wetness, *uv* for the UV and *BatteryVoltage* for battery voltage. For all variants the relay node has the CoAP server functionality. It is possible to have more than one relay node and therefore more than one CoAP server. For all variants the sensor nodes send multicast messages to the CoAP servers. In *Fog Request Method* (Figure 6.4b) the sensor nodes implement a CoAP server for receiving the *get data request*. After they received the request, they send the data like in *Forward Only Method* and *Relay Buffered Method*. The data that is sent is grouped as shown in Table 6.4. The NID is a unique identifier of the sensors in the network. The measurement value and the according time are 4 bytes large.

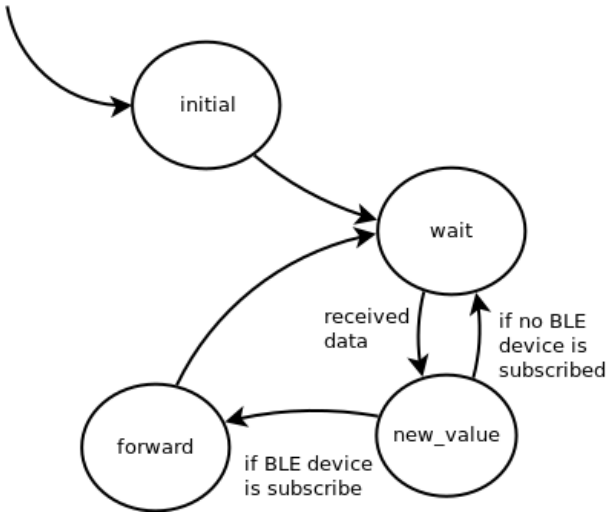

(a)

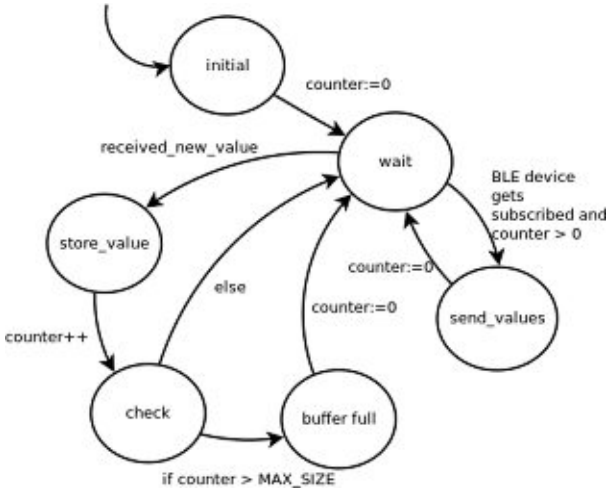

(b)

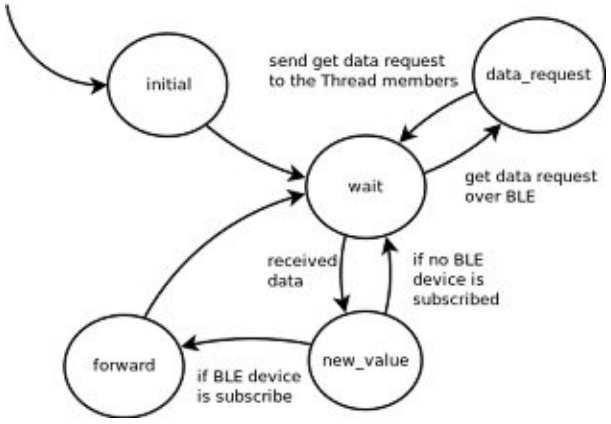

(c)

Figure 6.5: State machines for the relay node of a) *Forward Only Method*, b) *Relay Buffered Method* and c) *Fog Request Method*.

CHAPTER 7

Validation

The aim of this chapter is to evaluate the self-designed sensors against different criteria. First, the LWS is evaluated and calibrated. After that, the antenna is tested and the power consumption is examined. Finally, the reliability of the measurements of the sensors in the field tests is revealed. For this purpose, the sensors were mounted in the field, just as they would be used in a real-life use case.

7.1 LWS Area Evaluation

In this section the LWS is evaluated. This is necessary in order to assign the actual and possible leaf wetness values to an ADC value.

7.1.1 Comparison of Different PCB Tracks

In order to select the most sensitive and separable sensor area for the leaf wetness measurement, the sensors have been tested under different circumstances. Parameters that have been variated are the frequency of the PWM signal, its duty cycle and the sense time, which is the time to wait between setting the *SENSE_EN* to high and taking the first measurement value. The sensor surface to be tested is connected to the measuring device with a 15cm long cable. The measurement was performed for 4 different wetness states: dry, wetted, wet and sprayed. In the dry condition there is no water on the surface. In the wetted state, half of the area is covered with water and in the wet state, water covers the full area. In the sprayed condition, water was sprayed on the surface, so there are about 15 small drops on the surface. In Figure 7.1 to 7.4 the results of taking 31 samples in an interval of 5 minutes are presented for different parameters and conditions. Each of these measurements was taken for the wetness area with small, medium and large PCB tracks. Figure 7.1 b) to 7.4 b) shows the ADC value of the high and low measurements and Figure 7.1 a) to 7.4 a) shows the difference of the high and low value.

Table 7.1: Used parameters for comparing different PCB tracks.

Reference	PWM frequency [MHz]	Duty cycle [%]	Sense time [μs]
Measurement1	1	25	20
Measurement2	0.2	25	20
Measurement3	1	50	20
Measurement4	1	75	20

Table 7.2: Comparison of the difference from the mean values for different PCB tracks.

Reference	PCB Track	Difference of the mean value		
		Dry-Sprayed	Sprayed-Wetted	Wetted-Wet
Measurement1	small	127	114	30
	medium	121	139	34
	large	59	198	56
Measurement2	small	37	170	148
	medium	50	110	110
	large	39	5	145
Measurement3	small	124	282	139
	medium	219	139	139
	large	33	192	144
Measurement4	small	209	271	178
	medium	252	164	164
	large	52	183	179

Subtracting the low value from the high value increases the difference between the measurement values of the different wetness conditions and therefore enables better separability. Table 7.1 shows the parameters used for the comparison. For the PWM frequency 1MHz was chosen because it is the highest frequency which can be generated by the nRF52840 and the circuit was calculated for this condition. For testing purposes the frequency was set to 200kHz. Under this circumstance, the separability shown in Figure 7.2 is worse than for 1MHz because it is not possible to make an exact boundary between the different wet conditions. To find the best duty cycle, we compared three of them. Table 7.2 shows the differences in the mean values of the neighboring moisture states (Dry-Sprayed, Sprayed-Wetted and Wetted-Wet). A high value in Table 7.2 stands for a good separability between two wetness states. We want the value for all three states (Dry-Sprayed, Sprayed-Wetted and Wetted-Wet) to be as high as possible. The best separability of the different wetness conditions was achieved with a duty cycle of 75% and the small PCB tracks shown in Figure 7.4. The according mean values are marked green in Table 7.2.

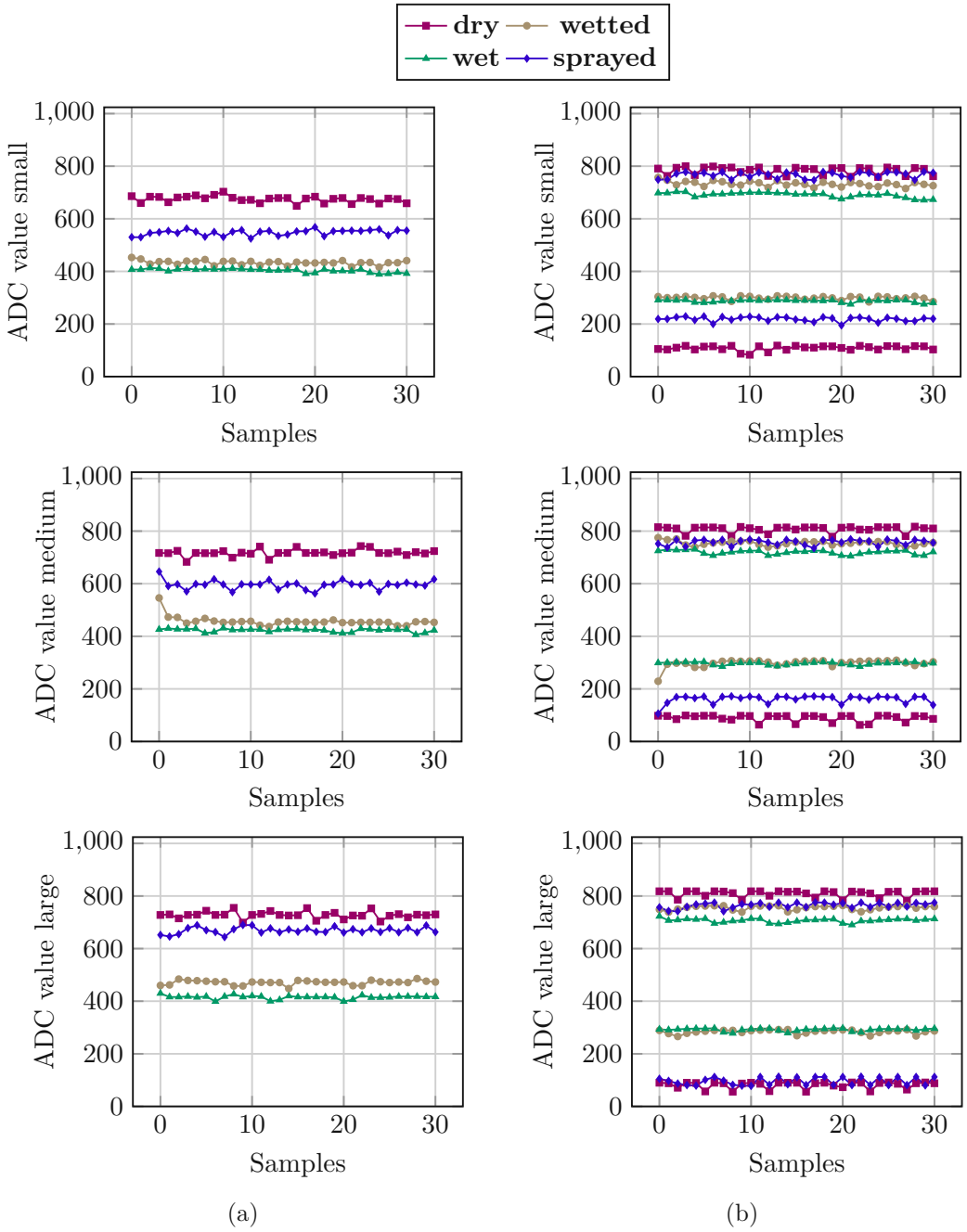

Figure 7.1: Measurement1 for a PWM frequency of 1MHz, a duty cycle of 25% and a sense time of 20μs. a) shows the difference of high and low values and b) shows the high and low values of the ADC

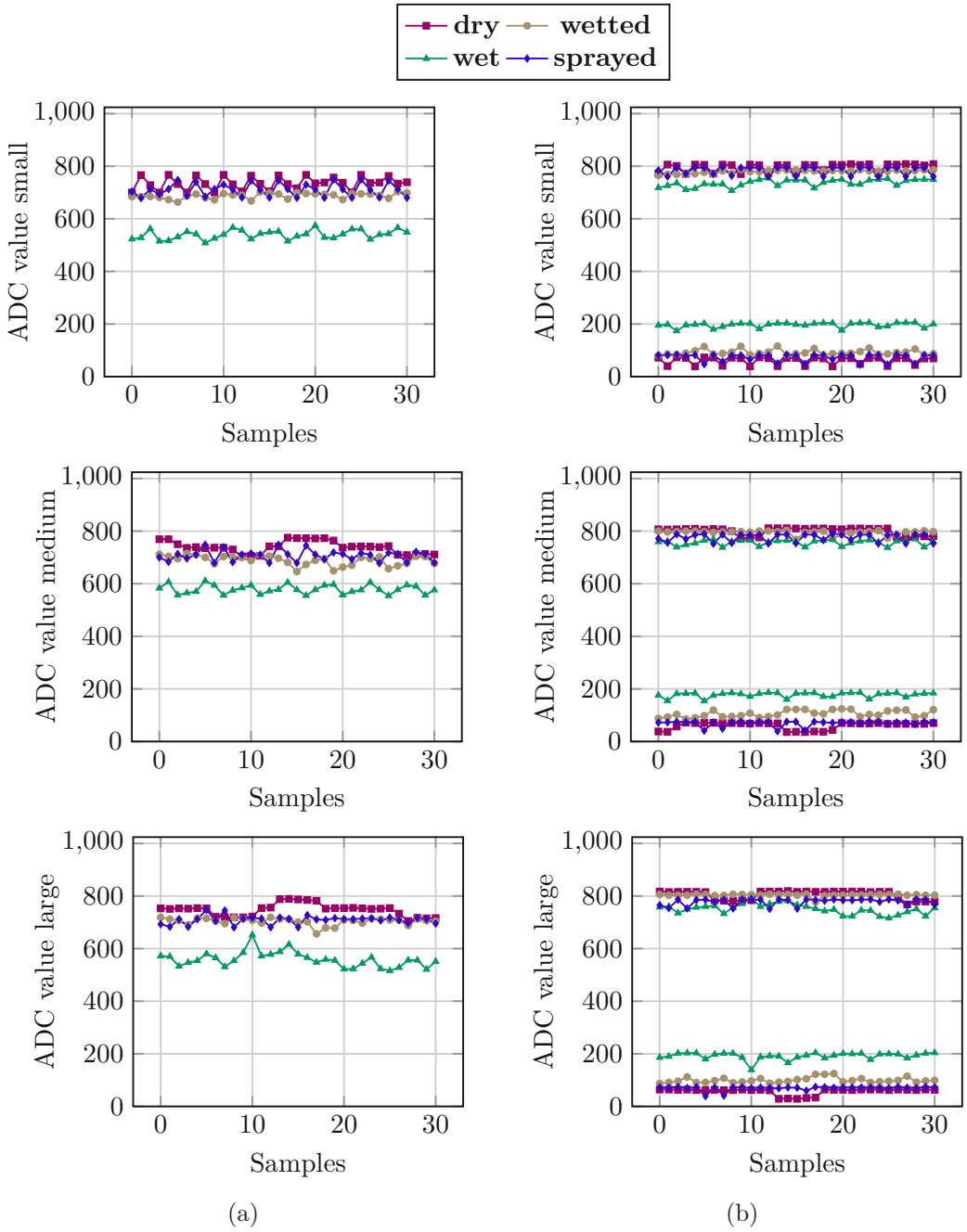

Figure 7.2: Measurement2 for a PWM frequency of 200kHz, a duty cycle of 25% and a sense time of 20μs. a) shows the difference of high and low values and b) shows the high and low values of the ADC

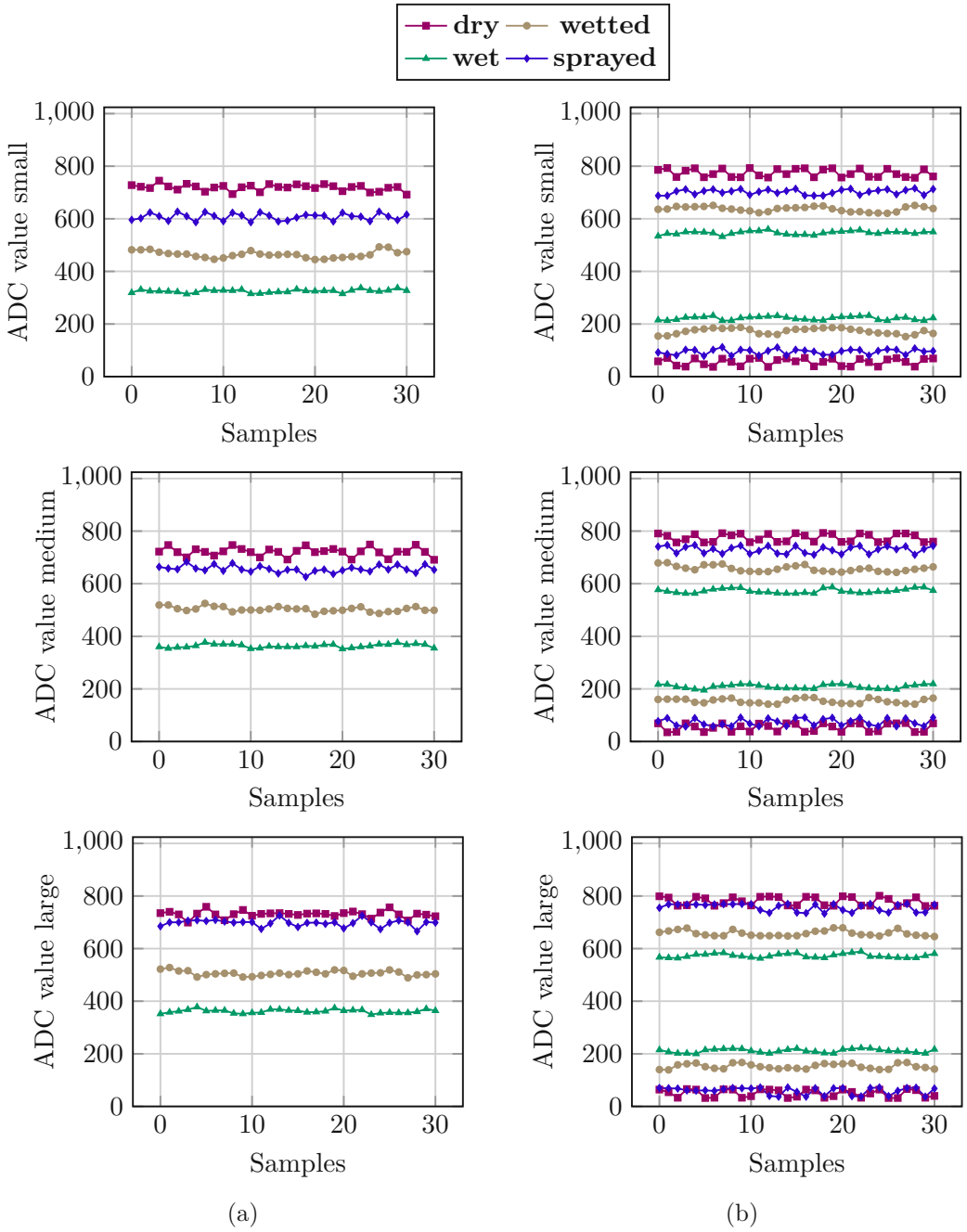

Figure 7.3: Measurement3 for a PWM frequency of 1MHz, a duty cycle of 50% and a sense time of 20μs. a) shows the difference of high and low values and b) shows the high and low values of the ADC

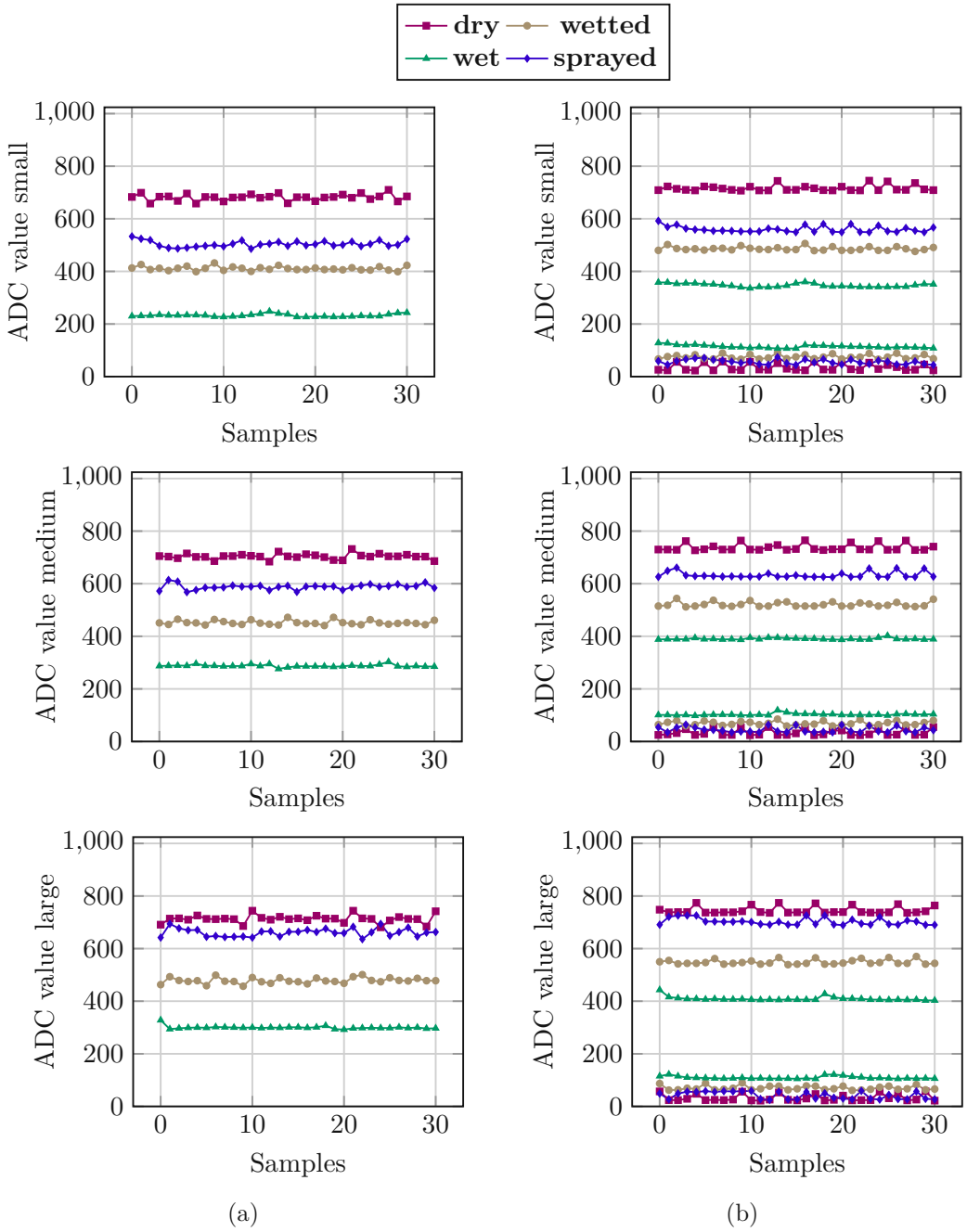

Figure 7.4: Measurement4 for a PWM frequency of 1MHz, a duty cycle of 75% and a sense time of 20μs. a) shows the difference of high and low values and b) shows the high and low values of the ADC.

Table 7.3: Measurement values of the sensor area.

x (ADC value)	y (Area)	leaf wetness [%]
750	0	0
650	1	10
560	2	20
460	3	30
420	4	40
396	5	50
370	6	60
349	7	70
330	8	80
307	9	90
269	10	100

7.1.2 Relationship of Leaf Wetness to Digital Value

In this section we assign a leaf wetness value to a digital value by dividing the sensor surface into 10 areas of equal size, which were successively covered with water. 0 stands for no water coverage, between 0 and 1 is the first area, between 1 and 2 is the second area and so on. The measured value when flooding the first area gives us the value for a 10 percent leaf wetness. If we cover the areas one and two, we get the value for a 20 percent leaf wetness. We carry out this measurement until all areas are covered and we reach the value for a 100 percent leaf wetness. Figure 7.5a illustrates the subdivision of the sensor area for the measurement and Figure 7.5b displays the results. From the resulting curve we see that the line is not linear. Therefore, we make a linear approximation that is illustrated in Figure 7.5b. In order to obtain the percentage leaf wetness y for a measured ADC value x, we have to look for the two closest known measuring points (x_0, y_0) and (x_1, y_1) from Table 7.3. This procedure is sketched in Figure 7.5b. At the end, we calculate y with the help of equation 7.1.

$$y = \frac{y_0(x_1 - x) + y_1(x - x_0)}{x_1 - x_0} \tag{7.1}$$

7.1.3 Calibration

Calibration is necessary if the sensors measure different values for the same environmental conditions. To determine the deviation between the sensors, 50 measurements were taken from four sensors at one-minute intervals for the three states dry, wetted and wet. The results are illustrated with box plots in Figure 7.6. To calibrate the sensor, we calculate the deviation of the median from the reference values in Table 7.3. Each measured value of the sensor must be corrected by this value. The values to be corrected for the four sensors are presented in Table 7.4.

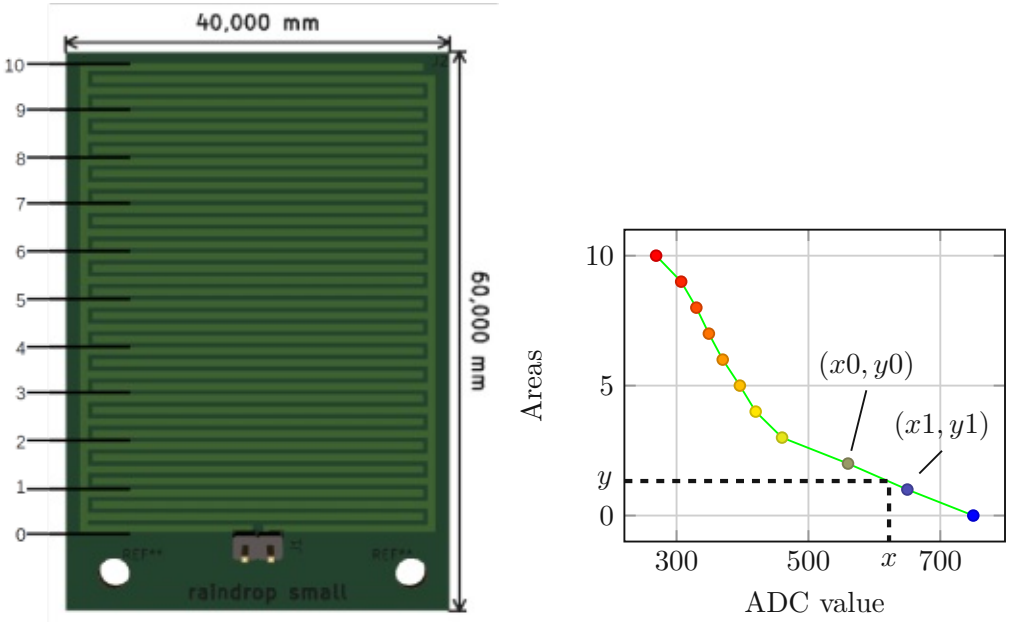

(a) (b)

Figure 7.5: Measurement to assign a leaf wetness value to a digital value. a) shows the subdivision of the sensor area and b) shows the measurement result for the wetted areas.

Table 7.4: Deviation from the reference values for different sensors.

sensor	correction value
0	-76
1	-49
2	-31
3	-49

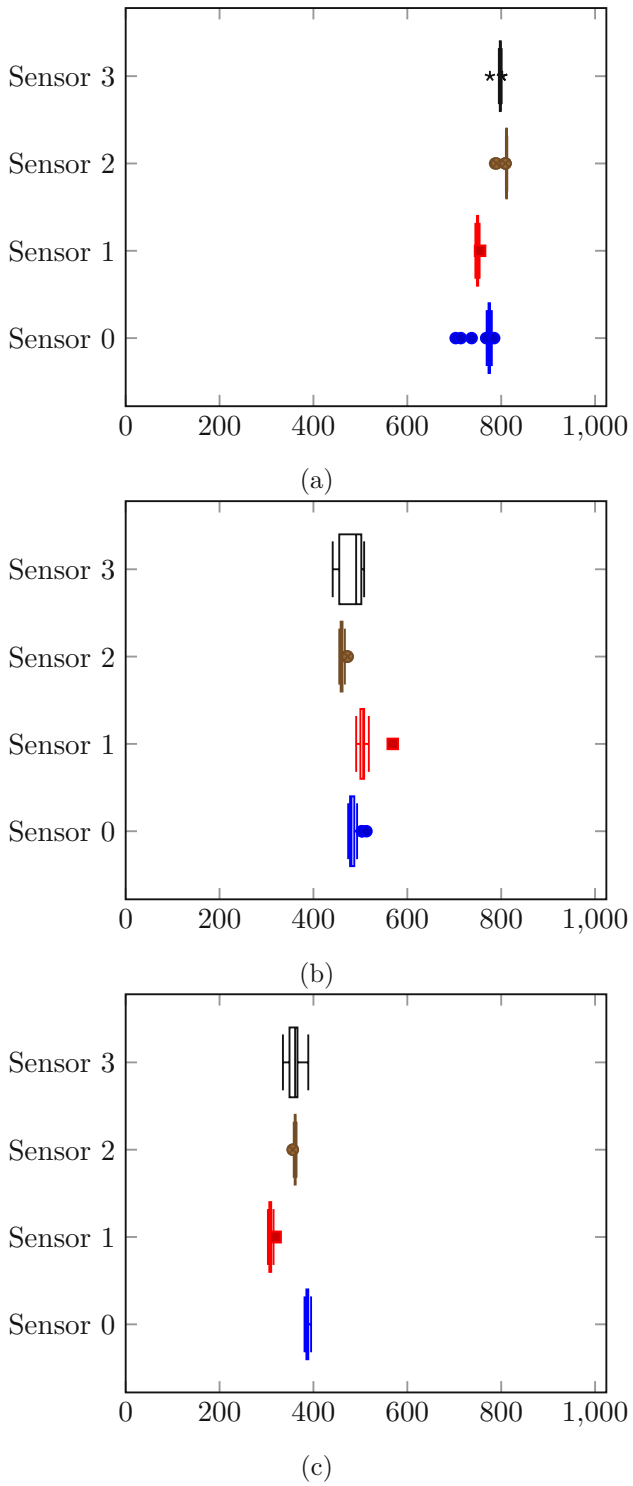

Figure 7.6: Box plots for the dry (a), wetted (b) and wet (c) states for the leaf wetness measurement for four sensors.

7.1.4 Comparison to Existing Sensors

A. Ghobakhlou et al. [GAS15] compare 6 different leaf wetness sensors in his paper, these are Hobby Boards LWS, Campell Scientific 237-L, Decagon Devices LWS, Pessl Instruments LWS, Painted Hobby Boards and Painted Campbell 237. To compare our sensors with these 6 sensors, two measurements were made over two days. At first, we compare the surfaces of our sensor and a real leaf. For this, we simultaneously put the same amount of water on both surfaces. Second, we measure how long it takes for these two surfaces to dry up. Finally, we have to different periods of time, one for the leaf and one for our sensor. The difference between these two time measurements is 11 minutes and is compared with the other 6 sensors in Figure 7.7. As you can see in Figure 7.7, the sensor built by the author takes as long as the other sensors to dry.

The second measurement compares the measured value of the sensor with the visual observation of actual wetness on the sensor surface. For this purpose, we wet the sensor and measure the time it takes the sensor surface to dry and the time it takes the measured value to signal a dry surface again. The difference between these two time measurements is 39 minutes and is compared with the other 6 sensors in Figure 7.7. As you can see in Figure 7.7, the sensor built by the author needs the most time to measure a dry surface again.

7.2 Antenna

The amplitude over the distance of the antenna is measured as shown in Figure 7.8a. For the measurement the nRF Connect software is provided by Nordic. Figure 7.8b illustrates the result, the sensor board is placed at different distances away from the nRF USB Dongle, which is used for the measurement. The z value was fixed at 0.5m. The free space path loss behaves as planned in Section 5.2 and corresponds to the reference design.

7.3 Power Management

In this section the power management is examined under real-life conditions. The solar panel has a size of about 20 x 20 cm and for the battery a capacity of 1.1Ah was chosen. Under full sunlight the battery was charged in about 1 hour. In Figure 7.10 the PV charging current under full sunlight is shown. The charging behavior is the same as described in the datasheet of the BQ25895 [Ins18]. The solar panel was placed in a way that no object can cast a shadow on it. Figure 7.9a shows the solar panel voltage over a period of 24 hours and Figure 7.9b shows the battery voltage. For loading the battery a minimum of 4.2V of solar panel voltage is required, this was configured in Section 6.1.7. The measurements were taken in winter in three different weather settings defined by the International Commission on Illumination (CIE) [CIE]: overcast sky, cloudy sky and clear sky.

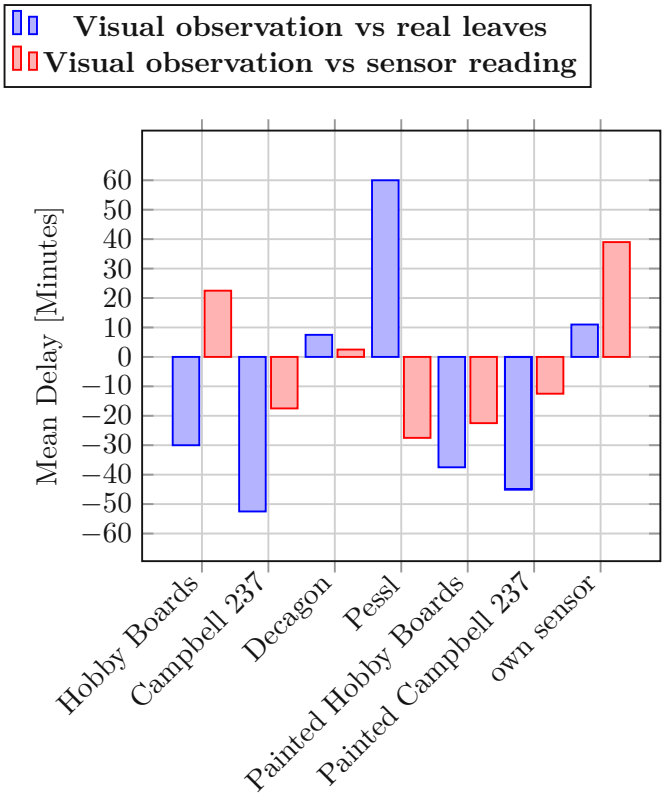

Figure 7.7: Comparison of own sensor dry-off against 6 sensor results from A. Ghobakhlou et al. [GAS15].

As we can see from the voltage curve in Figure 7.9a, it is not possible to load on an overcast day and in the other two cases, only at noon because at this point the sun light is highest and therefore the voltage is higher than 4.2V. The battery voltage measurement has the precondition that in all cases the battery voltage is the same at the beginning of the measurement. The minimum battery voltage is 3.3V and the maximal is 4.2V. When the sky is overcast, the battery voltage decreases by about 9 percent, when the sky is cloudy, it stays the same and when the sky is clear, the voltage increases by about 9 percent.

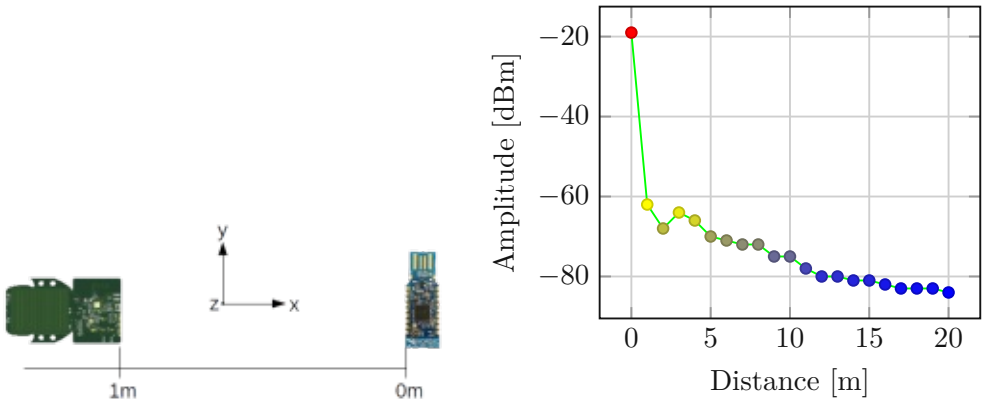

(a) (b)

Figure 7.8: a) shows the setup for the measurement of the amplitude of the antenna and b) shows the result.

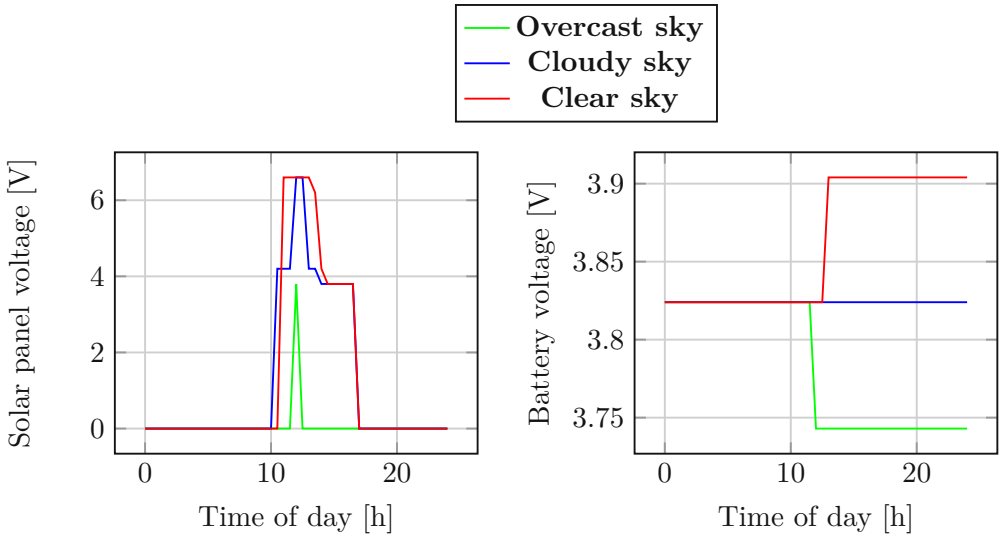

(a) (b)

Figure 7.9: Solar panel a) and battery b) voltages for different weather conditions.

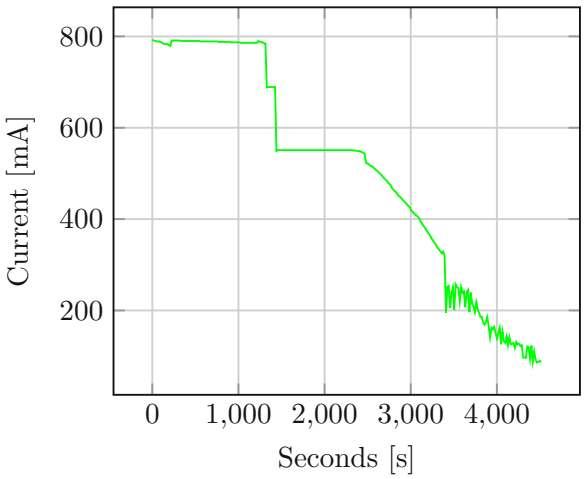

Figure 7.10: PV charging current under full sunlight.

Table 7.5: Price table of the components for one sensor and relay board.

Type	**Price** [€](09/2019)	**Seller**
Capacitors	5.34	From Mouser [Mou]
Resistors	1.9	
Inductors	0.72	
Diodes	1.14	
Crystals	2.02	
nRF52840	5.45	
BQ25895	2.85	
TPS2121	1.81	
VEML6070	2.36	
Case 100mmx60mm	6.15	
Other components	7.34	
PCB Board	5.9	From JLCPCB [JLC]
Assembly	5	Cost estimate from 7pcb [7PC]
9W solar panel	71.75	From Sparkfun [Spa]
Battery 1.1Ah	9.04	
Summary	**131.49**	

7.4 Expenditure on the Board

Table 7.5 lists the prices for the components of a sensor and their sellers. The assembly is based on a cost estimate because for the small number of 5 prototypes hand soldering is cheaper. The minimum quantity for the listed assembly price is 24 boards and the components must be purchased from the assembler. The total cost of about €131 does not meet our requirement of €110, which we have set in Chapter 3.1. But our sensor is still cheaper than the least inexpensive Waspmote for 240€, which we have compared in Chapter 2.

7.5 Field Test

For the field test four sensors were mounted outdoors. The aim was to test the whole network as shown in Figure 4.7. The recorded measured values were the power consumption of the relay and sensor node and the reliability of the leaf wetness, UV and battery voltage data. Figure 7.11a shows schematically the distances between the sensors. Figure 7.11b shows a picture of a mounted sensor in the vineyard, without the case, the solar panel and the battery installed.

(a) (b)

Figure 7.11: Field test setup. a) shows the schematic representation of the deployment of the sensors in the field and b) shows the photo of a mounted sensor node in a vineyard.

7.5.1 Power Consumption

The used ampere for the sensor and relay node for the three different variants are shown in Figure 7.12. The measurements were taken over a time period of one hour. The sensor nodes have taken one measurement every minute.

Forward Only Method The resulting average consumption is 15mA for the sensor node because the data is transmitted every minute immediately after taking the measurement and it needs more energy for that process. The relay node consumes 36mA, which is due to the permanent active Bluetooth connection. This is necessary because the relay node forwards received data immediately to the fog node.

Relay Buffered Method For this method the fog node collects the data every five minutes. Therefore, the relay node has to buffer five measurements for each sensor. In average the sensor node consumes 14.3mA and the relay node 34.5mA. The Bluetooth connection is active every five minutes.

Fog Request Method For this method the fog node collects the data every five minutes. Therefore, the Bluetooth and Thread connections are only active every five minutes. In average the sensor node consumes 12mA and the relay node 34.5mA.

Table 7.6: Comparison of power consumption of our sensor to already existing systems, which were discussed in Chapter 2.

System	Node Consumption [mA]	Relay/Gateway Consumption [mA]
Davis Instruments	12	25
Libelium	17	270
Own	15	36

On the one hand the power consumption of the relay node of the *Relay Buffered Method* and the *Fog Request Method* is the same because in both variants they manage the same tasks related to the receiving and sending of the data. On the other hand the sensor node for the *Relay Buffered Method* consumes more power because it sends the data every minute, whereas for the *Fog Request Method* the data is sent only every five minutes.

In Chapter 2 we compared existing measurement systems and discussed their power consumption. The gateway of the Davis Instruments EnviroMonitor mesh network consumes a minimum of 25mA and the node 12mA. The system from Libelium includes the Waspmote Plug & Sense, which consumes 17mA in the on state and 30μA in the sleep state. The Meshlium consumes 270mA. In Table 7.6 these values are compared to the power consumption of our sensor with the *Forward Only Method*. Our sensor node consumes in the on state as much current as other systems. It does not yet have a sleep state because in a thread network only a certain number of nodes are allowed to go to sleep to prevent the network from being destroyed and this requires further investigations into the software implementation. The relay node of our system needs more power than that of Davis Instruments but less than the one from Libelium. Our relay node needs this amount of power because it is waiting for incoming connections from Bluetooth and the Thread network.

7.5.2 Reliability

The reliability of the sensors was measured over a period of two days. Four sensors were configured, so one sensor value is recorded every minute. After that, it was checked whether the sensor data arrived correctly at the Raspberry Pi. The percentage evaluation of this measurement for the three different variants is shown in Figure 7.13. Since Thread uses UDP for transmitting data, which is connectionless and non-reliable, data could get lost. For each measurement type there is a separate CoAP resource, these are transmitted separately. Therefore, it can happen that, e.g. only the UV measurement value is lost at a certain time but leaf wetness and battery voltage reach their destination.

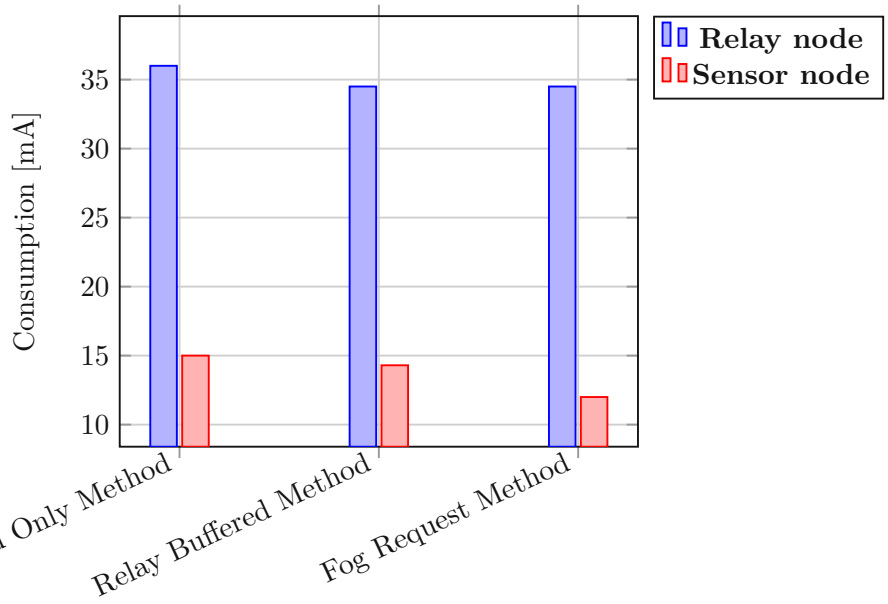

Figure 7.12: Average power consumption of the relay and sensor nodes for the three different transmission variants.

Forward Only Method The resulting reliability for the leaf wetness and UV measurement is 94%. For the battery voltage measurement it is 90%. With the *Forward Only Method* the thread network is more reliable because the data is sent directly to the fog node after each measurement. In this case the network has smaller intervals between data transfers, so the routes in the network and the roles of the nodes remain the same for a longer time. Since this method is centralized, it is very bad for reliability if a central node like the relay node or the fog device fails because all data is lost. But this did not happen during the test period.

Relay Buffered Method For this method the reliability for the leaf wetness is 87%, for the UV it is 91% and for the battery voltage measurement it is 90%. With this method data can be lost if the fog device does not fetch the data from the relay node in time and therefore the ring buffer overflows. In addition, as in the *Forward Only Method*, data can get lost in the network.

Fog Request Method For this method the reliability for the leaf wetness is 92.4%, for the UV it is 89% and for the battery voltage measurement it is 88.1%. With this method, as with *Relay Buffered Method*, data can get lost if the fog device does not fetch the data from the sensor nodes in time. Since each sensor stores its own data, it is less likely that the buffer will overflow because there is more storage space available.

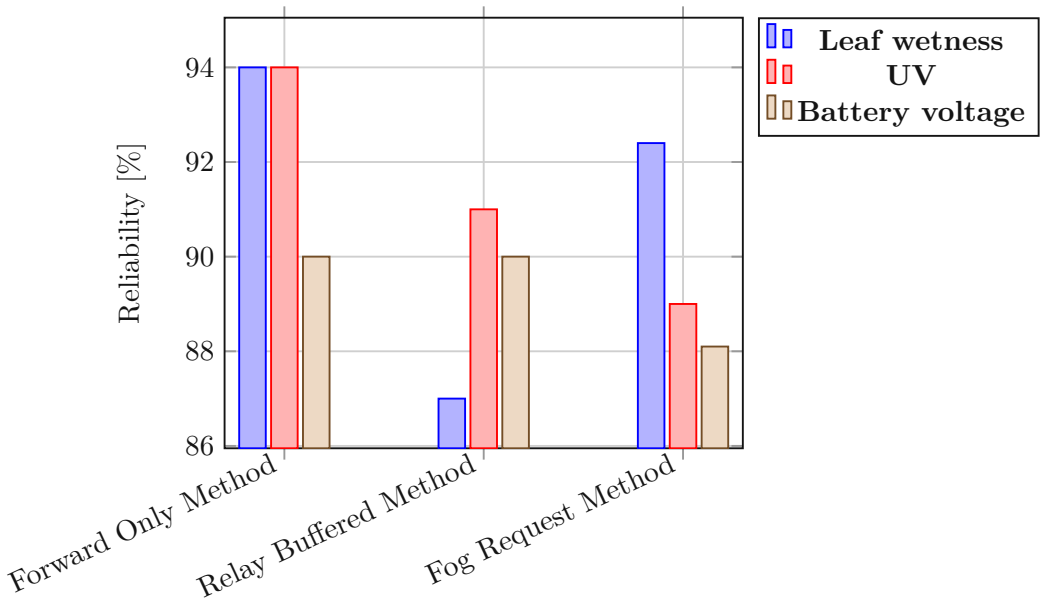

Figure 7.13: Percentage reliability of sensor data from four sensors over a period of 2 days.

CHAPTER 8

Conclusion

The aim of this thesis was to build an IoT sensor swarm for agricultural microclimate measurement. For this purpose, a prototype was built to measure the leaf wetness and UV radiation and it was tested for range, reliability and power consumption. The leaf wetness sensor imitates a leaf and measures the wetness on the sensor surface with the help of the change in capacitance. Three leaf wetness areas with different PCB tracks were compared. For transmitting the data, a mesh network was used and three possible transmission methods were evaluated. The power consumption is as good as with commercially available products. Nevertheless, there is still and always room for improvement, also in connection with reliability.

8.1 Outlook and Further Tasks

With this work several aspects were identified that can be improved to get a higher measurement reliability and consume less power. The following points should be considered in further research.

8.1.1 Sensor Manufacturing

The manufacturing of the sensors includes the steps: PCB manufacturing, PCB assembly, ordering all components and end testing. The equipment needed to manufacture the sensors and the companies that can take over steps from the manufacturing should already be analyzed and compared before the start of the development. This has to be done in order to avoid shortlisting products in the beginning that cannot be assembled later in the process. In our case, the placement, soldering and testing of the nRF52840 should be done by a professional company.

8.1.2 Power Consumption Optimization

The power consumption of the sensor node can be further reduced by improving the source code. This could be done by, for example, compressing the measurement data to decrease the necessary payload when transmitting. This has to be evaluated further by comparing the necessary power for compression versus the transmission power. Another possibility is to define certain nodes in the thread network as sleepy end devices. A sleepy end device turns off the radio for a predefined time. Afterwards it switches into sleep mode. Each sleepy end device needs a parent which buffers the messages when it is sleeping. Therefore, a sleeping mode is not intended for the parent. Only a small number of nodes in a thread network can go to sleep because the others have to keep the network running. However, an overall concept of the network to be built up is needed to use the maximum number of sleepy end devices. Another possibility to minimize the power consumption is to increase the measuring interval.

8.1.3 Increase Reliability

The reliability of the measured values can be improved by using check sums during transmission. Since Thread uses UDP for transmitting data, which is connectionless and non-reliable, data could get lost. Further data loss can occur if a sensor runs out of power and the data is not stored in a non-volatile memory. To prevent the non-volatile memory from overflowing, in addition to the internal flash memory of the nRF52840, an external flash can be installed. Another aspect to mention is, if the fog node misses any data, it could request a re-transmission from the sensor or the relay node.

CHAPTER 9

Appendix

This appendix includes the full schematic of the sensor board.

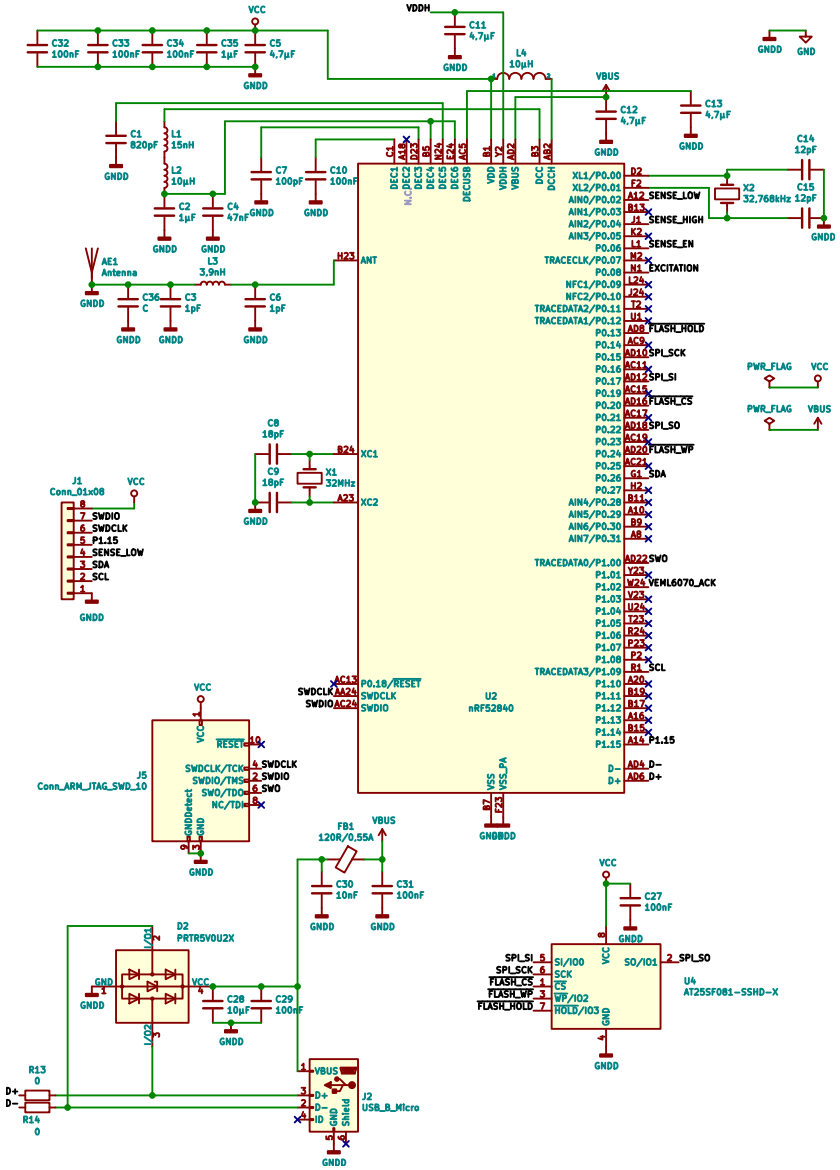

Figure 9.1: Schematic for the nRF52840.

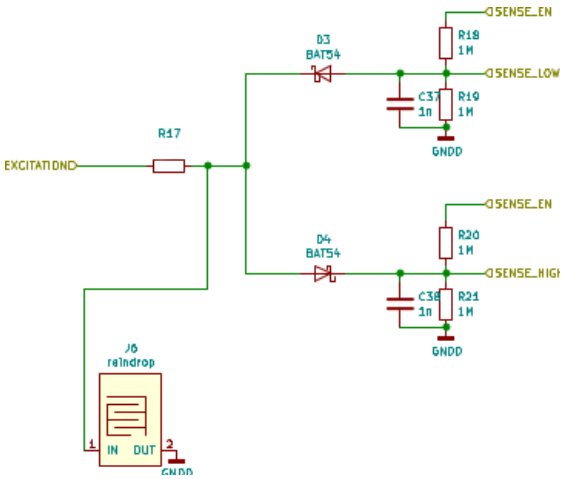

Figure 9.2: Schematic for the leaf wetness measurement.

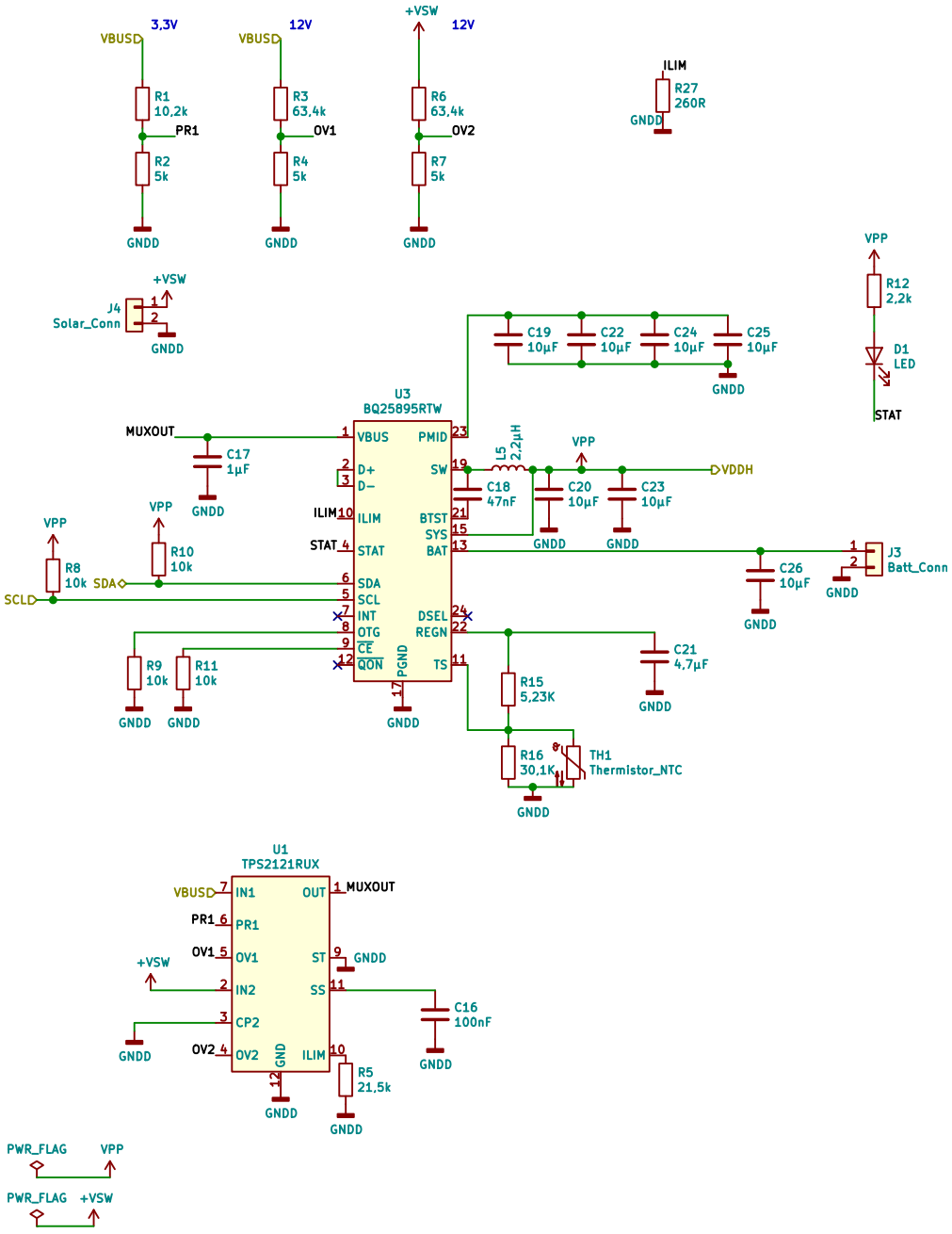

Figure 9.3: Schematic for the power management.

List of Figures

Acronyms

BLE Bluetooth Low Energy

NFC Near Field Communication

SoC System on Chip

RTOS Real Time Operating System

IoT Internet of Things

SPOF Single Point of Failure

OSI Open System Interconnection

ISO International Organization for Standardization

HTTP Hypertext Transfer Protocol

FTP File Transfer Protocol

DNS Domain Name System

SSL Secure Sockets Layer

TLS Transport Layer Security

MQTT Message Queuing Telemetry Transport

CoAP Constrained Application Protocol

PPTP Point to Point Tunneling Protocol

UDP User Datagram Protocol

DTLS Datagram Transport Layer Security

TCP Transmission Control Protocol

TLS Transport Layer Security

6LoWPAN IPv6 over Low power Wireless Personal Area Network

IEEE Institute of Electrical and Electronics Engineers

IP Internet Protocol

ARP Address Resolution Protocol

ICMP Internet Control Message Protocol

RFCOMM Radio Frequency Communication

SDP Service Discovery Protocol

L2CAP Logical Link Control and Adaptation Protocol

HCI Host Controller Interface

SPF Shortest Path Bridging

EIA Electronic Industries Alliance

SIG Bluetooth Special Interest Group

IETF Internet Engineering Task Force

IEEE-SA Institute of Electrical and Electronics Engineers Standards Association

IPv6 Internet Protocol Version 6

MTU Maximum Transmission Unit

AES Advanced Encryption Standard

CCM Counter with CBC-MAC

WPAN Wireless Personal Area Networks

PAN Personal Area Network

FFD Full Function Device

RFD Reduced Function Device

ISM Industrial, Scientific and Medical

LQI Link Quality Indication

CCA Clear Channel Assessment

ED Energy Detection

DSSS Direct Sequence Spread Spectrum

CSMA Carrier Sense Multiple Access

CA Collison Avoidance

CD Collison Detection

BE Beacon Enabled

NBE Non-Beacon Enabled

CAP Contention Access Period

CFP Contention Free Period

TDMA Time Division Multiple Access

BI Beacon Interval

BO Beacon Order

SD Superframe Duration

SO Superframe Order

NSFS Number of Superframe Slots

BSFD Base Super Frame Duration

SP Symbol Period

DVA Distance Vector Algorithm

FTD Full Thread Devices

MTD Minimal Thread Devices

REED Router Eligible End Device

FED Full End Device

MED Minimal End Device

SED Sleepy End Device

NCP Network Coprocessor

GFSK Gaussian Frequency Shift Keying

FHSS Frequency Hopping Spread Spectrum

REST Representational State Transfer

MQTT Message Queuing Telemetry Transport

IBM International Business Machines

OASIS Organization for the Advancement of Structured Information Standards

IPSec Internet Protocol Security

UVA Ultraviolet A

UVB Ultraviolet B

UVC Ultraviolet C

FDR Frequency Domain Reflectometry

TDT Time Domain Transmission

TDR Time Domain Reflectometry

UV Ultraviolet Radiation

I²C Inter-Integrated Circuit

PCB Printed Circuit Board

CCD Charge-coupled Device

CMOS Complementary metal-oxide-semiconductor

GSM Global System for Mobile Communications

GPRS General Packet Radio Service

UMTS Universal Mobile Telecommunications System

UHF Ultra-High-Frequency

LoRaWAN Long Range Wide Area Network

Edge Enhanced Data Rates for GSM Evolution

RS232 Recommended Standard 232

2G Second generation mobile network

3G Third generation mobile network

4G Fourth generation mobile network

SDK Software Development Kit

API Application-Programming-Interface

USB Universal Serial Bus

EOS Earth Observation Satellites

OTA Over The Air

SOC State Of Charge

LWD Leaf Wetness Duration

SIM Subscriber Identity Module

ADC Analog to Digital Converter

RAM Random Access Memory

IC Integrated Circuit

PWM Pulse Width Modulation

SPI Serial Peripheral Interface

MCU Microcontroller Unit

GPIO General Purpose Input Output

NTC Negative Temperature Coefficient

VPCC Voltage Proportional Current Control

VINDPM Voltage Input Dynamic Power Management

DPPM Dynamic Power Path Management

DPM Dynamic Power Management

MPPT Maximum Power Point Tracking

MPP Maximum Power Point

PPM Power Path Management

mux Multiplexer

Mux Multiplexer

MOSFET Metal Oxide Semiconductor Field Effect Transistor

DC Direct Current

PV Photovoltaic

LWS Leaf Wetness Sensor

CDC Capacitive to Digital Converter

Wh Watt hour

LED Light Emitting Diode

SWD Serial Wire Debug

LDO Low Dropout Regulator

SMD Surface Mounted Device

SMA SubMiniature version A

BALUN Balanced Unbalanced Network

DK Development Kit

GUI Graphical User Interface

MBR Master Boot Record

WDT Watchdog Timer

UUID Universally Unique Identifier

RPI Raspberry Pi

CSV Comma Separated Values

RTC Real Time Counter

NTP Network Time Protocol

EUI-64 64-Bit Extended Unique Identifier

CIE International Commission on Illumination

M2M Machine-to-Machine

LAN Local Area Network

WHO World Health Organization

DC/DC Buck regulator

List of Tables

Bibliography

[7PC] 7PCB. 7pcb, a pcb assembler. URL: https://www.7pcb.com/. [Online; last accessed: 2019-09-05].

[AAB+10] D. Allan, P. Ashwood-Smith, N. Bragg, J. Farkas, D. Fedyk, M. Ouellete, M. Seaman, and P. Unbehagen. Shortest path bridging: Efficient control of larger ethernet networks. *IEEE Communications Magazine*, 48(10):128–135, October 2010.

[Adca] Adcon. Adcon capacitive leaf wetness sensor. URL: https://www.adcon.com/products/sensors-284/wet-leaf-wetness-sensor-1759/. [Online; last accessed: 2019-09-05].

[Adcb] Adcon. Adcon weather station for agriculture. URL: https://www.adcon.com/solutions/precision-farming-99/. [Online; last accessed: 2019-09-05].

[AGM+15] A. Al-Fuqaha, M. Guizani, M. Mohammadi, M. Aledhari, and M. Ayyash. Internet of things: A survey on enabling technologies, protocols, and applications. *IEEE Communications Surveys Tutorials*, 17(4):2347–2376, 2015.

[ahd19] ahdb. Satellites for agriculture. URL: https://ahdb.org.uk/knowledge-library/satellites-for-agriculture, 2019. [Online; last accessed: 2019-09-05].

[AM12] N. Angkawisittpan and T. Manasri. Determination of sugar content in sugar solutions using interdigital capacitor sensor. *Measurement Science Review*, 12:8–13, 03 2012.

[Ann92] S. Ann. Ultraviolet radiation and plants: Burning questions. *The Plant cell*, 4:1353–1358, 12 1992.

[ASA+18] N. Ali, R. Saleem, P. Angelina, G. Mesut, and D. Behnam. Low-power wireless for the internet of things: Standards and applications. *IEEE Access*, PP:1–1, 11 2018.

[Aud08a] A. Audun. Selecting antennas for low-power wireless applications. URL: http://www.ti.com/lit/an/slyt296/slyt296.pdf, 2008. [Online; last accessed: 2019-09-05].

[Aud08b] A. Audun. Small size 2.4 ghz pcb antenna. URL: http://www.ti.com/lit/an/swra117d/swra117d.pdf, 2008. [Online; last accessed: 2019-09-05].

[Awt97] D. Awtrey. Transmitting data and power over a one-wire bus. *Applied Sensing Technology*, 1997.

[Awt98] D. Awtrey. The 1-wire weather station. *SENS(PETERBOROUGH, NH)*, 15(6):34, 1998.

[Bau08] K. Bauer. *Weinbau.* AV-Fachbuch. Österreichischer Agrarverlag, 2008.

[BKK+08] G. Bleyer, H.H. Kassemeyer, R. Krause, O. Viret, and W. Siegfried. „vitimeteo plasmopara“ – prognosemodell zur bekämpfung von plasmopara viticola (rebenperonospora) im weinbau. *Gesunde Pflanzen*, 60:91–100, 09 2008.

[BLSa] BLSIG. Bluetooth low energy mesh faq. URL: https://www.bluetooth.com/bluetooth-technology/topology-options/le-mesh/mesh-faq/. [Online; last accessed: 2019-09-05].

[BLSb] BLSIG. Bluetooth special interest group. URL: https://www.bluetooth.com. [Online; last accessed: 2019-09-05].

[BS01] J. Bray and C. F. Sturman. Bluetooth 1.1: Connect without cables, 2nd edition. URL: http://www.informit.com/articles/article.aspx?p=27591&seqNum=5, 2001. [Online; last accessed: 2019-09-05].

[Cama] Campbell. Campbell scientific capacitive leaf wetness sensor. URL: https://www.campbellsci.com/lws. [Online; last accessed: 2019-09-05].

[Camb] Campbell. Campbell scientific resistor based leaf wetness sensor. URL: https://www.campbellsci.com/237-l. [Online; last accessed: 2019-09-05].

[CCC51] D. Croney, J. D. Coleman, and E. W. H. Currer. The electrical resistance method of measuring soil moisture. *British Journal of Applied Physics*, 2(4):85–91, apr 1951.

[cco99] ccontrols. Understanding eia-485 networks. *Springer 1999 - theExtension*, 1, 1999. [Online; last accessed: 2019-09-05].

[CIE] CIE. International commission on illumination . URL: http://cie.co.at/. [Online; last accessed: 2019-09-05].

[Com06] Wikimedia Commons. Solar cell iv curve with mp. URL: https://commons.wikimedia.org/wiki/File:Solar-Cell-IV-curve-with-MPP.png, 2006. [Online; last accessed: 2019-09-05].

[Cop] R. Coppen. Oasis. URL: https://www.oasis-open.org/committees/tc_home.php?wg_abbrev=mqtt. [Online; last accessed: 2019-09-05].

[Cor] Davis Instruments Corporation. Davis instruments resistor based leaf wetness sensor. URL: https://www.davisinstruments.com/product/leaf-wetness-sensor-vantage-pro-and-vantage-pro2/. [Online; last accessed: 2019-09-05].

[CTGD09] F. Chen, T. Talanis, R. German, and F. Dressler. Real-time enabled ieee 802.15.4 sensor networks in industrial automation. *IEEE International Symposium on Industrial Embedded Systems.*, pages 136–139, 2009.

[Dav10] A. Davide. *Battery Management Systems for Large Lithium Ion Battery Packs*. EBL-Schweitzer. Artech House, 2010.

[Deb18] Open On-Chip Debugger. Open on-chip debugger. URL: http://openocd.org/, 2018. [Online; last accessed: 2019-09-05].

[Dev] Analog Devices. Analog devices ad7746, 24-bit, 2 channel capacitance to digital converter. URL: https://www.analog.com/en/products/ad7746.html. [Online; last accessed: 2019-09-05].

[Dif02] B. L. Diffey. Sources and measurement of ultraviolet radiation. *Methods*, 28(1):4 – 13, 2002.

[Dif13] B.L. Diffey. *Radiation Measurement in Photobiology*. Elsevier Science, 2013.

[DIN15] DIN. Preferred number series for resistors and capacitors (iec 60063:2015). URL: https://www.beuth.de/de/norm/din-en-60063/240741276, 2015. [Online; last accessed: 2019-09-05].

[Dja19] W. Djatmiko. Capacitance measurements system using rc circuit. *KnE Social Sciences*, 3:603, 03 2019.

[dp] dq pp. Mounting rope clamp. URL: http://dq-pp.com/stainless-steel-bolt-clip-from-pieces-p-6994.html. [Online; last accessed: 2019-09-05].

[Elea] SparkFun Electronics. Sparkfun soil moisture board. URL: https://www.sparkfun.com/products/13322. [Online; last accessed: 2019-09-05].

[Eleb] SparkFun Electronics. Veml6075 break out board. URL: https://www.sparkfun.com/products/15089. [Online; last accessed: 2019-09-05].

[FJ94] Z. Fedro and X. Jiannong. Soil moisture sensors 1. *Bulletin292*, 1994.

[Fou] Python Software Foundation. Python programming language. URL: https://www.python.org/. [Online; last accessed: 2019-09-05].

[fSI94] International Organization for Standardization (ISO). Information technology - open systems interconnection - basic reference model: The basic model. *ISO/IEC 7498-1*, 1994.

[GAS15] A. Ghobakhlou, F. Amir, and P. Sallis. Leaf wetness sensors - a comparative analysis. In *9th International Conference on Sensing Technology (ICST)*, pages 420–424, 12 2015.

[Gmba] Pessl Instruments GmbH. imetos weather station for agriculture. URL: http://metos.at/de/imetos33/. [Online; last accessed: 2019-09-05].

[Gmbb] Pessl Instruments GmbH. Metos pessl instruments resistor based leaf wetness sensor. URL: https://metos.at/portfolio/leaf-wetness/. [Online; last accessed: 2019-09-05].

[Goo] Google. Open thread. URL: https://openthread.io/. [Online; last accessed: 2019-09-05].

[Gro] Thread Group. Thread group. URL: https://www.threadgroup.org/thread-group#OurMembers. [Online; last accessed: 2019-09-05].

[Gup13] N. Gupta. *Inside Bluetooth Low Energy*. Artech House Remote Sensing Library. Artech House, 2013.

[GYYL09] K. Gill, S.-H. Yang, F. Yao, and X. Lu. A zigbee-based home automation system. *IEEE Trans. Consum. Electron*, 55:422–430, 2009.

[Her13] K.H. Hermann. *Der Photoeffekt: Grundlagen der Strahlungsmessung*. Vieweg+Teubner Verlag, 2013.

[Hol02] F. Hollósy. Effects of ultraviolet radiation on plant cells. *Micron*, 33(2):179 – 197, 2002.

[HP07] K.K. Hamamatsu Photonics. *PHOTOMULTIPLIER TUBES Basics and Applications*. Hamamatsu Photonics K.K. Electron Tube Division, 2007.

[HRG18] C. Hirsch, M. Redl, and R. Grosu. Towards an agricultural iot-infrastructure for micro-climate measurements. *Talk: Workshop on Smart Farming, Porto, Portugal*, 2018.

[IEEa] IEEE. Ieee 802.3. URL: http://www.ieee802.org/3/. [Online; last accessed: 2019-09-05].

[IEEb] IEEE. Ieee 802.3-2018 - ieee standard for ethernet. URL: https://standards.ieee.org/standard/802_3-2018.html. [Online; last accessed: 2019-09-05].

[IEEc] IEEE. IEEE standard association. URL: http://standards.ieee.org. [Online; last accessed: 2019-09-05].

[IEE12] *IEEE Standard for Local and Metropolitan Area Networks—Part 15.4: Low-Rate Wireless Personal Area Networks (LR-WPANs) Amendment 1: MAC Sublayer,* IEEE standard 802.15.4e-2012 (amendment to ieee standard 802.15.4-2011). pages 1–225, 2012.

[IETa] IETF. The internet engineering task force (IETF). URL: https://www.ietf.org. [Online; last accessed: 2019-09-05].

[IETb] IETF. Rfc4291. URL: https://tools.ietf.org/html/rfc4291. [Online; last accessed: 2019-09-05].

[IETc] IETF. Rfc6282. URL: https://tools.ietf.org/html/rfc6282. [Online; last accessed: 2019-09-05].

[IETd] IETF. Rfc7252. URL: https://tools.ietf.org/html/rfc7252. [Online; last accessed: 2019-09-05].

[IETe] IETF. Thread scope. URL: https://openthread.io/guides/thread-primer/ipv6-addressing. [Online; last accessed: 2019-09-05].

[Ily13] G. Ilya. Making the web faster with http 2.0. *Communications of the ACM*, 56(12):42–49, December 2013.

[Inca] Digi International Inc. Digimesh. URL: https://www.digi.com/products/tag/digimesh. [Online; last accessed: 2019-09-05].

[Incb] Silicon Laboratories Inc. Thread mesh network performance. URL: https://www.silabs.com/documents/login/application-notes/an1141-thread-mesh-network-performance.pdf. [Online; last accessed: 2019-09-05].

[Insa] Davis Instruments. Davis instruments capacitive leaf wetness sensor. URL: https://www.davisinstruments.com/. [Online; last accessed: 2019-09-05].

[Insb] Davis Instruments. Enviromonitor. URL: https://www.davisinstruments.com/solution/enviromonitor-affordable-field-monitoring-system/. [Online; last accessed: 2019-09-05].

[Ins14] Texas Instruments. Bq2403x. URL: http://www.ti.com/lit/ds/symlink/bq24038.pdf?keyMatch=BQ2403X&tisearch=Search-EN-everything, 2014. [Online; last accessed: 2019-09-05].

[Ins18] Texas Instruments. Datasheet of the bq25895 i2c controlled single cell 5-a fast charger with maxchargetm for high input voltage and adjustable voltage 3.1-a boost operation. URL: http://www.ti.com/lit/ds/symlink/bq25895.pdf, 2018. [Online; last accessed: 2019-09-05].

[Ins19] Texas Instruments. Datasheet of the tps212x 2.8-v to 22-v priority power mux with seamless switchover. URL: http://www.ti.com/lit/ds/symlink/tps2120.pdf, 2019. [Online; last accessed: 2019-09-05].

[Jaf14] T. Jaffey. Mqtt and coap, iot protocols. URL: https://www.eclipse.org/community/eclipse_newsletter/2014/february/article2.php, 2014. [Online; last accessed: 2019-09-05].

[Jha17] H. Jha. A study and comparison of wired, wireless and optical networks. 5:13109 – 13128, 2017.

[JLC] JLCPCB. Jlcpcb, a pcb manufacturer. URL: https://jlcpcb.com/. [Online; last accessed: 2019-09-05].

[JVR+19] P. Jitender, C. Vivek, P. Rishi, C. Sushabhan, M. Ranjan, M. Raj Gaurav, and K. Adesh. A review: Soil moisture estimation using different techniques. In *Intelligent Communication, Control and Devices*, pages 105–111, Singapore, 2019. Springer Singapore.

[KBD+99] U. Karsten, K. Bischof, H. Dieter, H. Tüg, and C. Wiencke. The effect of ultraviolet radiation on photosynthesis and ultraviolet-absorbing substances in the endemic arctic macroalga devaleraea ramentacea (rhodophyta). *Physiologia Plantarum*, 105:58 – 66, 01 1999.

[KC14] P. Karunakar and A. Chitneni. A comparative study of wireless protocols: Bluetooth, uwb, zigbee, and wi-fi. *Advance in Electronic and Electric Engineering*, 4:655–662, 09 2014.

[KiC] KiCad. Kicad eda, a cross platform and open source electronics design automation suite. URL: https://kicad-pcb.org/. [Online; last accessed: 2019-09-05].

[KK19] A. Khanna and S. Kaur. Evolution of internet of things (iot) and its significant impact in the field of precision agriculture. *Computers and Electronics in Agriculture*, 157:218 – 231, 2019.

[KM14] N. Kaur and S. Monga. Comparisons of wired and wireless networks: a review. *International Journal of Advanced Engineering Technology*, 5(2):34 – 35, 2014.

[LA16] D. Lechner and O. Aceña. Gattlib, python library to use the gatt protocol for bluetooth le devices. URL: `https://github.com/ev3dev/gattlib`, 2016. [Online; last accessed: 2019-09-05].

[Laba] National Renewable Energy Laboratory. Solar cell efficiency. URL: `https://pvdpc.nrel.gov/`. [Online; last accessed: 2019-09-05].

[Labb] Descartes Labs. Descartes labs. URL: `https://www.descarteslabs.com/`. [Online; last accessed: 2019-09-05].

[Labc] Silicon Labs. Sensor puck. URL: `https://www.silabs.com/products/development-tools/sensors/environmental-biometric-sensor-puck-starter-kit`. [Online; last accessed: 2019-09-05].

[LGL+] J.D. Longstreth, F.R. de Gruijl, J.C. van der Leun, M. L Kripke, and Y. Takizawa. Effects of increased solar ultraviolet radiation on human health. *Ambio*, 24.

[Lib] Libelium. Libelium waspmote. URL: `http://www.libelium.com/products/waspmote/`. [Online; last accessed: 2019-09-05].

[Lim] Arm Limited. Mbedos. URL: `https://os.mbed.com/docs/mbed-os/v5.14/reference/thread-tech.html`. [Online; last accessed: 2019-09-05].

[LL15] I. Lee and K. Lee. The internet of things (iot): Applications, investments, and challenges for enterprises. *Business Horizons*, 58(4):431 – 440, 2015.

[LLC] SEGGER Microcontroller Systems LLC. Segger j-link. URL: `https://www.segger.com/products/debug-probes/j-link/`. [Online; last accessed: 2019-09-05].

[MFP+16] V. Montone, C.W. Fraisse, N.A. Peres, P.C. Sentelhas, M. Gleason, M. Ellis, and G. Schnabel. Evaluation of leaf wetness duration models for operational use in strawberry disease-warning systems in four us states. *International Journal of Biometeorology*, 60(11):1761–1774, Nov 2016.

[MLPP16] J. Morales, N. A. Lopez, J. Parado, and J. Pasaoa. A comparative study of thread against zigbee, z-wave, bluetooth, and wi-fi as a home-automation networking protocol., 11 2016.

[MLS12] H. Mittelbach, I. Lehner, and S. I. Seneviratne. Comparison of four soil moisture sensor types under field conditions in switzerland. *Journal of Hydrology*, 430-431:39 – 49, 2012.

[Mon13] V.O. Montone. *Leaf Wetness Duration Modeling and Spatialization to Optimize Fungicide Application in Strawberry Production Systems*. University of Florida Digital Collections. University of Florida, 2013.

[Mor12] M. Morris. Comparison of rechargeable battery technologies. *ASME Early Career Technical Journal*, 11:148–155, 11 2012.

[Mou] Mouser. Mouser, a electronic component seller. URL: `https://www.mouser.at/`. [Online; last accessed: 2019-09-05].

[MPB+16] B. Milija, S. Petar, K. Bozo, Đ. Slobodan, and P. Tomo. A private iot cloud platform for precision agriculture and ecological monitoring. *Computers and Electronics in Agriculture*, 140:255 – 265, 06 2016.

[MRC+17] Y. Murillo, B. Reynders, A. Chiumento, S. Malik, P. Crombez, and S. Pollin. Bluetooth now or low energy: Should ble mesh become a flooding or connection oriented network? In *2017 IEEE 28th Annual International Symposium on Personal, Indoor, and Mobile Radio Communications (PIMRC)*, pages 1–6, 2017.

[Nai17] N. Naik. Choice of effective messaging protocols for iot systems: Mqtt, coap, amqp and http. In *2017 IEEE International Systems Engineering Symposium (ISSE)*, pages 1–7, Oct 2017.

[Nin12] J. Ning. Adi capacitance-to-digital converter technology in healthcare applications. URL: `https://www.analog.com/en/analog-dialogue/articles/capacitance-to-digital-converter-technology-healthcare.html`, 2012. [Online; last accessed: 2019-09-05].

[OBL+15] R. Ojo, P. R. Bullock, J. L'Heureux, Powers, H.J. McNairn, and A. Pacheco. Calibration and evaluation of a frequency domain reflectometry sensor for real-time soil moisture monitoring. *The Soil Science Society of America, Inc.*, 2015.

[PAM17] N. Poursafar, M. E. E. Alahi, and S. Mukhopadhyay. Long-range wireless technologies for iot applications: A review. In *2017 Eleventh International Conference on Sensing Technology (ICST)*, pages 1–6, 2017.

[Pan13] K. Pandya. Network structure or topology. *International Journal of Advance Research in Computer Science and Management Studies*, 1:22 – 27, 2013.

[PDHM14] R. Priyanka, S. K. Deep, C. Hakima, and B. Marie. Wireless sensor networks: a survey on recent developments and potential synergies. *The Journal of Supercomputing*, 68(1):1 – 48, 2014.

[PRSBR17] J. Prasanth Ram, T. Sudhakar Babu, and N. Rajasekar. A comprehensive review on solar pv maximum power point tracking techniques. *Renewable and Sustainable Energy Reviews*, 67:826 – 847, 2017.

[RSPAM19] A. K. Rêgo Segundo, E. Pinto, G. Almeida, and P. Monteiro. Capacitive impedance measurement: Dual-frequency approach. *Sensors*, 06 2019.

[San14] L. Sanchez. Smartsantander: Iot experimentation over a smart city testbed. *Computer Networks*, 61:217–238, 2014.

[SBV+19] A. Singh, A. Bhardwaj, CL. Verma, VK. Mishra, A. Singh, S. Arora, N. Sharma, and R. Ojha. Soil moisture sensing techniques for scheduling irrigation. *Journal of Soil Salinity and Water Quality*, 11(1):68 – 76, 2019.

[Sci] Campbell Scientific. Cs616 capacitive soil measurement board. URL: `https://www.campbellsci.de/cs616-reflectometer`. [Online; last accessed: 2019-09-05].

[Sem] Nordic Semiconductor. Nordic nrfjprog. URL: `https://www.nordicsemi.com/Software-and-tools/Development-Tools/nRF-Command-Line-Tools`. [Online; last accessed: 2020-11-22].

[Sem16] Nordic Semiconductor. Datasheet of the nrf52840. URL: `https://infocenter.nordicsemi.com/pdf/nRF52840_OPS_v0.5.pdf`, 2016. [Online; last accessed: 2019-09-05].

[Sem18a] Nordic Semiconductor. Nordic memory layout libraries. URL: `https://infocenter.nordicsemi.com/index.jsp?topic=%2Fcom.nordic.infocenter.sdk5.v15.2.0%2Flib_bootloader.html`, 2018. [Online; last accessed: 2019-09-05].

[Sem18b] Nordic Semiconductor. Nordic multiprotocol. URL: `https://www.nordicsemi.com/Products/Low-power-short-range-wireless/Multiprotocol`, 2018. [Online; last accessed: 2019-09-05].

[Sem18c] Nordic Semiconductor. Nordic softdevice s140. URL: `https://infocenter.nordicsemi.com/pdf/S140_SDS_v1.1.pdf`, 2018. [Online; last accessed: 2019-09-05].

[Sem19] Vishay Semiconductors. Datasheet of the veml6070 uva light sensor with i2c interface. URL: https://www.vishay.com/docs/84277/veml6070.pdf, 2019. [Online; last accessed: 2019-09-05].

[Sem20] Nordic Semicondutor. nrf52840 development kit. URL: https://infocenter.nordicsemi.com/index.jsp?topic=%2Fug_nrf52840_dk%2FUG%2Fnrf52840_DK%2Fgetting_started.html, 2020. [Online; last accessed: 2020-11-22].

[Sho] Farm Shots. Farm shots. URL: http://farmshots.com/. [Online; last accessed: 2019-09-05].

[SKB18] S. Sen, J. Koo, and S. Bagchi. Trifecta: Security, energy efficiency, and communication capacity comparison for wireless iot devices. *IEEE Internet Computing*, 22(1):74–81, 2018.

[SMG04] P. Sentelhas, J.E.B.A. Monteiro, and T.J. Gillespie. Electronic leaf wetness duration sensor: Why it should be painted. *International journal of biometeorology*, 48:202–5, 06 2004.

[Sol] Solargis. Solargis map for austria. URL: https://solargis.com/maps-and-gis-data/download/austria. [Online; last accessed: 2019-09-05].

[Sol18] Low Power Radio Solutions. 2.4ghz compressed stubby / whip antenna. URL: https://lprs.co.uk/assets/files/downloads/ant-ss24g-antenna-datasheet-v1.5.pdf, 2018. [Online; last accessed: 2019-09-05].

[Spa] Sparkfun. Sparkfun, a electronic component seller. URL: https://www.sparkfun.com/. [Online; last accessed: 2019-09-05].

[SPS+12] B. Sameer, A. Paventhan, A. Salkrishna, V. Gayathri, and R. N.Mohan. Leveraging coap towards monitoring agriculture sensor network. *Wireless Communication and Sensor Networks*, 12 2012.

[SSS+06] C. Sicora, A. Szilárd, L. Sass, E. Turcsányi, Z. Máté, and I. Vass. *UV-B and UV-A Radiation Effects on Photosynthesis at the Molecular Level*, pages 121–135. 07 2006.

[Staa] RFC Internet Standard. Transmission control protocol. URL: https://tools.ietf.org/html/rfc793. [Online; last accessed: 2019-09-05].

[Stab] RFC Internet Standard. User datagram protocol. URL: https://tools.ietf.org/html/rfc768. [Online; last accessed: 2019-09-05].

[Ste16] H. Stefan. Heimautomation mit knx, dali, 1-wire und co. *Rheinwerk Computing*, 2016.

[SWA13] M. Shiraz, Md. Whaiduzzaman, and G. Abdullah. A study on anatomy of smartphone. *Journal of Computer Communication and Collaboration*, 1:24–31, 06 2013.

[TG15] Inc Thread Group. Thread commissioning. URL: https://www.threadgroup.org/Portals/0/documents/support/CommissioningWhitePaper_658_2.pdf, 2015. [Online; last accessed: 2019-09-05].

[TGL+07] F. Tang, M. Guo, M. Li, Y. Yang, D. Zhang, and Y. Wang. Wireless mesh sensor networks in pervasive environment: a reliable architecture and routing protocol. In *2007 International Conference on Parallel Processing Workshops (ICPPW 2007)*, pages 72–72, Sep. 2007.

[Upt19] E. Upton. Raspberry pi specification. URL: https://www.raspberrypi.org/blog/raspberry-pi-4-on-sale-now-from-35/, 2019. [Online; last accessed: 2019-09-05].

[Vit] Vitimeteo. Vitimeteo - forecasting models, weather data and monitoring for viticulture. URL: https://www.vitimeteo.at/. [Online; last accessed: 2019-09-05].

[VTC17] P. Vosoughi, P. Taylor, and H. Ceylan. Impacts of internal curing on the performance of concrete materials in the laboratory and the field. *INTRANS PROJECT REPORTS*, 11 2017.

[W3C] World Wide Web Consortium W3C. W3c - http. URL: https://www.w3.org/Protocols/. [Online; last accessed: 2019-09-05].

[Wil11] B. Will. Time domain transmission sensors for soil moisture measurements. In *Proceedings of the 19th Telecommunications Forum (TELFOR)*, pages 16–19, 2011.

[YKX+17] Y. Liu, K. Tong, X. Qiu, Y. Liu, and X. Ding. Wireless mesh networks in iot networks. In *2017 International Workshop on Electromagnetics: Applications and Student Innovation Competition*, pages 183–185, May 2017.

[Zig] ZigBee. ZigBee. URL: http://www.zigbee.org. [Online; last accessed: 2019-09-05].